Natural Product Reports

ROYAL SOCIETY OF CHEMISTRY

REVIEW

View Article Online
View Journal | View Issue

Cite this: *Nat. Prod. Rep.*, 2024, **41**, 1723

Structural diversity and chemical logic underlying the assembly of monoterpene indole alkaloids oligomers†‡

Pierre Le Pogam * and Mehdi A. Beniddir *

Received 28th February 2024

DOI: 10.1039/d4np00011k

rsc.li/npr

Covering: up to 2024

This review aims to draw a parallel between all known oligomers of monoterpene indole alkaloids (MIAs) by illustrating the chemical logic underlying their assembly. For this purpose, oligomeric MIAs were first comprehensively listed and organized according to the names of the backbones of their constitutive monomers and the binding sites. From this extensive list, an oligomer network was generated and unprecedented MIA statistics were mined and shared herein. Subsequently, oligomeric MIAs were categorized according to the number of connections instigated between their monomeric components (single, double, triple, and mixed tethering), then subdivided according to the uniqueness or combination of oligomerization assembly reactions. This effort outlined oligomerization trends in a scaffold-specific manner, and established binding reactivity patterns facilitating the comprehension of the associated biosynthetic processes. At last, this review illustrates a unique initiative in crafting a comprehensive repository of machine-readable metadata for MIA oligomers that could be leveraged for chemoinformatic purposes.

Équipe, Chimie des Substances Naturelles, Université Paris-Saclay, CNRS, BioCIS, 17 avenue des Sciences, 91400 Orsay, France. E-mail: pierre.le-pogam-alluard@universite-paris-saclay.fr; mehdi.beniddir@universite-paris-saclay.fr

† We dedicate this manuscript to Nicole Kunesch in recognition of her seminal contribution to the classification of MIA oligomers.

‡ Electronic supplementary information (ESI) available. See DOI: https://doi.org/10.1039/d4np00011k

Mehdi A. Beniddir

Mehdi Beniddir is a Full Professor of natural products chemistry at the Faculty of Pharmacy of Paris-Saclay University. He graduated in pharmacy and received his MSc degree from Paris-Sud University in 2009. He obtained his PhD under the guidance of Dr Françoise Guéritte and Dr Marc Litaudon at the Institut de Chimie des Substances Naturelles (ICSN-CNRS) in 2012. He was subsequently a post-doctoral fellow of Prof. Erwan Poupon at Paris-Saclay University. His research interests include the streamlined discovery of intricate natural substances from plants, marine invertebrates, and micro-organisms using prioritization strategies integrating the principles of decision theory to mimic the chemist's intuition in targeting natural substances.

1 Introduction

From an evolutionary standpoint, oligomerization is an energetically economical biosynthetic strategy that nature commonly adopts to generate complex natural product architectures in short order.[1,2] These compounds arise biosynthetically from the union of a monomeric building block with itself or another moiety that, sometimes, does not belong to the genuine oligomer family.

With presumably more than 4000 members, Monoterpene Indole Alkaloids (MIAs) represent one of the most structurally diverse groups of alkaloids. Owing to their hybrid biosynthetic origin and to the inherent reactivity of strictosidine (**1**) (Fig. 1) as their nearly unique precursor and to that of its early derivatives, MIA compounds arise as an impressive array of structural variants disclosing complex, polycyclic scaffolds. This catalogue of intriguing molecules has been tantalizing the interest of both natural product and organic chemists' communities since the 1950s. The diverse bioactivities of many MIAs also contributed to the stern research endeavors geared towards this iconic structural class, now comprising sustained efforts to unveil the biosynthetic gene clusters[3] leading to pharmacologically-relevant structures to secure their supply using engineered hosts.[4–6]

The outstanding chemodiversity of MIAs relies on the oligomerization of monomeric units, using a wealth of different assembly modes to bridge their constitutive components (Fig. 1). Notably, little is known about the biochemical basis of those bridging reactions, despite their high potential. For instance, more than 700 MIA dimers, anhydrovinblastine (**2**) (Fig. 1), a biosynthetic precursor of the anticancer drugs vinblastine (**3**) and vincristine, is the sole oligomer for which the dimerization step has been deciphered.[7] Remarkably, the chemical basis underpinning these associations has not been comprehensively considered so far. As a result of the interest represented by these structures, the topic of bisindole alkaloids has been reviewed four times with three of them being a contribution to different issues of the Alkaloids: Chemistry and Biology series. A first review, published in 1969, reveals a more pronounced emphasis on the dimerization modes of MIAs among the different reviews proposed in the field, although it is limited to asymmetrical dimers and is considered obsolete today due to the number of MIA dimers isolated since this review was published.[8] Since then, three further reviews

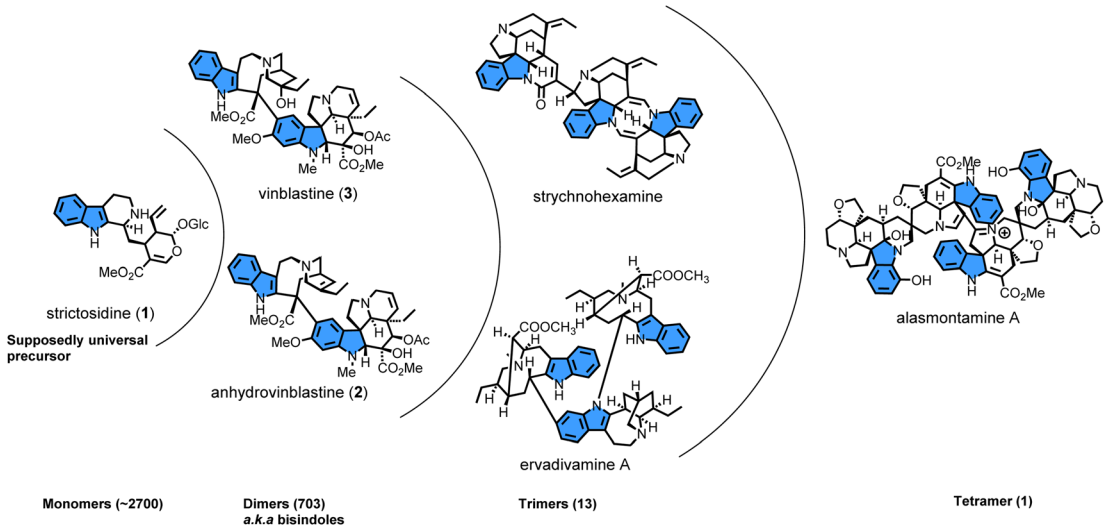

Fig. 1 Overview on MIA oligomers.

have been devoted to updating the diversity of bisindole alkaloids, with varying degrees of emphasis on monoterpene indole alkaloids.[9–11] Thus, all these contributions covered the subject in a similar way but across different periods of time, with an emphasis on the monomeric components and few details regarding the chemical logic underlying their dimerization.

In stark contrast with these former contributions, this review aims to draw a parallel between all known MIA oligomers by illustrating the chemical logic underlying their assembly. For this purpose, oligomeric MIAs will first be classified according to the connections instigated between their monomeric components. At this level, a distinction is envisaged between compounds with a single intermonomeric connectivity and those with two or more intermonomeric connectivities. A further benefit of this review will be the ability to establish the dominant patterns of heterodimeric MIAs, which were only considered in Szabó's 2008 review (Scheme 10),[12] but on a limited set of compounds and with a limited structural accuracy. Outlining these dimerization trends in a scaffold-specific manner established binding reactivity patterns and facilitated the comprehension of the associated biosynthetic processes.

Additionally, our bibliographic survey also covered pseudodimeric structures (*viz.* combining both a MIA and either a tryptamine or an iridoid unit) and even hybrid structures including both a MIA and a biosynthetically unrelated partner insofar as these latter often capitalize on the same reactivity logic (Fig. 2). Although the partners likely to couple with MIAs have therefore been considered very broadly, we have adhered to a strict biosynthetic definition of the notion of MIA, limiting ourselves to molecules derived from strictosidine, as the supposedly universal precursor of all members of this phytochemical class.[13] Interested readers are referred to a specialized literature for further insight into such tryptamine–iridoid alkaloids, obtained apart from the canonical strictosidine pathway.[14,15]

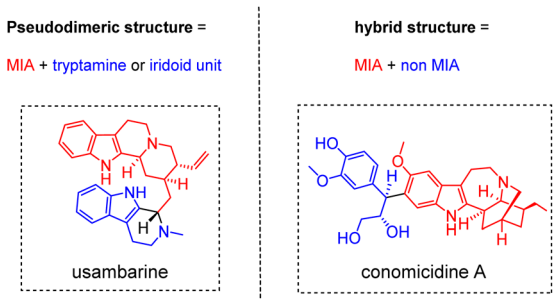

Fig. 2 Examples of pseudodimeric and hybrid structures.

2 Comprehensive analysis of oligomeric MIA chemical space

2.1 Mining monoterpene indole alkaloid oligomers literature

The comprehensive listing of the impressive number of MIA oligomers required extensive database explorations, including Reaxys, SciFinder Scholar, and the Dictionary of Natural Products. Initially, the four above mentioned reviews were merged and used as a starting point. Next, well-tailored structural queries, based on constitutive generic skeletons, (See ESI‡) allowed for the completion of this review effort. To the best of our knowledge, the latest attempt to document the basic MIA scaffolds can be found in the Dictionary of Alkaloids where 42 skeletons had been distinguished. Building upon this effort, 78 additional skeletons were identified, defined structurally (see ESI‡) and used to chart the MIA oligomers listing. Ultimately, an up-to-date, metadata-enriched comprehensive listing of more than 950 MIA oligomers was obtained (see ESI‡) and organized according to the skeleton names of the constitutive monomers and the bridging sites. Notably, this listing has been uploaded to LOTUS[16] to share this knowledge with the community.

2.2 MIA oligomers statistics

The data gathered in the MIA oligomer listing allowed, for the first time, the drawing of a global interconnection landscape for this family of natural products. As such, an oligomer network (Fig. 3) was crafted from this data and interesting statistics were obtained. As of 2024, 703 dimers, 13 trimers and only one tetramer have been reported. Accordingly, the 703 known dimers seem to be dominated by 25 MIA skeletons. Some MIA subtypes are notably prevalent to capture the diversity of MIA dimers with no less than 222 such compounds comprising an aspidospermane unit, 187 molecules containing a vobasane unit and 162 revealing an ibogane-type component. The predominance of aspidospermane is in fact even greater than it may seem at first glance since almost half of aspidospermane-comprising MIA dimers are of the bis-aspidospermane subtype (102 entries), whereas bis-vobasane and bis-ibogane type dimers are far less represented (7 and 6 entries, respectively). Other prevalent contributors to the chemical space of MIA dimers include macrolane-based compounds (67 macrolane units in strict MIA dimers), eburnane (46 such compounds), corynantheane (42 entries) and pleiocarpamane (39 strict MIA dimers). It is interesting to note that this predominance of MIA scaffolds is also encountered to some extent for trimers and the unique tetramer with the aspidospermane scaffold vastly dominating this chemical space (20 units out of 43 building blocks when considering all 13 trimers and alasmontamine (A) followed by the vobasane unit (8 monomers out of 43)). One hundred pseudodimers have been identified in the literature, two-thirds of them incorporating a second tryptamine unit (74 entries). A huge majority of compounds comprising an additional tryptamine unit derive from a corynantheane-type MIA (70) with the few others being related to vobasane-type MIAs. The 26 pseudodimers featuring an additional iridoid unit are mostly found in *Gelsemium*-type scaffolds (mainly gelsedane and humanteninane) and, to a lesser extent, are associated with a few aspidospermane or strictosidine-type MIAs. To complete this overview, an array of extraneous units that have been involved in interunit connections were unveiled during our literature survey, including methylene group,[18] urea group,[19] acetonic group,[20] pyrocatechuic group,[21] thioether bridge,[22,23] sugars[24] or in the diversification of MIAs through the incorporation of unrelated biosynthetic units such as various products related to the shikimic acid pathways,[25,26] gallic acid derivatives,[27,28] anthranilic acids[29] derivatives; (104 entries), flavonoids (6 compounds), canthinones (8 compounds) and various other miscellaneous products. Before getting to the heart of the matter, we feel it is important to mention that some MIA skeletons incorporate a biosynthetic element other than tryptamine and secologanin in their core constitution. O'Connor's[30] recent elucidation of the biosynthetic pathways of strychnine demonstrated that this scaffold relies on the incorporation of a malonyl-CoA unit, which had been assumed for nearly 60 years on the basis of chemical reactivity considerations and radiolabelling studies.[31,32]

3 Intermonomeric connection analysis in oligomeric MIAs

During our bibliographic survey, it became apparent that many oligomerization sequences were, in some way, stringently associated with the biosynthesis of strict MIA dimers, whereas some others are geared towards the incorporation of alternative biosynthetic units. To highlight these considerations,

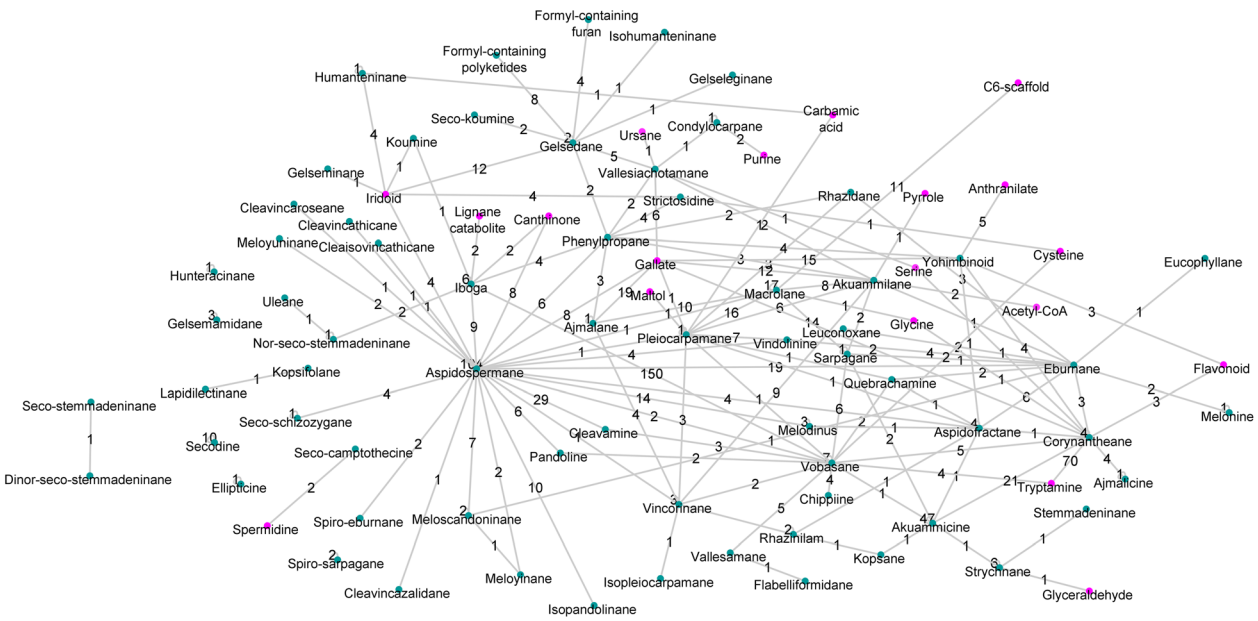

Fig. 3 MIA oligomer network (trimers and tetramer are excluded) generated with Cytoscape 3.8.0.[17] Self-loops refer to dimers comprising two components having the same MIA skeleton. Numbers on the edges define the number of oligomers pertaining to specific skeletons. Purple nodes are non-MIA counterparts. A machine-readable version of this figure is accessible as a ESI.‡

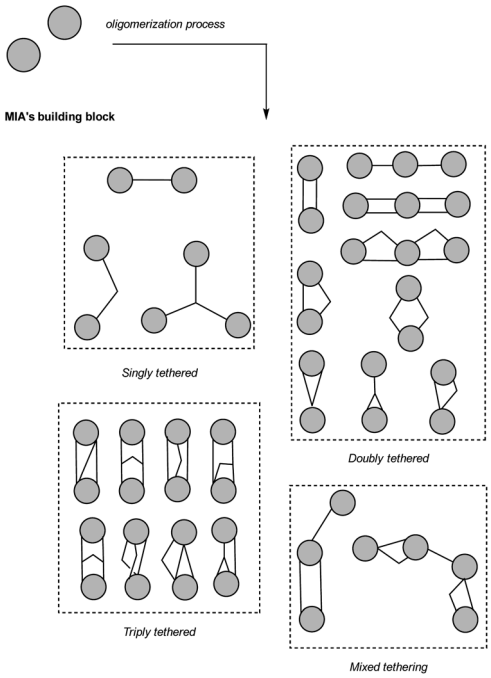

Fig. 4 Overview of reported bridging modes in MIA oligomers.

a comprehensive list of simplified models of all MIA skeletons is provided as a ESI‡ indicating bridging sites and involved coupling partners (S1, ESI‡). Moreover, to follow the logic of this review, a reactivity table is also provided as a ESI (S2, ESI‡). This table classifies all[33] of the MIA oligomers covered by our study according to the putative sequence of reactivity that led to their final scaffold with a distinct colour code to instantly highlight their gross constitution (*viz.* strict MIA constitution, pseudodimer with additional tryptamine unit, pseudodimer with additional iridoid unit, MIA with extraneous phenylpropanoid or gallate unit (*sensu lato*) and MIA with various other units). Inspired by the first classification system proposed by Kunesch *et al.*[8] for monoterpene bisindole alkaloids in 1969, a deep analysis of the wealth of the MIA oligomers led us to classify this fascinating family according to the number of bridges instigated between the constituting units (single, double, triple, and mixed tethering) as illustrated in Fig. 4. Then, in each tethering mode, some cornerstone oligomers were addressed to illustrate a unique chemical logic or a combination of assembly reactions (See S2, ESI‡, for a comprehensive list of MIA related to a chemical logic). To make it easier for readers to follow the numbering system used in this review, we have decided to use the Le Men and Taylor MIA biosynthetic numbering.[34] This section will detail the above-mentioned assembly reactions.

3.1 Singly-tethered oligomers

A retro-oligomerization analysis conducted on the singly-tethered MIA oligomers revealed the implication of four assembly mechanisms.

3.1.1 Electrophilic aromatic substitution-driven oligomerization. Considering the resonance contributors related to the indolic system found in most MIAs reveals that all non-bridgehead carbons can serve as a functional carbanion equivalent to trigger nucleophilic attack.[35,36] The presence of *ortho*-oxygenated functionality at the site triggering the nucleophilic attack is often encountered, but it is not a strict structural requirement. Conversely, indoline-containing MIA subtypes are prone to instigating nucleophilic attack involving their electron-rich C-10 and/or C-12 sites. For this reactivity, seven types of electrophilic motifs will be covered.

3.1.1.1 Indoleninium and quinone methide. The electrophilic nature of vobasinol C-3 provides an explanation for the wealth of MIA dimers disclosing a 3-vobasinyl residue. Indeed, a vast array of MIA subtypes are known to react with this monomer, in a seemingly indistinct manner. Our literature survey indicated that no less than 150 vobasane-ibogane (Fig. 1, see S2, ESI‡) dimers have been reported to date, all of which derive from a conjugate 1,6-addition on the electrophilic C-3 position of the vobasane scaffold, with the possibility of involving additional reactions in the context of more sophisticated coupling strategies. This mere reactivity scheme is illustrated through the examples of the vallesamane/vobasane-type pseudovobparicine (**4**)[37] and the recently reported vobasane/tryptamine pseudodimer pyrrovobasine (**5**) (Fig. 5).[38] This reactivity is highly predominant when considering the vobasane building block as a whole since vobasane-comprising dimers involving akuammicine (1 entry), aspidospermane (2 entries), sarpagane (5 entries), vallesamane (5 entries), vincorinane (2 entries) and bis-vobasane dimers (7 entries) use its C-3 position as an electrophilic center, even though a few of them instigate partner-dependent multiple connections as will be developed later on. Quite remarkably, it seems that only the recently described

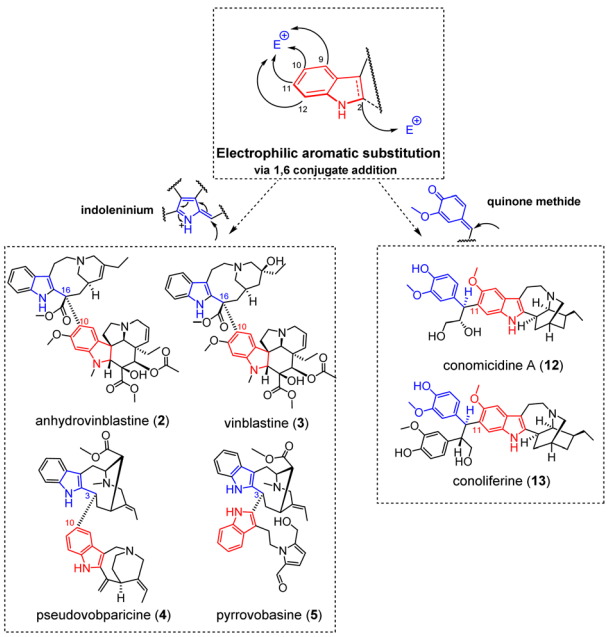

Fig. 5 Singly-tethered oligomers resulting from an electrophilic aromatic substitution on an indoleninium (by 1,6-conjugate addition) or a quinone methide. Note that cleavamine-derived scaffolds resulting from this reactivity are outlined in Fig. 6.

ligustrinine (**114**) (Fig. 35) enters a dimerization process that does not involve the vobasinyl electrophilic C-3 position.

The aspidospermane/cleavamine-type, exemplified by the illustrious anticancer agents vinblastine (**3**) and vincristine, are presumed to be obtained following a related biosynthetic scenario, although this implies more preliminary rearrangements to install a reactive indoleninium moiety compared with vobasinyl-comprising dimers. An oxidase or peroxidase-mediated oxidation of an ibogane-type MIA would first avail a 7-hydroperoxyindolenine intermediate (Fig. 6). Different oxidation mechanisms have been proposed for this purpose, involving either a radicalar mechanism (darkness, triplet oxygen) or a ionic mechanism (light, singlet oxygen).[39] The easy elimination of this peroxy group is inferred to initiate a rearrangement of the ibogane scaffold to both disrupt the C-16–C-21 bond and establish a $\Delta^{2,16}$ function, thereby installing a reactive indoleninium moiety as outlined in Fig. 5. This structural motif is easily amenable to an electrophilic aromatic substitution involving the C-10 site of the aspidospermane-type vindoline unit on the C-16 site of the cleavamine unit *via* 1,6-addition, instigating the canonical C-10–C-16 connectivity, represented by 29 natural derivatives.[40] This bridging mode largely dominates the diversity of cleavamine-comprising MIA dimers reported to date, especially when having in mind that further structures are presumed to derive from these MIA dimers through rearrangement of their cleavamine unit. Most rearrangements affecting the cleavamine component were reported to proceed from derivatives bearing a 15–20 epoxide function. Transannular cyclizations could then occur to create either a 7–15 or a 7–20 bond to yield either vincathicine (**6**) or the recently reported isovincathicine (**7**) (Fig. 6).[41] As per vincathicine (**6**), this biosynthetic path has been experimentally validated from leurosine (**8**).[42,43] A last unique example of MIA dimer stemming from this intermediate is roseadine (**9**).[44] Again, this scaffold would require a 15–20-epoxycleavamine derivative to undertake an alternative 2–15 transannular cyclization. Rearomatization of the indolic system through fragmentation of the C-2–C-16 bond and simultaneous installment of the $\Delta^{16,17}$ double bond would then avail roseadine (**9**). Very recently, vincazalidine A (**10**)[45] was reported as a new MIA dimer from *Catharanthus roseus*, apparently corresponding to a new rearrangement of the cleavamine subunit of leurosine (**8**). This rearrangement would result from an unprecedented mechanism initiated by the heteronucleophilic attack of the alicyclic nitrogen N-4 onto the carbonylic position of the methylester moiety at C-22 to install a remarkable site being simultaneously connected to a charged nitrogen atom and to two oxygenated functionalities (a methylether and an alcohol). The newly obtained alcohol group at C-22 could then undertake an heteronucleophilic attack at the C-20 epoxidated site to afford the final, *trans*-diol containing vincazalidine A (**10**).[45] The most obvious biosynthetic derivatives of cleavamine/aspidospermane dimers are pandoline/aspidospermane type dimers (6 such products are described that also disclose a C-10 to C-16 connection). These compounds were found to co-occur in *Catharanthus* species, further supporting the hypothesis of a biosynthetic interrelationship.[46] Oxidation-based sequences have been supported by various organic chemistry reports,[42,47] apparently involving nucleophilic attack of the indolic $\Delta^{2,7}$ enamine on a $\Delta^{3,4}$ iminium functionality to install the additional C-3–C-7 connectivity, also accounting for the indolenine status of the pandoline component as in cycloleurosine (**11**).[46] To provide a complete overview of cleavamine reactivity, the occurrence of MIA dimers disclosing other connections should be pointed out. Firstly, three vobasane/cleavamine dimers, capuvosine and its derivatives,[48] involve an aromatic electrophilic substitution of cleavamine C-11 on the C-3 electrophilic position of a vobasane residue, bypassing the usual cleavamine-driven reactivity to follow the expected reaction with a vobasane-like residue, as outlined at the beginning of this section. Analogous pandoline/aspidospermane dimers have been described from the same plant source (capuvosidine).[49] Remarkably, one sole monomeric cleavamine seems to be known to date: capuronine.[49] Conversely, pandoline-type MIAs often occur as monomeric MIAs. Quite remarkably, monomeric pandolines are not supposed to arise from an aspidospermane precursor as described earlier but would instead be based on a Diels–Alder reaction proceeding from a *seco*-stemmadeninane precursor.[50] As a consequence, monomeric pandolines display a $\Delta^{2,16}$

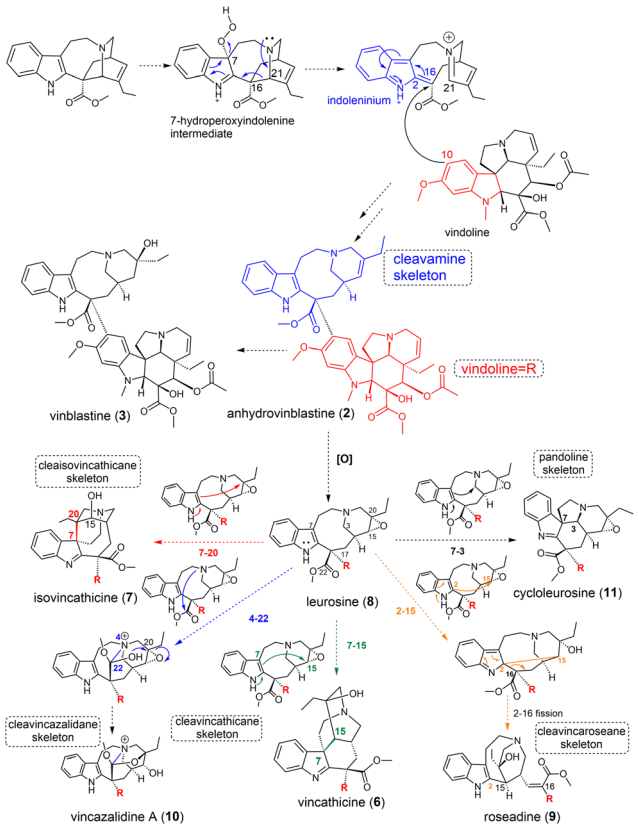

Fig. 6 Proposed biosynthetic path to cleavamine-containing MIA dimers and possible rearrangements into cleavamine-derived MIA subtypes. Note that most of the derived scaffolds (cleaisovincathicane, cleavincathicane, cleavincaroseane and cleavincazalidane) are exclusive to the dimeric condition and are all known so far from a unique compound.

function[51] instead of an indolenine nucleus as it appears in dimeric MIAs such as cycloleurosine (**11**).

Unsurprisingly, the cleavamine-derived cleavincathicane/cleaisovincathicane/cleavincarosean/cleavincazalidane have not been identified as monomeric MIAs to date. Finally, 1,6-additions may be directed towards coniferyl/*p*-coumaryl alcohol-derived quinone methides (Fig. 5), availing hybrid MIA/hydroxycinnamyl conjugates such as conomicidines A (**12**) and B,[52] or towards a lignan-derived quinone methide to provide conoliferine (**13**) and isoconoliferine.[53]

3.1.1.2 Iminium. A large number of MIA dimers are obtained through a coupling of indolic sites to the C-16 position of an eburnane residue (see S1, ESI‡) as in the eburnane/aspidofractane-type pleiomutine (**14**) (Fig. 7).[54] Such dimers arise as a consequence of a nucleophilic attack on a C-16 carbinolamine/$\Delta^{1,16}$ iminium and account for the constitution of an important number of MIA dimers (more than 40 entries). The electrophilicity of eburnane C-16 position is a key to understand the constitution of most eburnane-containing dimers, although a few of them instigate several connections in the end. This logic also extends to the eburnane-like constitution of the meloyuninane subtype, accounting for the C-10–C-16 connection appearing in angustifonines A (**15**)[55] (Fig. 7) and B. It seems that only one eburnane-containing dimer, namely vobtusamine (**124**)[56] (Fig. 37), does not involve the eburnane C-16 position. In a vast majority of cases, the nucleophilic attack is triggered by aromatic sites of the other MIA component. Biomimetic strategies have been undertaken to access such derivatives, sometimes failing to reach the sought-after dimeric structure as in the example of leucophyllidine (**16**)[57] (Fig. 7) where a regioisomer had been obtained instead (disclosing a C-12–C-16 connectivity instead of the awaited C-10–C-16 bonding).[58] A parallel can easily be drawn with the pseudodimeric structures of bonafousine (**17**)[59] (Fig. 7)/isobonafousine associating an ibogane subunit to a building block of as yet unknown biogenetic origin, somehow evocative of a tetracyclic eburnane analogue. The α-oxygenated C-12 position of the ibogane subunit could trigger a nucleophilic attack on an iminium involving any of the two nitrogen atoms of the structure to afford these isomers. Notably, this reactivity involving an electrophilic aromatic substitution and an iminium is part of a much wider ensemble and can account for the constitution of many MIA dimers, spanning across a considerable number of scaffolds. A few illustrations of structurally diverse MIA dimers arising from this reactivity are given in Fig. 3. For example, plumocraline (**18**) (Fig. 7) relies on the C-10-triggered electrophilic aromatic substitution of an akuammilane component on a $\Delta^{1,2}$ indoleninium-containing pleiocarpamane. Some dimers are supposed to arise from electrophilic aromatic substitution on iminium ions involving the alicyclic nitrogen.[60] As such, criophylline (**19**)[61–63] (Fig. 7) involves a $\Delta^{3,4}$ iminium moiety of the aspidospermane-type pachysiphine being attacked by the C-10 position of a *seco*-schizozygane-type andrangine subunit. Melosuavine C (**20**)[64] (Fig. 7) seemingly relies on the electrophilic aromatic substitution of the C-10 site of an aspidospermane unit on a $\Delta^{4,5}$ iminium-containing Melodinus-type monomer whereas uncaramine (**21**)[65] (Fig. 7) and callophyllines[66] derive from a $\Delta^{4,21}$ iminium-containing yohimbinoid unit. Structural oddities may rely on similar reactivities from different substrates. The partner initiating the nucleophilic attack may be structurally different at first. One such example is the electrophilic aromatic substitution triggered by a flavonoid aromatic position on a $\Delta^{4,21}$-containing corynantheane in epicatechocorynantheine A (**22**) (Fig. 7),[67] a reactivity also stepping in the biosynthesis of further rubiaceous flavoalkaloids known as uncariagambiriines.[68,69] Another possibility is that of an alternative iminium-containing structure as the electrophilic partner, as observed in the case of the aspidospermane-containing melofusinine A (**23**) (Fig. 7),[70] that involves the $\Delta^{1,2}$ iminium function of nitrogenated iridoid unit.

The unique C-2–C-10 tethering encountered in the bis-aspidospermane scaffold of tabernaebovine (**24**) (Fig. 7) deserves to be developed in the context of electrophilic aromatic substitution.[71] Plausible mechanisms to provide this unique connectivity rely on conjugate nucleophilic additions from C-10 to a *N*-methylquebrachamine half. A 21-keto-containing quebrachamine unit had been selected by Movassaghi to reach tabernaebovine scaffold.[72] A $\Delta^{4,21}$ quebrachamine iminium can also be envisaged to afford the ring closure leading to the bis-aspidospermane constitution of the second aspidospermane unit. Finally, an indoleninium-type aspidospermane scaffold cannot be ruled out either.

3.1.1.3 α,β-Unsaturated carbonyl and imine. This category of electrophilic motifs is associated with more stringent structural requirements and is therefore associated with a limited set of MIA subtypes. As such, the monoterpenic component of macrolane-type MIAs is prone to different scaffold-specific electrophilic aromatic substitutions. This scaffold name derives from macroline, a key entry to macrolane-based MIA dimers,

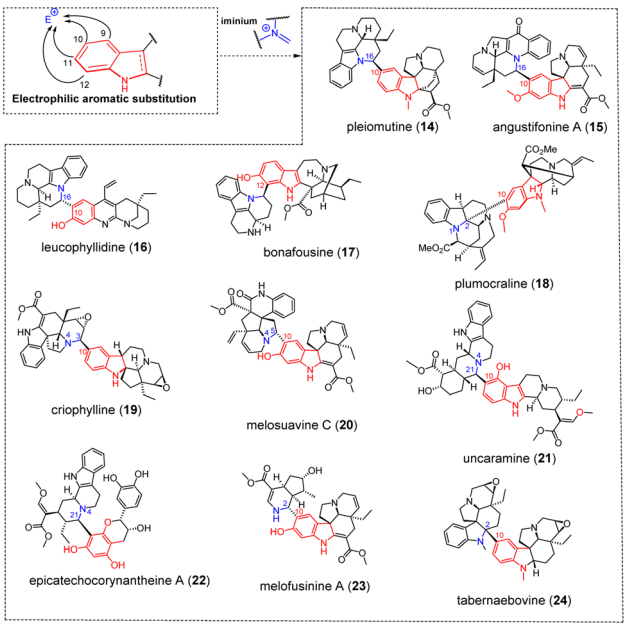

Fig. 7 Singly-tethered oligomers resulting from an electrophilic aromatic substitution on an iminium.

comprising a highly reactive α,β-unsaturated carbonylic group. Its characteristic constitution had been suggested to be biosynthetically related to sarpagane-type MIAs and notably comprises two distinct forms which can be rationalized with regards to a freely-rotatable, open dialdehydic intermediate.[73] An etherification occurring between an oxygenated substituent at C-19 and the –CH_2OH group leads to the so-called type-A macroline (*e.g.* macroline) whereas a similar reaction involving an oxygenated substituent at C-21 and the same –CH_2OH moiety rather leads to a type-B macroline (*e.g.* ring E *seco*-talcarpine) (Fig. 8).[74] It can be noted that macroline itself does not seem to have been isolated yet as a natural product so that it only exists as a putative biosynthetic cornerstone towards dimeric MIAs. Notably, macroline has a limited shelf life as it spontaneously cyclizes into the more stable dihydroalstonerine.[75] A 1,4-Michael addition on the C-21 position of the enone group of a type A-macroline supposedly gives access to perhentinine-type MIA dimers that may undertake subsequent hemiketalization to afford alstomacrophylline (**25**)-type derivatives (Fig. 9),[76] featuring a diagnostic connection between an aromatic site of the MIA partner initiating the electrophilic aromatic substitution and the macrolane C-21 site. A type B macroline reactive unit reveals an alternative, α,β-unsaturated aldehyde-based Michael acceptor granting access to angustilongine A (**26**)-type dimers (Fig. 9). This second classical type of macrolane-based MIA dimers discloses a connection between an aromatic site and macrolane position C-19. One can note that an alternative mechanism has been proposed for the coupling of ring A-oxygenated macroline-type alkaloids, based on a Friedel–Crafts alkylation process stabilized by an oxonium ion.[75]

The monoterpenic component of the akuammicine scaffold is associated with a specific reactivity giving rise to specific singly and doubly-tethered MIA dimers when it reveals an exomethylene–indolenine conjugate susceptible to nucleophilic attacks. Such oligomers comprise the kopsane/akuammicine-type arbolodinine C (**27**) that derives from an electrophilic aromatic substitution triggered by the C-10 site of the kopsane subunit on the electrophilic C-22 exomethylenic position of the akuammicine component (Fig. 9).[77]

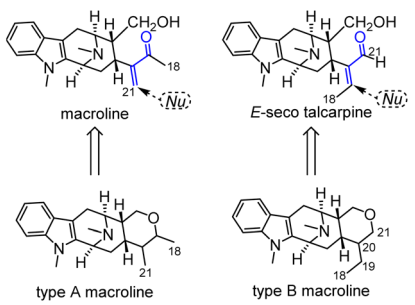

Fig. 8 Structural features of interest to decipher the dimerization trends of macrolanes and scaffolds of the so-called types A and B macrolanes. Electrophilic sites are highlighted in blue for both scaffold subtypes. Note that anhydromacrosalhine methine, a key nucleophilic partner for the dimerization of some macrolanes, differs from the gross structure given to type B macroline by the existence of two unsaturations (*viz.* $\Delta^{18,19}$ and $\Delta^{20,21}$).

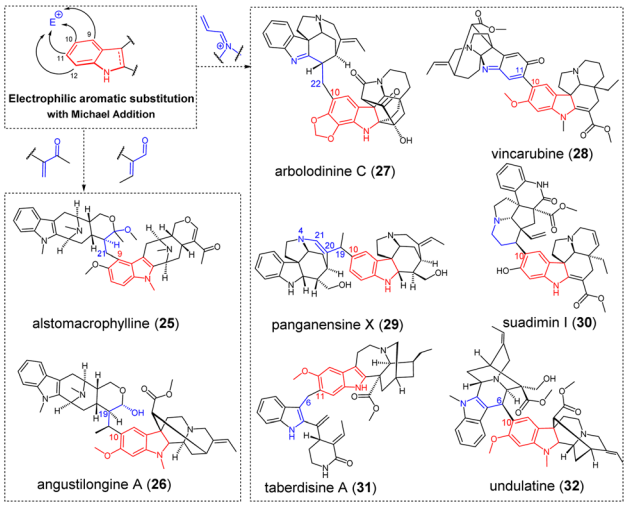

Fig. 9 Singly-tethered oligomers resulting from an electrophilic aromatic substitution on an α,β-unsaturated carbonyle or imine.

Dimeric MIAs featuring diaryl connections are often presumed to derive from a radical coupling and, as such, the topic will be mostly covered in the next section. A dozen compounds link the C-10 position of an indoline-containing MIA, a nucleophilic site of great generality, to a recurring C-11 position of a vincorinane component featuring a constant α-oxygenated functionality. An oxidative coupling has been proposed to step in the dimerization of such compounds, without much detail (see next section for further discussion).[78] Alternatively, an indolenine-containing akuammilane could install an electrophilic quinone-imine. This hypothesis is supported by the occurrence of quinone-imine containing dimers (*e.g.* vincarubine (**28**),[59] rausutrine, rausutranine[79]).

Bis-akuammicine dimers also comprise very unusual connectivities involving their ethylidenic/ethylic side chain. As such, panganensines X/Y (**29**)[80] feature a C-10 to C-19 connection. While the C-10 position is a very common nucleophilic site, a $\Delta^{19,20}$ conjugated-$\Delta^{4,21}$ iminium can be proposed to account for C-19 electrophilicity that is prone to undergo a 1,4-Michael addition. A similar mechanism has been proposed to incorporate a third nitrogen during the biosynthesis of arboflorine.[81] Likewise, a conjugated iminium-type electrophilic partner probably steps in the biosynthesis of suadimin I (**30**).[82] A related mechanism involving a conjugated indoleninium as the electrophilic moiety can account for the C-6–C-11 connectivity appearing in the *nor-seco*-stemmadeninane/ibogane taberdisines A (**31**)-B (Fig. 9).[83] Finally, a unique intermonomeric connection appears in undulatine (**32**).[84] While the C-10 position of the akuammilane component acts as a classical electron-rich partner, the involvement of the C-6 position of the sarpagane unit as a nucleophilic site is highly unusual. Here again, an α,β-unsaturated indoleninium system could explain the electrophilicity of C-6. Alternatively, it was suggested that the coupling reaction should proceed from a 6-hydroxylated sarpagane derivative (6-hydroxylated sarpagane[85] analogues had seldom been described). An hemisynthetic investigation using

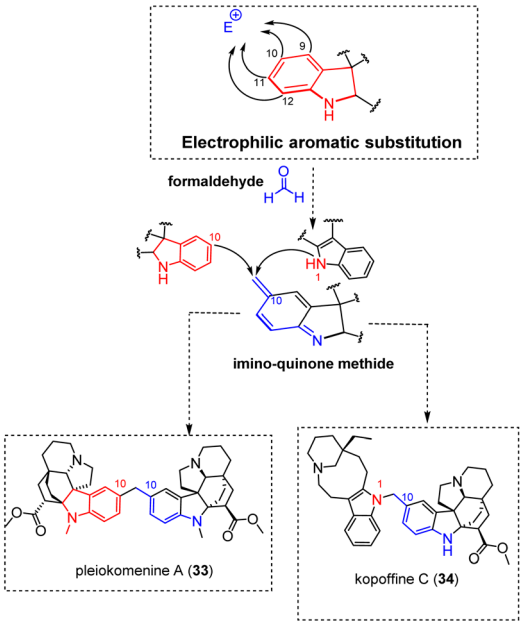

Fig. 10 Putative biosynthetic path to singly-tethered methylene-bridged MIA dimers.

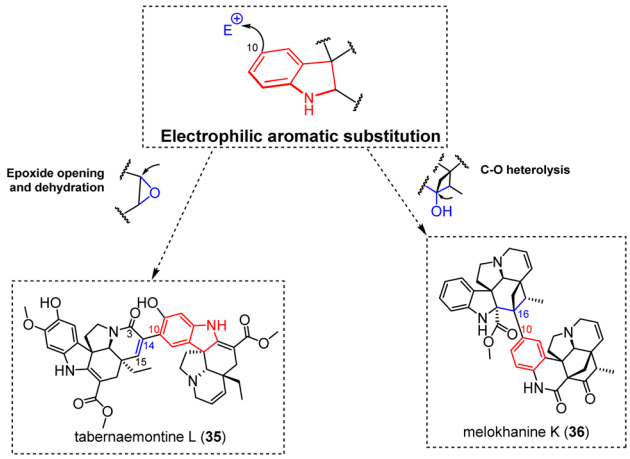

Fig. 11 Singly-tethered oligomers resulting from an electrophilic aromatic substitution on an epoxide or a carbocation.

DDQ as a coupling agent gave support to this putative reactivity.[86]

3.1.1.4 Formaldehyde. As stated in Section 2.2, extraneous units such as formaldehyde have been involved as the electrophilic partner in such reactions, as exemplified by pleiokomenine A (**33**) and kopoffine C (**34**) (Fig. 10), among many others. Such a reaction has been proposed to provide a *para* iminoquinone methide moiety that could further be prone to undergoing different kinds of nucleophilic attack. As per pleiokomenine A (**33**), the electron-rich C-10 site of an additional aspidofractane unit is presumed to trigger this electrophilic aromatic substitution.[18] Kopoffine C (**34**) seems to arise as a consequence of an heteronucleophilic attack instigated by the N-1 nitrogen of the quebrachamine unit on a similar *para* iminoquinone methide of the aspidofractane counterpart.[87] Methylene-bridged dimeric natural products as a whole have been recently reviewed.[88]

3.1.1.5 Epoxide-ring opening and nucleophilic attacks towards a hydroxylated site. The recently reported bis-aspidospermane-type tabernaemontine L (**35**) (Fig. 11) appears to reveal a unique example of connectivity among electrophilic aromatic substitution-driven and singly-tethered MIA dimers.[89] Although unique, the C-10–C-14 connection appearing in this dimer is relatable to an electrophilic aromatic substitution targeting the C-14 position of a 14,15-epoxide-containing aspidospermane unit. Subsequent dehydration could then install the $\Delta^{14,15}$ functionality appearing in tabernaemontine L (**35**). From a biosynthetic point of view, this dimerization mechanism is supported by the known presence of such 3-oxo-14,15-epoxide-containing aspidospermanes,[90,91] and analogous building blocks are proposed to step in the biosynthesis of various aspidospermane-based doubly-tethered dimers (*e.g.* conophylline (**90**)) and trimers (*e.g.* taberdivarine A (**91**)) (Fig. 25), as discussed in more detail below. The meloscandoninane-meloyinane type melokhanine K (**36**)[92] represents a markedly different situation (Fig. 11). Its intermonomeric connectivity implies an electrophilic aromatic substitution into the meloyinane C-16 position. For this purpose, the C-16 hydroxylated monomeric precursor was reported from a plant pertaining to the same genus a few years ago, namely meloyine A.[93] Even though the hydroxy group is not generally accepted as a good leaving group *per se*, an array of different hydroxy activation strategies has been reported to step in natural products biosynthesis.

3.1.2 Radical coupling-driven oligomerization. Most MIA dimers resulting from radical coupling involve the establishment of connections between the benzene rings of the indole/indoline systems, the regioselectivity of which is often directed by the *ortho*-occurrence of oxygenated functionalities. As these binding sites are poorly influenced by the nature of the monoterpenic component, scaffold-specific bridging modes are rather uncommon within this specific kind of dimeric MIAs. An array of dimeric MIAs disclosed in Fig. 12–15 illustrates these different possibilities.

3.1.2.1 Ortho–ortho diphenol and O-ortho phenol coupling products. The 9,9-bonded bis-ibogane type pendulifloramine (**37**),[94] the 11,12-bonded aspidospermane-ibogane type tetrastachynine (**38**),[95] the 10,10-bonded bis-aspidospermane type *N*-acetyl-16,17-dihydroxyaspidospermidine (**39**)[96] and the 9,12-bonded bis-hunteracinane type blumeanine (**40**) are canonical *ortho–ortho* phenolic oxidative coupling products (Fig. 12). Notably, the *O*/*ortho* regioisomer of tetrastachynine (**38**), namely tetrastachyne (**41**), was co-isolated with it.[95] Such MIA dimers appear to be very unusual, although a closely related analogue was later isolated.[97]

The connection mode of the bis-sarpagane-type dispegatrine (**42**)[98] is consistent with a canonical *ortho–ortho* phenolic oxidative coupling. Nevertheless, the phenolic oxidative coupling of its monomeric component, spegatrine, could provide dispegatrine (**42**), but with a very modest yield of 0.25%. Conversely, Cook *et al.* were able to complete the synthesis of

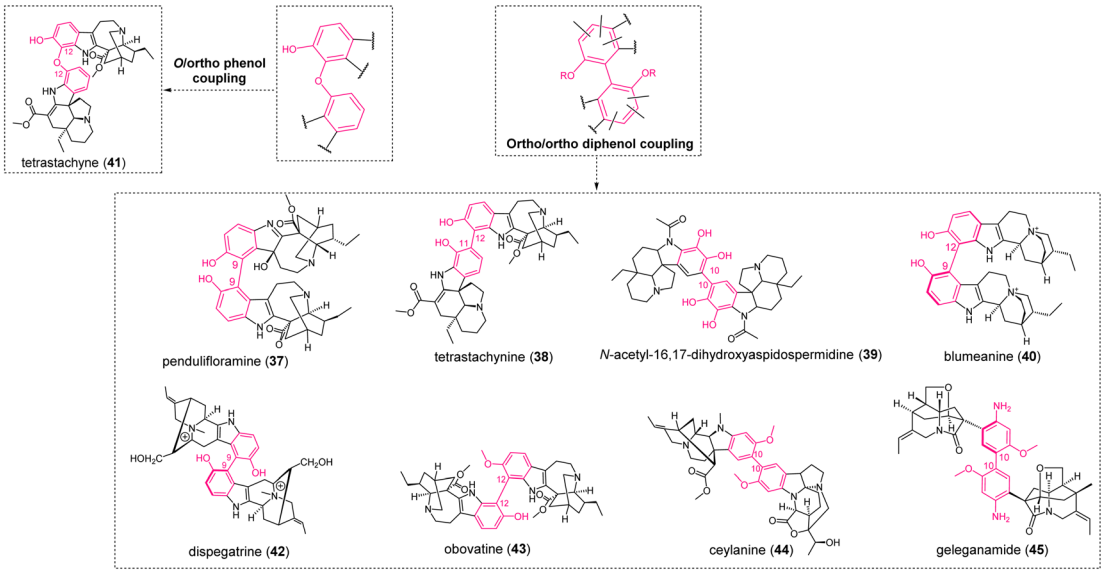

Fig. 12 Singly-tethered oligomers resulting from *ortho*/*ortho* diphenol coupling and *O*/*ortho* phenol coupling. Color coding has been added for clarity but it does not indicate any chemical sense.

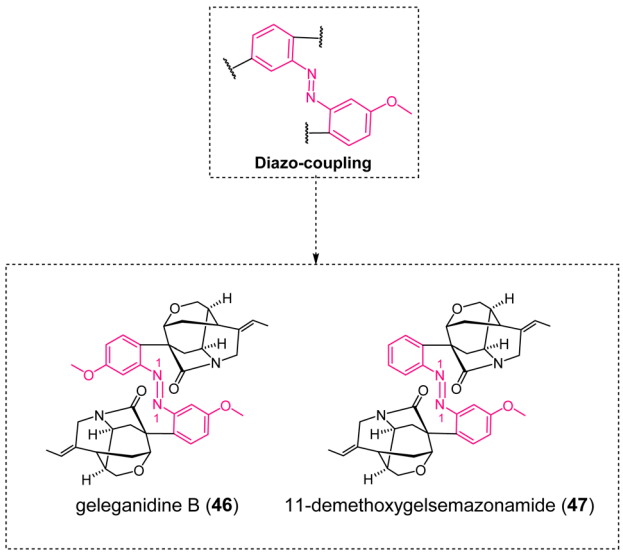

Fig. 13 Singly-tethered oligomers resulting from diazo-coupling. Color coding has been added for clarity but it does not indicate any chemical sense.

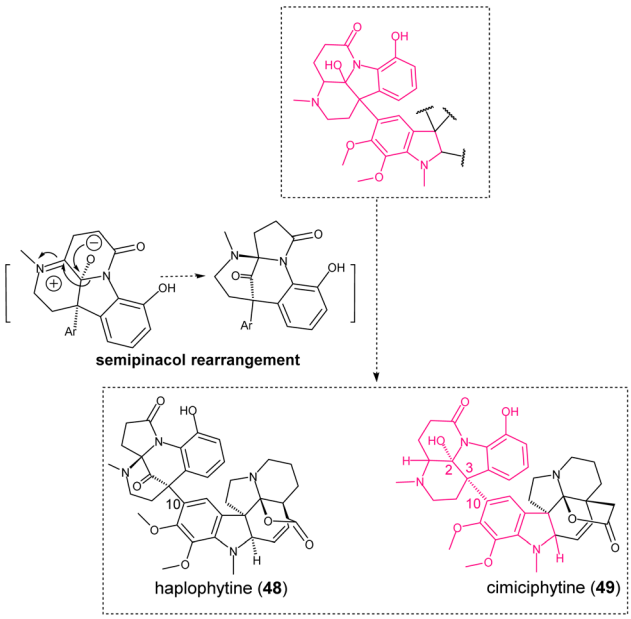

Fig. 14 Singly-tethered haplophyton alkaloids. Color coding has been added for clarity but it does not indicate any chemical sense.

dispegatrine (**42**) with a much higher yield using a non-phenolic oxidative dimerization process.[99] Intermolecular non-phenolic oxidative dimerizations of complex aryl substrates are known to be very rare but is documented for some indolic substrates.[100] Notably, the formation of a single atropodiastereomer during Cook synthesis could finalize the structure assignment of dispegatrine (**42**) as its axial chirality had been overlooked in the original phytochemical report. The *P*-configuration of dispegatrine (**42**) biaryl axis would be related to an internal asymmetric induction originating from the steric hindrance related to the sarpagane cage-like structure.[99] A few analogues reveal a biaryl junction contiguous to other oxygenated functionalities. One such example is the 12,12-bonded bis-ibogane-type obovatine (**43**),[101] where the *ortho*-arranged substituents to the biaryl axis are a phenol and a methoxy group. In this context, it can be envisaged that the methoxylation occurs after the dimerization process. This assumption is further supported by the co-isolation of its diphenolic analogue, namely bis[11-hydroxycoronaridinyl-12-yl].[101] More generally speaking, such biosynthetic assumptions (methoxylation after coupling) have received support from biosynthetic investigations carried out

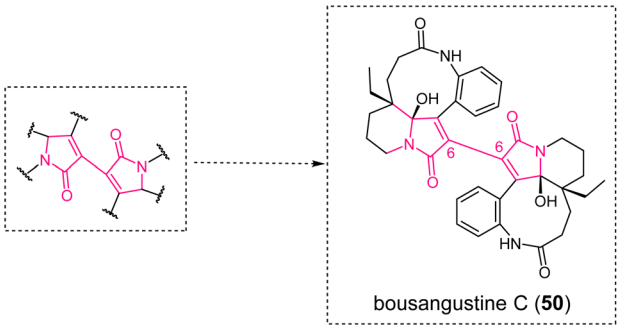

Fig. 15 Singly-tethered leuconolam-derived dimers. Color coding has been added for clarity but it does not indicate any chemical sense.

on fungal dimeric polyketides deriving from oxidative phenolic coupling.[102] Likewise, the vincorinane/isopleiocarpamane-type ceylanine (**44**)[103] or the bis-vincorinane-type peceylanine feature two methoxy groups being *ortho*-disposed to the biaryl connection, these methoxylations presumably occurring after dimerization. Again, this hypothesis is supported by the co-isolation of related dimers disclosing a furanic connection (*e.g.* peceyline (**153**)) that suppose the existence of dimeric intermediates revealing phenolic groups instead of the methoxy groups finally appearing in ceylanine (**44**) and peceylanine (see Fig. 49 for doubly-tethered oligomers resulting from radical coupling). Similarly, the spectroscopic data of geleganamide (**45**) indicated a dimeric structure of two gelsemamidane-type MIA alkaloids connected through a C-10–C-10 bond.[104] A possible biogenetic access to this compound could also benefit from an amino radical. Such a rare substituent for a MIA tryptaminic benzene originates from the hydrolytic cleavage of the indolic pyrrole, as sometimes observed for gelsedane-type MIAs.[105,106] An amino-derived radical could result in a spin density at the *para*-amino C-10 position, accounting for the intermonomeric connectivity of geleganamide (**45**).[107]

3.1.2.2 Diazo-coupled MIA dimers. Alternatively, such secondary amine-containing gelsemamidane-type MIAs can lead to aromatic azo compounds such as geleganidine B (**46**)[19] and 11-demethoxygelsemazonamide (**47**) (Fig. 13).[106] Although corroborated by several reactivity reports dealing with structurally diverse aniline derivatives,[108] natural azo products are extremely rare. Prior to geleganidine B (**46**), it seems that only one natural azo compound had been reported (from the macromycete *Agaricus xanthodermus*), whose artefactual nature has been suggested since its first isolation and structure elucidation.[109] These *N*,*N*-coupled MIA dimers are somehow evocative of some *N*,*N*-coupled indolosesquiterpene dimers known as dixiamycins, that were proved to originate from a radical-based mechanism.[110] Such singly bonded *N*,*N*-bonded MIA dimers (*viz*. radical processes occurring from a secondary amine) still have to be reported.

3.1.2.3 Haplophyton alkaloids. Apocynaceous plants of the genus *Haplophyton* produce unique heterodimers featuring inter-indolic connectivities invariably associating an aspidospermane-type MIA monomer with a canthinone-type nucleus through a C-10–C-3 connection.[111] These iconic structures, including haplophytine (**48**) and cimiciphytine (**49**) (Fig. 14), were first isolated from *Haplophyton cimicidum*.[112,113] Interestingly, the canthinone-type component sometimes occurs as a quinolinone derivative and the ability of these two forms to interconvert has been experimentally validated as a semipinacol-type rearrangement,[114] as evidenced since the early report of haplophytine (**48**) by Yates, Cava and co-workers.[111] The biosynthetic relevance of this rearrangement is emphasized by the co-occurrence of hybrid dimers associating an identical aspidospermane unit and both forms of the canthinone/quinolinone counterpart within producing plants.[111,115] The total synthesis of haplophytine (**48**) represented an important synthetic challenge owing to the steric impediments of the coupling process between the aspidospermane component and the C-3 position of the canthinone unit. Synthetic attempts by Corey *et al.* emphasized the trend of different mono- and bicyclic aspidospermane mimics to initiate electrophilic aromatic substitution α to the iminium nitrogen instead of the desired γ-position. Likewise, electrophilic aromatic substitution strategies targeting 2,3-epoxide-containing canthinone analogues resulted in the formation of C-10–C-2 bonded analogues (electrophilic aromatic substitution) or a 11-O–C-2 connected dimer (heteronucleophilic attack) but failed to establish the desired C-10–C-3 connectivity.[116] Later attempts of electrophilic aromatic substitution proved successful but these synthetic works used a tricyclic indolenine-containing canthinone-mimic with a leaving group at C-3, which can hardly be related to a biosynthetic coupling process.[117,118] Nicolaou suggested that the coupling between the canthinone and aspidospermane components of haplophytine (**48**) should result from an oxidative coupling reaction. The desired junction could be experimentally formed from simplified analogues, giving further support to this biosynthetic hypothesis.[119]

3.1.2.4 Leuconolam-derived dimer. Finally, the bis-rhazinilam constitution of bousangustine C (**50**) (Fig. 15), involving a C-6–C-6 connection, is seemingly unique as a MIA dimer as it does not involve the benzenoid ring of the indolic system. Even in the broader context of natural products, it seems difficult to find molecules deriving from a similar reactivity. Tryptamine-based dimers involving a similar coupling position have been repeatedly described in the group of bisindolylmaleimide/indolocarbazoles, but the coupling mechanism involving an enamine radical[120] is difficult to reconcile with the specific example of bousangustine C (**50**). Likewise, the joined motifs of bousangustine C (**50**) are structurally evocative of bipyrrole alkaloids like isochrysohermidin[121] or speranberculatin A.[122] Nevertheless, elegant synthetic works by Boger *et al.* established that these compounds derived from a well-precedented addition-elimination sequence involving the uptake of singlet oxygen by a suitable bipyrrole precursors, that have been co-isolated in both cases,[123] so that these compounds can hardly be related to bousangustine C (**50**) either. An oxidative single electron transfer at N-1 followed by deprotonation at the N-1 position of leuconolam has been proposed to avail a neutral radical. This radical could then relocate to C-6 to

account for the connection appearing in this intriguing compound.[124]

3.1.3 Enamine reactivity-driven oligomerization. An important reactivity feature likely to provide MIA oligomers is linked to the nucleophilic attack triggered by the enamine functions. Our literature survey suggested us to distinguish MIA oligomers according to the nature of the electrophilic partner.

3.1.3.1 Iminium. A first group of electrophilic partners for enamine-driven dimerization reactions comprises iminium-containing metabolites (Fig. 16), as can be produced through Polonovski-type reaction.[125] Although simple, this mechanism enables straightforward access to a large number of structurally diverse MIA dimers. The C-14–C-5 connectivity of the bis-aspidofractane type arbolodinine A (**51**)[77] is easily relatable to a nucleophilic attack of the tetrahydropyridine-type $\Delta^{3,14}$ enamine of a first unit to the $\Delta^{4,5}$ iminium function of another aspidofractane-type component. The structurally-intriguing gabonine (**52**),[126] featuring two ibogane-derived units, is supposed to dimerize upon nucleophilic attack of a $\Delta^{5,6}$ enamine on a $\Delta^{4,21}$ iminium of the other subunit. It seems that this dimer stands among the very scarce number of MIA dimers incorporating Witkop–Winterfeldt oxidized[127] subunits (along with melotenuine C[128]), although several examples of such monomeric MIAs exist.[129,130] With this in mind, it can also be assumed that the nucleophilicity of the α-carbonylated position C-6 could be sufficient to trigger the nucleophilic attack. A related mechanism can be invoked to decipher the inter-monomeric connection appearing in panganensine R (**53**).[80] This rare scaffold could be obtained considering a nucleophilic attack instigated by a dienamine function involving the $\Delta^{18,19}$ vinylic function of a first akuammicine-type monomer on a $\Delta^{4,21}$ iminium-containing akuammicine derivative, resulting in a rare C-18–C-21 junction. Alternatively, 2-pyrroline-type enamine partners could be involved. This reactivity accounts for the intermonomeric connection appearing in the bis-aspidospermane-type melosine A (**54**),[131] that results from the nucleophilic attack of a $\Delta^{5,6}$ enamine-containing unit to a $\Delta^{3,4}$ iminium-containing coupling partner. This reaction is somewhat reminiscent of the coupling mode evoked in the coupling of the two vobtusine blocks as it appears in alasmontamine A (**159**) (Fig. 52).[132]

3.1.3.2 Aldehyde. Enamine-containing MIAs can also target aldehyde functions as electrophilic partners (Fig. 17). The tetrahydropyridine-derived $\Delta^{5,6}$ enamine, as in the case of serpentinine derivatives (*e.g.* 20′-episerpentinine (**55**)), can enable such reactivities. An enamine-driven aldolization of ajmalicine C-6 to the aldehydic C-17 position of the corynantheane northern unit is presumed to assemble the complete scaffold of serpentinines/moandaensines,[133–135] resulting in the final compound after dehydration and a thermodynamically-favoured rearomatization of ajmalicine C-ring. A similar process from the $\Delta^{5,6}$ enamine of a strictosidine-type MIA to the aldehydic moiety of secologanin readily accounts for the pseudodimeric constitution of neonaucleoside B (**56**).[136] Gelsedane-type MIAs are prevalent contributors to enamine reactivity-driven dimerizations. These dimerization trends can be explained by the presence of pyrrole rings and of 2-ethylidene-substituted pyrrolidines in the monoterpenic part of several such MIAs, structural features that are rare for any MIA. With regard to dimers obtained through an enamine-driven nucleophilic attack on an aldehydic function, the case of gelsecorydine A (**57**)[137] is worth being highlighted. The nucleophilic attack would be triggered by the enamine (=2-ethylidenepyrrolidine) form of a gelsedane-type gelsenicine derivative, accounting for the nucleophilicity of its C-19 position, towards the C-21 aldehydic function of vallesiachotamine. The nucleophilic attack of a similar gelsedane 2-ethylidenepyrrolidine function (at C-19)

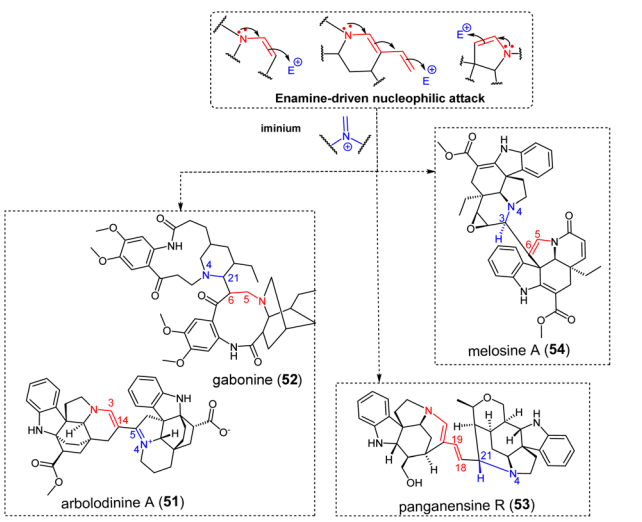

Fig. 16 Singly-tethered MIA oligomers resulting from an enamine-driven nucleophilic attack on an iminium.

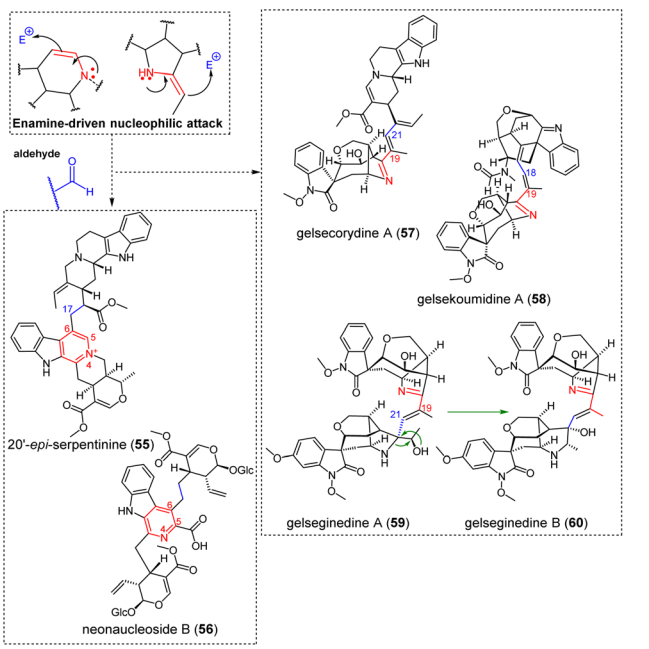

Fig. 17 Singly-tethered MIA oligomers resulting from an enamine-driven nucleophilic attack on an aldehyde and the rearrangement of gelseginedine A into gelseginedine B.

on a putative α,β-unsaturated aldehyde-containing *seco*-koumine at C-18 is presumed to afford the intriguing gelsedane-*seco*-koumine constitution of gelsekoumidine A (**58**).[138] The *seco*-koumine appendage does not appear to have been reported from a monomeric MIA so far. It can be hypothesized that the different constitution of the recently reported gelseginedine A (**59**)[139] stems from the enamine-induced nucleophilic attack of the C-19 position of the gelsedane component on the C-21 aldehyde site of a gelseleginane homologue, a MIA subtype previously assumed to correspond to a biosynthetic intermediate between humanteninane and gelsedane scaffolds.[140] It has been proposed that co-isolated gelseginedine B (**60**) corresponds to a derivative of this earlier dimer by ring expansion of its gelselegine pyrrole in the corresponding piperidine, resulting in a hitherto unprecedented MIA scaffold.

3.1.3.3 Formaldehydes, α,β-unsaturated carbonyls and indoleninium. Extraneous units may also be incorporated after nucleophilic attack of formaldehyde by an enamine function. As in the former subsection, this reactivity often steps in the dimerization of several MIA obtained from gelsemiaceous source. Such scaffold-specific reactivity can rely on the 2-ethylidenepyrroline system (nucleophilic C-19 position) to provide a side chain including an exomethylene function, possibly amenable to epoxidation. An epoxide ring-opening initiated by another 2-ethylidenepyrroline nucleophilic attack system (again from C-19) of a second gelsedane subunit can be presumed to yield the connectivity observed in geleganimine A (**61**) (Fig. 18).[104] Aside from MIA partners, electrophilic sites appearing on a wealth of different phytochemicals are prone to such dimerization processes, mostly aldehydic-containing substances but also α,β-unsaturated exomethylenes as encountered in iridoid monoterpenes, leading to compounds such as gelsamydine (**62**) (Fig. 18).[141] Likewise, rhazinilam-type MIAs are prone to a dienamine-triggered nucleophilic attack on formaldehyde that can readily afford derivatives revealing either an aldehydic or an exomethylenic function at C-5 position. This exomethylenic function is prone to undergoing a nucleophilic attack involving different possible partners. For example, an heteronucleophilic attack initiated by an indolinic N-1 position can be invoked to account for the constitution of the aspidofractane/rhazinilam-based kopoffine A (**63**) (Fig. 18) and of the kopsane/rhazinilam-based kopoffine B.[87] Alternatively, a dienamine nucleophilic attack triggered from a first rhazinilam monomer on a C-5 exomethylene-substituted rhazinilam can lead to the dimeric scaffold of bousangustine B. An additional nucleophilic attack initiated by the dienamine function of a third rhazinilam unit can yield the trimeric bousangustine A (**64**) (Fig. 18).[124] The vallesamane/vobasane dimer vobparicine (**65**) (Fig. 18),[142] can be assembled following a conjugate 1,6-addition of the conjugated system appearing in the $\Delta^{16,22}$-exomethylene-containing apparicine on the electrophilic C-3 of vobasinol.

3.1.3.4 Quinone methide. Finally, the unique structures of inaequalisines A (**66**) (Fig. 19) and B introduced a C-7 located phenylpropene unit that acted as a dearomatizing unit, a structural trait having no precedent in the wide phytochemical class of MIAs. More generally, such phenylpropene-pyrroloindolines are very rare in the plant kingdom with only two other occurrences: angelicastigmin[143] and utilisin.[144] Although rare, it is quite straightforward to understand the constitution of this unusual MIA that seems to rely on an enamine attack on a feruloyl-type *para*-quinone methide.[25] It should be noted that the proposed biosynthesis pathway of ineaqualisines would proceed from an indole-containing quebrachamine precursor which would subsequently rearrange into the final rhazidine appendage.[25]

3.1.4 (Hetero)nucleophilic coupling-driven oligomerization. Many different MIA dimerization processes are based on nucleophilic attacks initiated either by carbon or by heteroelements. A selection of MIA dimers obtained using this reactivity

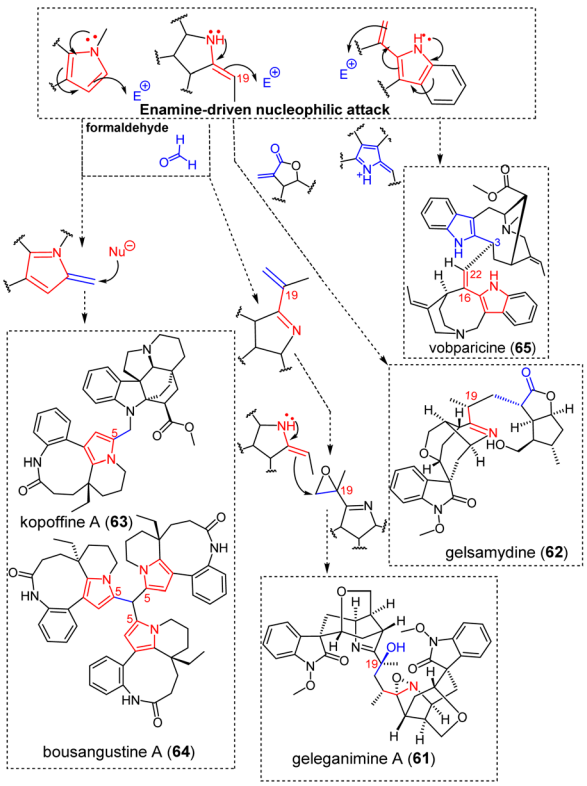

Fig. 18 Singly-tethered MIA oligomers resulting from an enamine-driven nucleophilic attack on formaldehyde or on an α,β-unsaturated carbonyl.

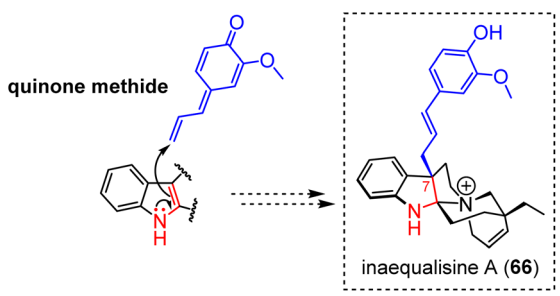

Fig. 19 Singly-tethered MIA oligomers resulting from an enamine-driven nucleophilic attack on a conjugated quinone methide.

is disclosed below according to the nature of the electrophilic partner.

3.1.4.1 Formaldehyde. Some of these dimerization sequences require precise structural features, which probably explains the relatively low number of MIA dimers obtained in this way. Several such bis-aspidospermanes seem to depend on both (i) the existence of a secondary alcohol function at C-18 and (ii) the occurrence of a $\Delta^{14,15}$ functionality (see for example fusiformine A for a relevant monomeric constituent).[145] Aspidospermane-type MIAs disclosing these substituents may trigger nucleophilic attack of the 18-OH group on the $\Delta^{14,15}$ functionality to trigger nucleophilic attack on an extraneous formaldehyde, to install an electrophilic site at C-14 along with a classical hexacycle framework featuring an additional tetrahydrofuran ring (relatable to modestanine monomers).[146] This reactivity can yield MIA dimers such as voacinol (**67**)[147] or voacandimine C (**68**)[148] (Fig. 20) type structures, only deriving from the bis-tetrahydrofuran containing dimer by the reductive ring opening of one or two such rings. Regarding voacinol (**67**), it is also possible that an extraneous water unit triggers the 1,4-Michael addition, which would be consistent with the occurrence of a $\Delta^{14,15}$ moiety after dehydration (see sungucine (**76**) in the next section for a related mechanism). The synthesis of voacinol (**67**) and voacandimine C (**68**) by Movassaghi *et al.* supported this putative biosynthetic scenario, although an enamine-type reactivity was retained as the second dimerization step.[149] The aspidospermane/ibogane biscarpamontamine A (**69**) (Fig. 20) is supposed to be obtained as a consequence of a similar, enol ether-like scheme, but followed by a nucleophilic attack initiated by the N-1-position of an ibogane unit on the C-14 electrophilic site of the aspidospermane unit.[128] MIA dimers incorporating extraneous methylenic units can also be related to a direct heteronucleophilic attack by a nitrogen atom. The bis-aspidospermane melofusine I (**70**)[150] (Fig. 20) can be inferred to derive from an heteronucleophilic attack on a formaldehyde unit, subsequent dehydration and further heteronucleophilic attack of the resulting iminium by a further aspidospermane unit. Alternatively, heteronucleophilic attack on a formaldehyde unit may be initiated from the alicyclic nitrogen, as in the case of geleganidine C (**71**) (Fig. 20).[19] In this latter dimer, this extraneous unit is later oxidized to an urea group.

3.1.4.2 Iminium. Diverse (hetero)nucleophilic attacks targeting iminium functions have been reported. Here again, the structural specificities of certain MIA subtypes are sometimes involved in these reactive pathways. Enol ether-containing macrolanes are one such example. A putative macrolane monomer of salient biosynthetic interest, anhydromacrosalhine-methine (Fig. 8), is presumed to trigger a nucleophilic attack on a $\Delta^{3,4}$-containing aspidospermane to afford the macrolane/aspidospermane-type pandicine (**72**)[151] (Fig. 21) (as demonstrated by Cook *et al.* based on biomimetic synthesis[152]) or on a pleiocarpamane indoleninium to yield macrocarpamine.[153]

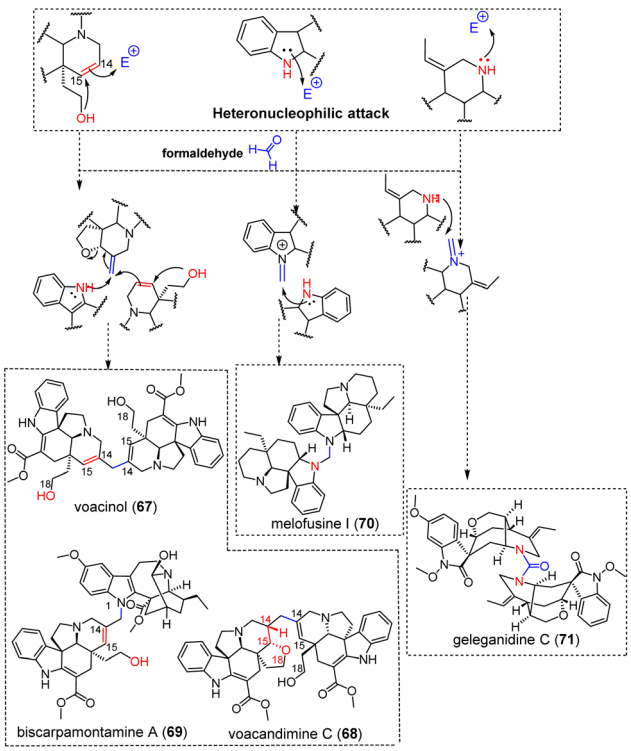

Fig. 20 Singly-tethered oligomers resulting from an heteronucleophilic attack on formaldehyde (see S2‡ for a comprehensive listing, red- and blue-colored moieties refer to nucleophilic and electrophilic sites, respectively).

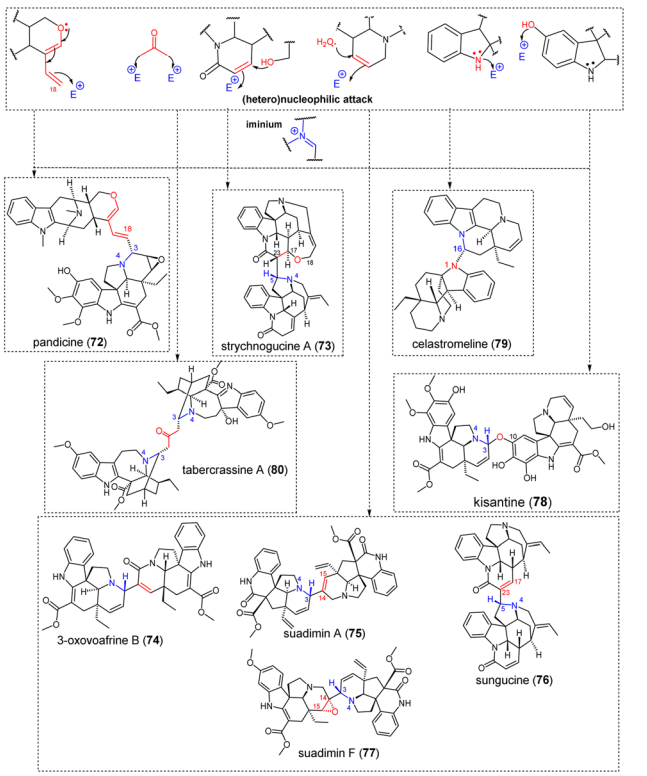

Fig. 21 Singly-tethered oligomers resulting from an (hetero)nucleophilic attack on an iminium (see S2‡ for a comprehensive listing, red- and blue-colored moieties refer to nucleophilic and electrophilic sites, respectively).

Likewise, Gan and Cook could synthesize macrocarpamine from pleiocarpamine and anhydromacrosalhine methine (Fig. 8).[154] Remarkably, the dimerization process of strychnogucine A (**73**)[155] (Fig. 21) may result from the heteronucleophilic annulation of a 18-OH function on the $\Delta^{17,23}$ functionality of a *seco*-F ring strychnine precursor initiating a nucleophilic attack on a $\Delta^{3,4}$ iminium-containing akuammicine electrophilic partner. This is somehow reminiscent of that having led to voacinol (**67**) and voacandimine C (**68**). In some cases, the driving force to initiate a nucleophilic attack does not rely on a heteronucleophilic attack based on an oxygen functionality already located on the reactive monomer, but rather seems to depend on the involvement of an extraneous water unit. One such example is that of the bis-aspidospermane 3-oxovoafrine B (**74**) (Fig. 21).[69] Again, a monomeric aspidospermane unit containing a $\Delta^{14,15}$ functionality should be considered to undergo an heteronucleophilic attack by a water molecule that could be combined with the coupling to an iminium-containing electrophilic partner. This readily accounts for the constitution of 3-oxovoafrine B (**74**)[69] but also for the bis-Melodinus-type suadimin A (**75**), or the bis-akuammicine sungucine (**76**) (Fig. 21).[155,156] In all these cases, the hydroxy group having initiated this sequence is ultimately eliminated by dehydration, resulting in $\Delta^{14,15}$ functions. This double bound can be subsequently epoxidized, as observed in suadimin F (**77**) (Fig. 21).[82]

The bis-aspidospermane-type kisantine (**78**) (Fig. 21) enters a unique category as the nucleophilic attack seems to result from a phenate function at C-10 on a $\Delta^{3,4}$ iminium-containing aspidospermane as an electrophilic partner.[157] Likewise, the constitution of the melonine/eburnane-type celastromeline (**79**)[158] (Fig. 21) is straightforward to delineate as it merely results from an heteronucleophilic attack triggered by melonine N-1 on the C-16 of an eburnane unit, previously presented as an electrophilic site of considerable generality. It should be noted that this structure is at high risk of being erroneous as we revised the structure of melonine in 2021.[159]

Tabercrassine A (**80**) (Fig. 21) is an intriguing dimer disclosing two ibogane-type units bridged by an extraneous acetone unit connecting their C-3 positions. Such compounds are presumed to be artifacts arising from the nucleophilic attack of an acetone methyl group on a $\Delta^{3,4}$-iminium containing ibogane-type MIA. Accordingly, ibogane monomers disclosing a 3-oxopropyl group (*e.g.* 3-(2′-oxopropyl)-coronaridine)[20] are in line with this speculative biosynthetic scenario.[160,161] A nucleophilic attack triggered by the remaining methyl group of acetone on another $\Delta^{3,4}$ iminium-containing ibogane unit can give access to tabercrassine A (**80**)/3,3′-(oxopropyl)dicoronaridine dimers.

3.1.4.3 Indoleninium. The constitution of the bis-vobasane-type bisnicalaterine A (**81**)[162] denotes a 1,6-addition triggered by an indolic nitrogen N-1 on the electrophilic C-3 residue of another vobasine molecule. Other bis-vobasane dimers obtained through an analogous reactivity are the so-called theionbrunonines A (**82**)-C that feature a unique S heteroatom connecting the C-3 site of two vobasinyl residues (Fig. 22).[22,23] These structures were speculated to result from the nucleophilic attack of a 3-SH containing vobasane residue to the C-3 position

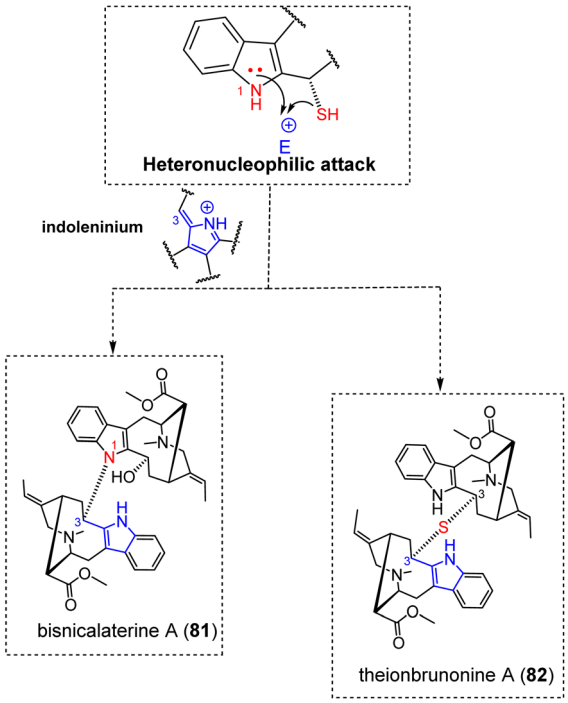

Fig. 22 Singly-tethered oligomers resulting from an heteronucleophilic attack on an indoleninium (see S2‡ for a comprehensive listing).

of vobasinol. The occurrence of a very unusual thiol substituent in this tentative substrate was presumed to arise from a 1,6-addition of cysteine on the electrophilic C-3 site of vobasine. Cysteinyl-comprising MIAs have seldom been reported to occur comprising mappiodoside I,[26] and, mostly, the related pagisulfine,[163] that could afford the desired precursor under the action of a cysteine C-S lyase. This assumption found later support through the isolation of the sought-after monomer, hemitheion, from the same plant a few years later.[164]

3.1.4.4 α,β-Unsaturated carbonyl and imine. Heteronucleophilic attacks can also proceed through an aza-Michael-based dimerization (Fig. 23). The constitution of some dimers obtained following these reactions is easy to explain, such as the akuammicine/aspidofractane-type arbolodinine B (**83**).[77] This dimer presumably derives from the nucleophilic attack of the N-1 position of an aspidofractane on the C-22 position of the conjugated exomethylene-indolenine system of the akuammicine-type valparicine. Conversely, angustiphylline (**84**), comprising two unusual building blocks, *viz.* an uleane and a *nor-seco*-stemmadeninane unit, requires some reactivity prior to dimerization.[165] The biosynthetic pathway to angustiphylline (**84**) would be initiated from a N-4-oxidized stemmadeninane followed by a Potier–Polonovski fragmentation and excision of C-5 to afford a ring-opened conjugated indoleninium. A nucleophilic attack by the N-4-nitrogen of the uleane-type alstilobanine C on this open conjugated indoleninium ion would then provide angustiphylline (**84**).[165] Although unusual as a dimerization mechanism, it is worth noting that alstilobanine C itself was proposed to derive from a Potier–

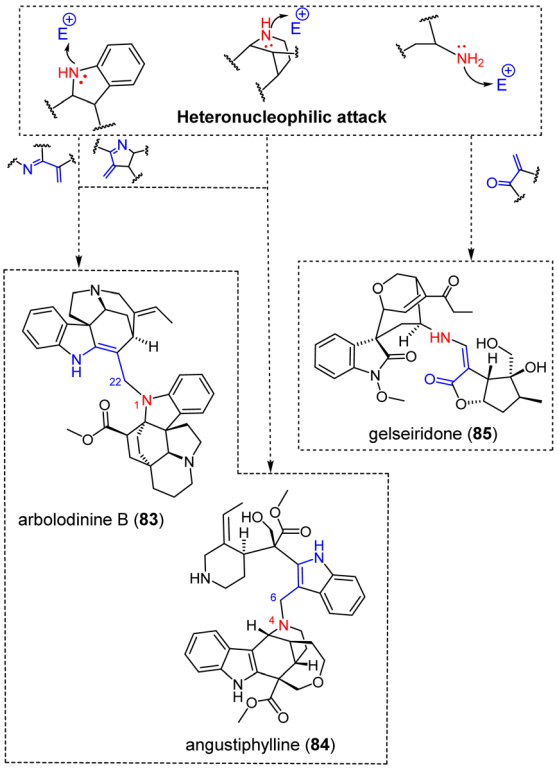

Fig. 23 Singly-tethered oligomers resulting from an heteronucleophilic attack on an α,β-unsaturated carbonyl/imine (see S2‡ for a comprehensive listing).

Polonovski-initiated fragmentation and recyclization proceeding from stemmadenine.[166] Potier and Janot proposed that the apparicine scaffold is also biosynthetically derived from stemmadeninane by this mechanism, and several examples of monomeric MIAs from *Alstonia* indicated that this reactivity (*i.e.*, fragmentation-excision(s)) played an important role in the structural diversification of stemmadeninane-type MIAs.[167–169] It can be assumed that the recently reported scholaphylline derives from a similar reactivity, with the monomeric block initiating the heteronucleophilic attack lacking two carbon units compared with stemmadenine.[170] Again, monomeric scaffolds of this constitution have already been reported, and a biosynthetic link to stemmadenine has been suggested elsewhere.[171] As a last example of aza-Michael derived MIA pseudodimer, gelseiridone (**85**) is a further example of gelsedane-type MIA bonded to an additional iridoid unit. This biosynthesis would proceed from a gelsedane-type gelsenicine derivative having underwent an imine hydrolytic cleavage to release a secondary amine group, able to initiate an aza-Michael addition on the conjugated α,β-unsaturated carbonyl function of 7-deoxygelsemide as an iridoid.[172] Finally, the ring opening of the dihydropyran moiety of this iridoid unit provides the definite structure of gelseiridone (**85**).

3.1.4.5 Carboxylic acid derivatives and aldehyde function. A very large number of MIA derivatives result from the condensation of different MIAs with diverse shikimic acid-derived building blocks. Our bibliographic survey enabled us to locate 98 adducts between MIAs and such gallic acid/cinnamic acid derivatives and, seldom, anthranilic acid derivatives.[29] While some remarkable, C–C or multiply bonded adducts with shikimic acid derivatives have already been covered (conomicidine A (**12**), conoliferine (**13**) and inaequalisine A (**66**)) or will be developed in the dedicated section (kanluaengoside C (**93**), voacalgine A (**146**), bipleiophylline (**147**), and pleiomaltinine (**148**)), a vast majority of these hybrid natural substances (almost 9 out of 10) arise from the esterification of a MIA alcohol group on a phenolic carboxylic acid group or, in a few cases, from an amidification initiated by the indole/indoline nitrogen for some aspidospermane-type[173] or ajmaline-type MIA (*e.g.* alstiphyllanine I (**86**)) (Fig. 24).[28] Although the structural requirements are seemingly scarce for the MIA component to initiate such reactions, it is intriguing to note that these esterification-derived adducts are limited to a few MIA subtypes with the most prevalent contributors being yohimbinoids (24 esters on either 17-OH or 18-OH, with raugustine (**87**)[27] as an illustration), ajmalane (15 esters on 17-OH and 7 amides on N-1), akuammilanes (15 esters on 17-OH) and aspidospermanes (11 esters on 19-OH and 4 amides on N-1). To a lesser extent, adducts on vallesiachotamane and strictosidine have also been reported. In mappiodoside J (**88**) the alcohol group of a sugar unit esterifies the carboxylic acid group of an extraneous cinnamate unit.[26]

Heteronucleophilic attack from the alicyclic nitrogen of a strictosidine derivative on the aldehydic group of a second secologanin unit can readily account for the constitution of the pseudodimeric neonaucleoside A (**89**), later shown to be structurally equivalent to bahienoside A through total synthesis.[174]

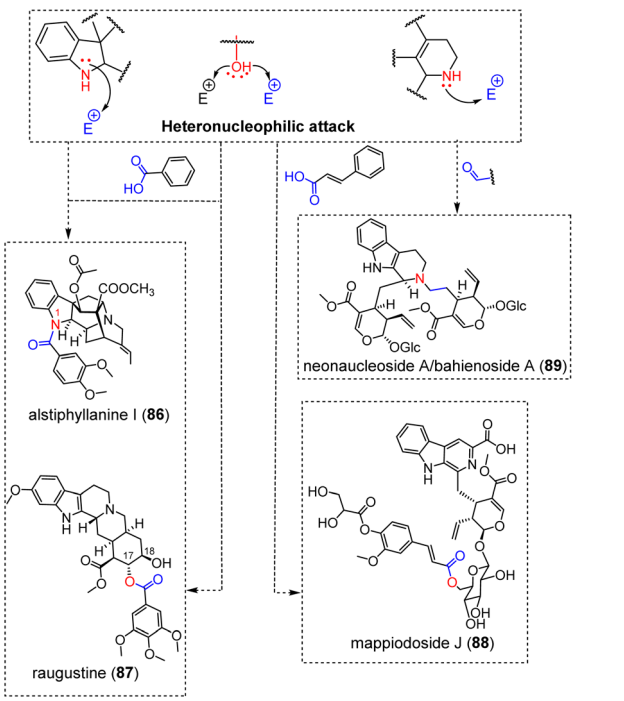

Fig. 24 Singly-tethered oligomers resulting from an heteronucleophilic attack on carboxylic acids or aldehydes (see S2‡ for a comprehensive listing).

3.2 Doubly-tethered oligomers

A retro-oligomerization analysis conducted on the doubly-tethered MIA oligomers revealed the implication of five reactive sequences.

3.2.1 Doubly-tethered oligomers resulting from an electrophilic aromatic substitution associated to an heteronucleophilic attack. Electrophilic aromatic substitutions have formerly been presented as a privileged strategy to trigger MIA dimerization. This section covers a selection of cornerstone MIA oligomers implying a combination of electrophilic aromatic substitutions and heteronucleophilic annulations, according to the nature of the involved electrophilic partner.

3.2.1.1 Iminium. As already seen above, electrophilic aromatic substitutions often involve iminium-type electrophilic partners (Fig. 7). Such products may lead to doubly-tethered MIA dimers provided that some structural requirements are met. Furan-bridged MIA dimers (*e.g.* conophylline (**90**)) (Fig. 25) would require two additional structural features, *i.e.* a phenol group contiguous to the site initiating the electrophilic aromatic substitution and an epoxide moiety next to the site of the electrophilic partner. In the specific example of the bis-aspidospermane conophylline (**90**) (Fig. 25), this further nucleophilic attack is conducted by the 11-OH group on the epoxide unit at C-14 to install this furanic junction.[47] The tris-aspidospermane-type taberdivarine A (**91**)[175] (Fig. 25) features two such connections (it should be noted that this name had been formerly given to an unrelated vobasane/quebrachamine dimer).[176] A unique instance of doubly-tethered eburnane/aspidospermane dimer is represented by bisleuconothine B (**92**) (Fig. 25).[177] The first connection between the two building blocks befits the usual connection mode involving eburnane-type MIAs, *i.e.* an electrophilic aromatic substitution on an $\Delta^{1,16}$ iminium resulting in a typical C-16–C-10 connection. The final scaffold could be reached from this singly-tethered intermediate, with the second connection being established after nucleophilic attack of a C-9 phenol function on the C-2 site of an indoleninium-type eburnane presumed to be obtained after an enamine-driven hydroxylation at C-7.

3.2.1.2 Quinone methide. Likewise, the structure of the cinnamyl-vallesiachotomane-type kanluaengoside C (**93**)[178] (Fig. 26) is reminiscent of that of electrophilic aromatic substitution-derived conjugates such as conomicidine A (**12**) (Fig. 5). The first connection again relies on an electrophilic aromatic substitution between the vallesiachotamane C-9 position and a cinnamyl-derived *para*-quinone methide. The second connection depends on both the presence of an *ortho*-phenolic group to the site having initiated the electrophilic aromatic substitution and the occurrence of a carboxylic acid group on the cinnamyl conjugate enabling a subsequent lactonization.

3.2.1.3 Formaldehyde. The strained pleiocarpamane scaffold is associated with an inherent electrophilicity at C-7 along with a pronounced nucleophilicity at C-2, accounting for the propensity of this MIA subtype to afford doubly-tethered MIA dimers involving these two positions.[179] One such example is that of the pleiocarpamane/rhazidine type goniomedine A (**94**) (Fig. 27).[180,181] Electrophilic aromatic substitution by the C-10 site of the rhazidine component is first proposed to install a *para*-iminoquinone methide group, that could be prone to undergo a $\Delta^{2,7}$ enamine nucleophilic attack from the pleiocarpamane to afford an indoleninium-comprising pleiocarpamane as a singly-tethered intermediate. The occurrence of a C-11 phenolic group on the rhazidine component enables an heteronucleophilic annulation on a pleiocarpamane indoleninium to afford the dihydropyran intermonomeric junction. A bis-aspidospermane dimer, melomorsine (**95**) (Fig. 27),[182] seems to be obtained through a comparable mechanism. In this case, an exomethylene-type N-1 iminium could be added by the *ortho*-oxygenated C-10 position of the other subunit. The resulting indoleninium ion might then undergo a nucleophilic attack by the phenate at C-11 to install the oxazole core appearing in melomorsine (**95**).

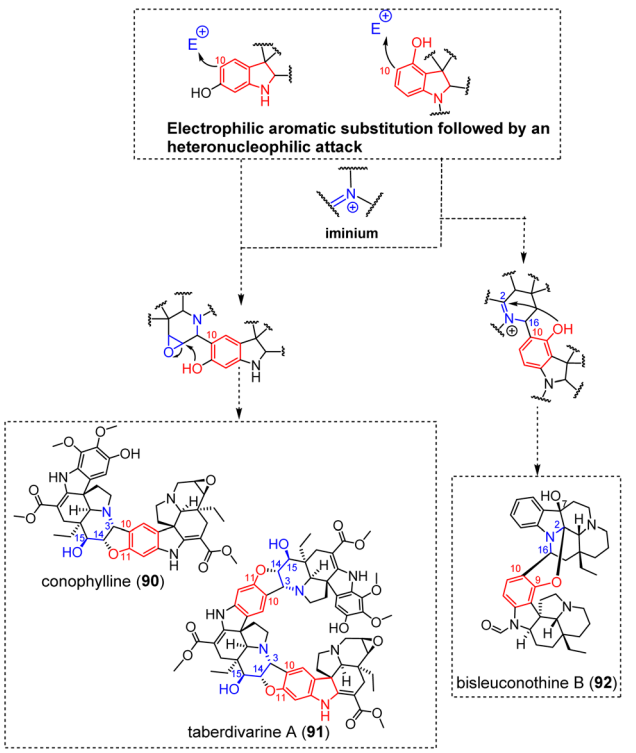

Fig. 25 Doubly-tethered oligomers resulting from an electrophilic aromatic substitution on an iminium associated to an heteronucleophilic attack (see S2‡ for a comprehensive listing).

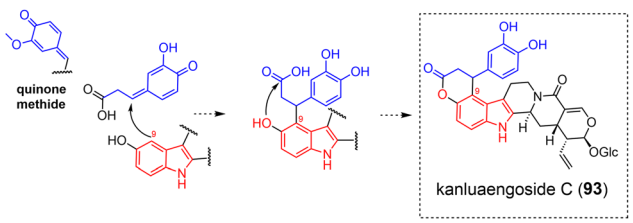

Fig. 26 Doubly-tethered oligomers resulting from an electrophilic aromatic substitution on a quinone methide associated to an heteronucleophilic attack (see S2‡ for a comprehensive listing).

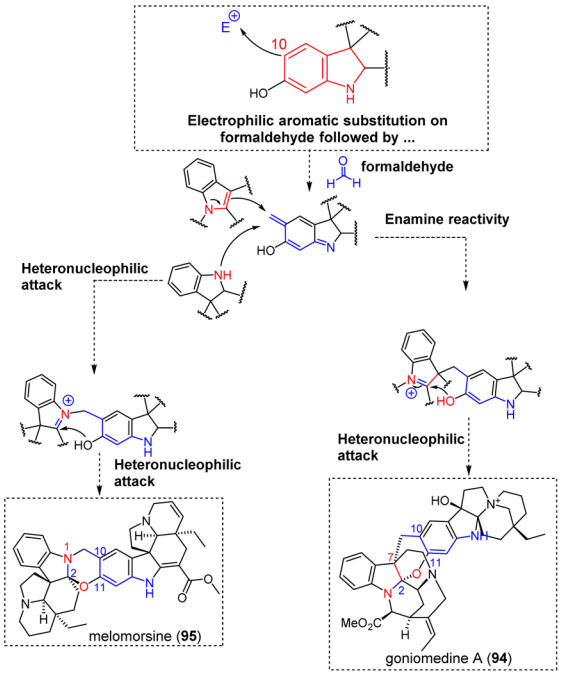

Fig. 27 Doubly-tethered oligomers resulting from an electrophilic aromatic substitution on a formaldehyde unit associated to an heteronucleophilic attack (see S2‡ for a comprehensive listing).

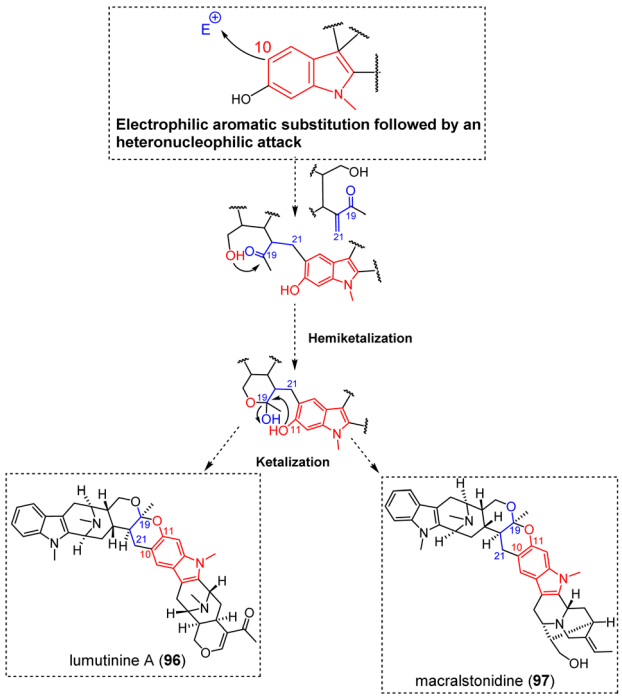

Fig. 28 Doubly-tethered oligomers resulting from an electrophilic aromatic substitution on an unsaturated carbonyl associated to an heteronucleophilic attack (see S2‡ for a comprehensive listing).

3.2.1.4 α,β-Unsaturated carbonyl. Lumutinines (herein exemplified by lumutinine A (**96**)) are doubly-tethered bis-macrolane-type MIA dimers and macralstonidine (**97**)[183] is a macrolane/sarpagane dimer (Fig. 28). These compounds disclose a tetrahydropyranic junction and are presumed to derive from the 1,4-Michael addition of the electron-rich C-10 position of a macrolane or sarpagane residue on the exomethylenic position C-21 of a type A-macrolane (Fig. 8) to afford an hydroxyketone, prone to ring closure *via* hemiketal formation, and final ketalization triggered by a phenolic group at C-11.[184] Biomimetic synthesis of macralstonidine (**97**) from macroline and N_a-methylsarpagine gave support to this dimerization scenario.[185] As formerly noted for some singly-tethered bis-macrolane dimers, an alternative dimerization mechanism to lumutinine A (**96**) relying on a Friedel–Crafts-based sequence has been suggested elsewhere.[186]

3.2.1.5 Indoleninium. The constitution of the ibogane/vobasane/vobasane trimer divaricamine A (**98**)[187] (Fig. 29) is easily relatable to the electrophilic nature of the C-3 position of vobasane-type MIAs. The middle vobasane unit undergoes an electrophilic aromatic substitution by an ibogane C-10, instigating the usual 1,6-conjugate addition when a vobasane is involved as an electrophilic partner. The connection between the vobasane building blocks results from a similar 1,6-conjugate addition but results from an heteronucleophilic attack triggered by the N-1 atom of the middle vobasane unit on the C-3 site of the other vobasane component.

3.2.2 Doubly-tethered oligomers resulting from two electrophilic aromatic substitutions. The trimeric constitution of the eburnane/aspidospermane/eburnane bousigonine B (**99**)[188] (Fig. 30) is relatable to two electrophilic aromatic substitution reactions initiated by the C-10 and C-12 positions of the central aspidospermane component on the C-16 electrophilic sites of both peripheric eburnane units.

The recently isolated aspidospermane/cleavamine/aspidospermane MIA trimer, vincarostine A (**100**) (Fig. 30),[189] incorporates an anhydrovinblastine substructure linked to another aspidospermane unit (vindoline) *via* an unprecedented aspidospermane 10-cleavamine 6 bond. This unique bond was assumed to be generated by the Polonovski reaction of anhydrovinblastine *N*-oxide with the introduction of vindoline as nucleophile at C-6 (through its electron-rich C-10 site).

3.2.3 Doubly-tethered oligomers resulting from *N*-mediated heteronucleophilic attack. *N*-mediated heteronucleophilic attacks reported in this section have been categorized according to five distinct assembly reactions.

3.2.3.1 Aza-Michael addition. The only ellipticine-comprising MIA dimer described to date, the bis-ellipticine-type strellidimine (**101**) (Fig. 31) obtained from *Strychnos dinklagei*, features a fused oxazole system as an intermonomeric junction. A putative biosynthetic scenario to this structure proceeds from an oxidized 10-hydroxyellipticine derivative (*i.e.* oxidized to a *para* quinone imine), thereby revealing an α,β-unsaturated indolenine prone to undergo heteronucleophilic attack at C-9 initiated by the dihydropyridine nitrogen N-4 of the other subunit. The quaternary adduct could then rearrange *via* heteronucleophilic annulation to a thermodynamically-favoured system featuring the final oxazole junction, with the rearomatization of the 10-hydroxyellipticine being a likely driving force.[190] Likewise, the hexacyclic constitution of the recently reported alstoscholarinine A[191] features an oxazolidine

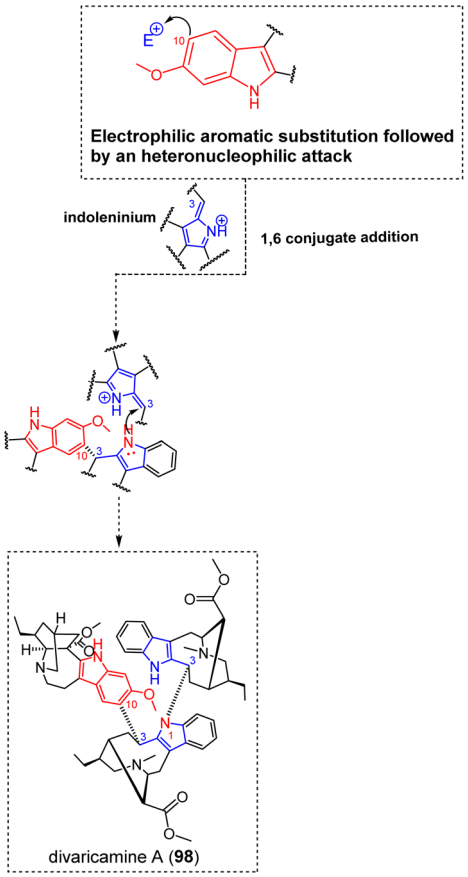

Fig. 29 Doubly-tethered oligomers resulting from an electrophilic aromatic substitution on an indoleninium associated to an hetero-nucleophilic attack.

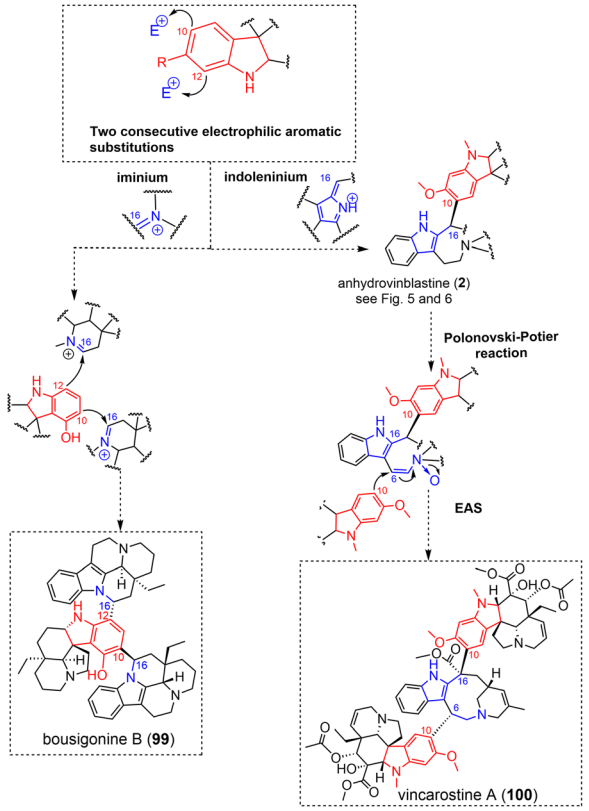

Fig. 30 Doubly-tethered oligomers resulting from two electrophilic aromatic substitutions (EAS) on iminium or indoleninium (see S2‡ for a comprehensive listing).

nucleus that is presumed to arise from two consecutive Mannich-type condensations initiated by glycine on (i) the C-17 alcohol group of the corynantheane-type isositsirikine and then (ii) the C-19 position of an oxidized derivative, resulting in an intermediate dihydropyridinium derivative. Subsequent dihydroxylation would then set the stage for the final dehydrative etherification of the reduced glycine analogue affording the hexacyclic, oxazolidine-containing structure.

The doubly-tethered bis-akuammicine leucoridine A (**102**) (Fig. 31) is an interesting case first involving an aza-Michael type 1,4 addition from the N-1 position of the anhydropereirine unit on the C-22 position of the conjugated exomethylene-indolenine system of the dihydrovalparicine electrophilic partner (see arbolodinine B (**83**) for an analogous singly-tethered MIA dimer (Fig. 23)).[192] A subsequent enamine-driven nucleophilic attack on the C-22 site of the conjugated exomethylene-indoleninium unit of the anhydropereirine component yields the doubly-tethered constitution of leucoridine A (**102**). A biomimetic dimerization of dihydrovalparicine to leucoridine A has been accomplished a few years later. DFT calculations favoured a stepwise aza-Michael sequence rather than an alternative hetero-Diels–Alder cycloaddition.[193] A similar stepwise Aza-Michael reaction can readily account for the structure of the bis-condylocarpane-type leucofoline (**103**) (Fig. 31).[194] The bis-aspidospermane type anhydrohazuntiphyllidine reveals a similar intermonomeric connectivity with its hydroxylated derivative, hazuntiphyllidine (**104**) (Fig. 31), revealing an additional OH group at the C-2 position of the southern aspidospermane unit.[195] Interestingly, hazuntiphyllidine (**104**) was shown to exist in two distinct structural forms in solution, depending on the solvent used. The analysis of hazuntiphyllidine (**104**) in DMSO-d_6 revealed a leucofoline-like spiranic junction. Conversely, NMR analysis in C_6D_6 determined an additional ether connectivity resulting from heteronucleophilic attack of the 2-OH function on the C-2 position of the southern indolenine-containing component. To the best of our knowledge, this solvent-dependent number of intermonomeric connections is the unique documented example within MIA oligomers.

The bis-akuammicine type bisleucocurine A (**105**)[196] (Fig. 31) can be related to a similar dimerization mechanism. As already envisaged in the frame of leucoridine A (**102**), a singly-tethered intermediate could result from the aza-Michael type 1,4-addition from anhydropereirine N-1 into the C-17 position of the conjugated exomethylene-indoleninium of the electrophilic partner. Ring closure would then result from a C-12 initiated electrophilic aromatic substitution on the C-2 position of the indoleninium-oxidized electrophilic motif. It can be noted that an equally satisfactory biosynthetic scenario could rely on a Mannich-type heteronucleophilic attack from

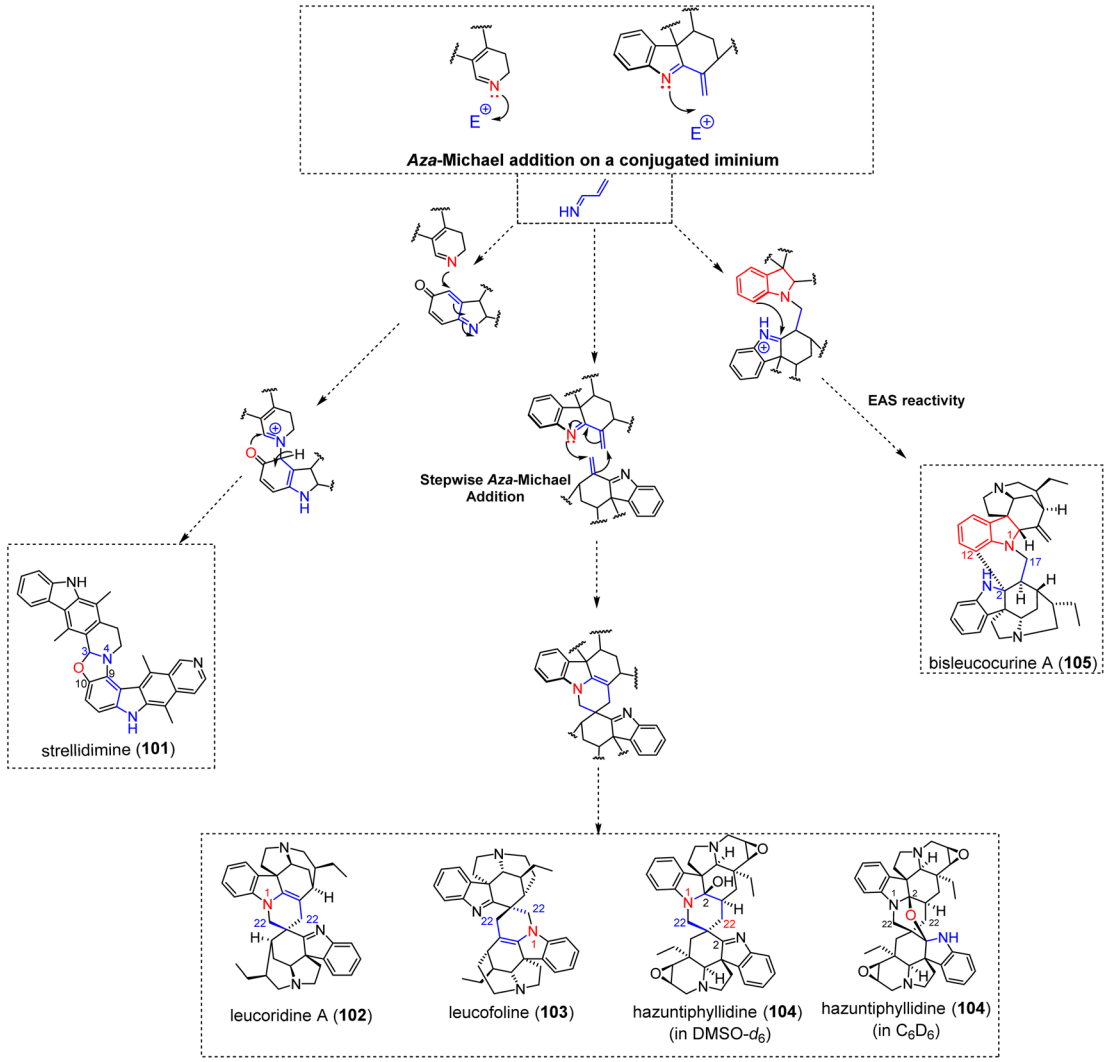

Fig. 31 Doubly-tethered oligomers involving an aza-Michael addition on a conjugated iminium.

anhydropereirine N-1 on the aldehydic function of 18-deoxy Wieland–Gumlich aldehyde.

The dimerization of the akuammicine/strychnane-type strychnobaillonine (**106**)[197] (Fig. 32) can be supposed to proceed *via* an aza-Michael addition of an akuammicine indoline nitrogen into the C-17 strychnane position, taking benefit of the signature α,β-unsaturated lactame system (Δ^{17-23} functionality) of such analogues (the use of this functionality in the frame of a dimerization is somehow reminiscent of the path to strychnogucine A (**73**) and sungucine (**76**)). The second connection between the two units would then be related to an aldolization reaction directed towards the C-17 position of the akuammicine unit.

The recently reported ajmalane/macrolane-type alsmaphylline A (**107**) (Fig. 32) features an original intermonomeric connectivity.[198] The dimerization would first involve an aza-Michael addition of ajmaline N-1 on the C-21 position of an alstonerine α,β-unsaturated ketone system (cyclized, $\Delta^{20,21}$-containing form of a type B macrolane) (Fig. 8). The unconjugated C-19 ketone group from the macroline unit could then be prone to undergo an electrophilic aromatic substitution from the ajmalane unit C-12 position. This dimerization scheme is highly reminiscent of that proposed to yield the structurally-related alstonisidine (**108**) (Fig. 32).[199] This molecule was proposed to result from the aza-Michael addition of an ajmaline indoline N-1 on the C-21 site of the conjugated exomethylene of the type A-macroline (Fig. 8) to yield an alternative singly-tethered intermediate that could lead to an hemiketal group with the nearby CH_2OH group (alstomacroline-type intermediate). A subsequent electrophilic aromatic substitution by the C-12 position of the ajmalane on this hemiketalic C-19 position can then install the second intermonomeric bond to provide the final frame of alstonisidine (**108**). This assumption has been supported by early biomimetic syntheses.[200,201]

3.2.3.2 Pictet–Spengler. Pseudodimeric structures such as usambarine (**109**) (Fig. 33), tchibangensine and cinchophyllamine are presumed to derive from a Pictet–Spengler condensation between the aldehydic function at the C-17 position of a corynantheal/corynantheidal-like precursor and a tryptaminic derivative.[109] As an illustration, Seguin and Koch achieved the

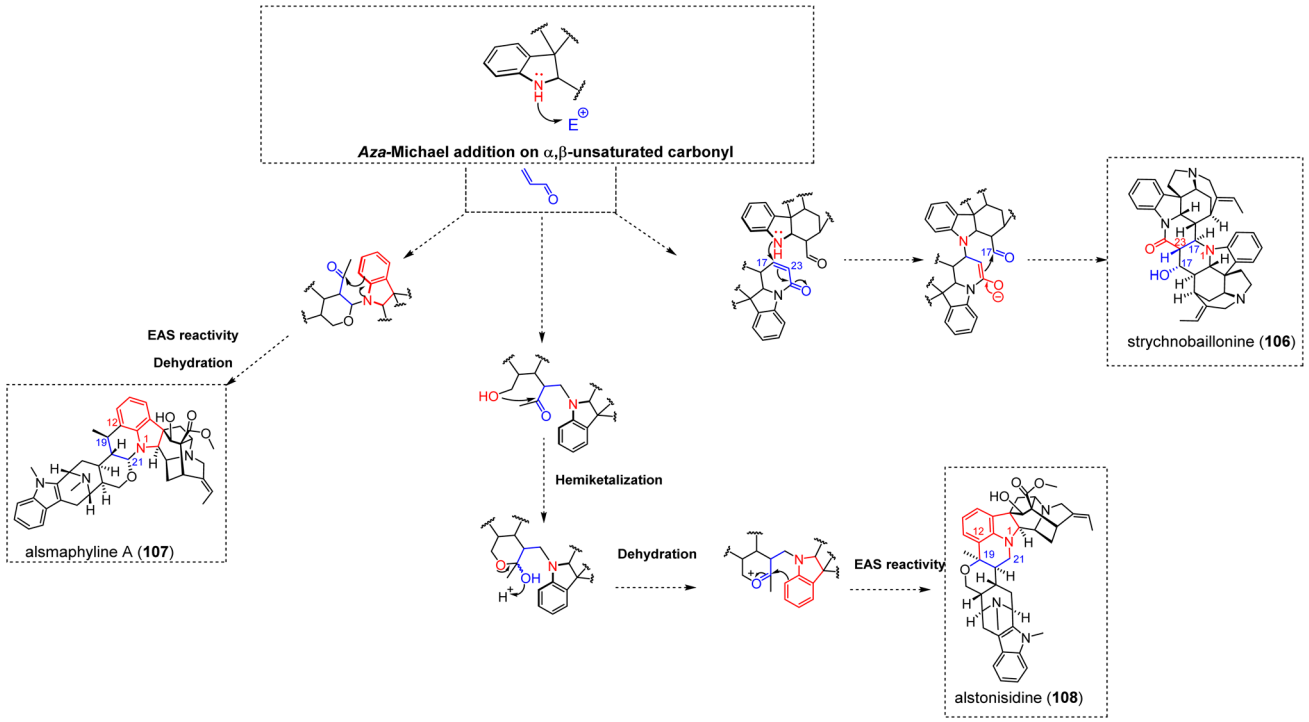

Fig. 32 Doubly-tethered oligomers involving an aza-Michael addition on an α,β-unsaturated carbonyl.

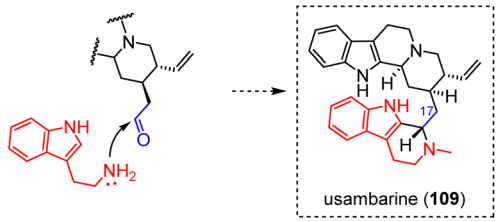

Fig. 33 Example of doubly-tethered pseudodimer resulting from a Pictet–Spengler reaction.

hemisynthesis of usambarine by Pictet–Spengler condensation between corynantheidal and *N*-methyltryptamine.[202] Likewise, strychnofolines[111] and barterines[112] involve the same reaction but proceed from a spiro-oxindole-containing MIA. Although this reaction had not been considered earlier in this review, Pictet–Spengler reaction is of extreme importance to the wide MIA structural class. Strictosidine (**1**), as the universal precursor to MIAs, derives from a Pictet–Spengler condensation between tryptamine and the aldehyde-containing monoterpene, secologanin. This reactivity is highly reminiscent of the biosynthetic steps leading to the emetine-type ipecac alkaloids, although incorporating a dopamine instead of tryptamine in that case.[203]

3.2.3.3 Mannich reaction combined to enamine and electrophilic aromatic substitution reactivities. Stepwise reactions related to enamine reactivity and electrophilic aromatic substitution are often proposed to step in the dimerization of pleiocarpamane-containing compounds (*e.g.* pycnanthine (**110**), pycnanthinine (**111**) and contortarine A (**112**)[204]) (Fig. 34). The first step to initiate such dimerization relies on the heteronucleophilic attack of formaldehyde by diverse indolines (pycnanthine = a vindolinine, pycnanthinine[205] = an aspidospermane and contortarine A = an aspidofractane) to install a nucleophilic exomethylene-type N-1-iminium. This functional group can undergo an enamine nucleophilic attack to yield a C-7 substituted singly-tethered intermediate disclosing a pleiocarpamane indoleninium. The second inter-unit bonding is obtained through an electrophilic aromatic substitution triggered by the C-12 position on the pleiocarpamane C-2 indoleninium.[205]

3.2.3.4 N,O-ketalization. A few MIA dimers feature a characteristic junction composed of an 1,3-oxazinane such as geissospermine (**113**),[206] geissolosimine,[207] ligustrinine (**114**)[208] (Fig. 35) and strychnobiline.[209] This junction is implemented thanks to an heteronucleophilic attack from the akuammicine component N-1 atom to the C-17′ aldehydic function of the corynantheane counterpart to give rise to a *N*,*O*-hemiketal function. Further heteronucleophilic attack of this group by the C-17 OH group of the akuammicine would then yield the *N*,*O*-ketal function, thereby installing the final 1,3-oxazinane ring. As an example, the akuammicine/corynantheane-based geissospermine (**113**) involves the 17-hydroxylated akuammicine-type geissoschizoline. A similar process is supposed to step in the biosynthesis of ligustrinine (**114**) *via* an heteronucleophilic attack of the vobasine N-4 into the C-17′ aldehydic site of the sarpagane component. The resulting *N*,*O*-hemiketal may then evolve into a *N*,*O*-ketal after an heteronucleophilic attack by the vobasane 17-OH group. The illustrious bis-akuammicine-type caracurine V (**115**)[210] (Fig. 35) probably arises through a similar dimerization mechanism. Two distinct

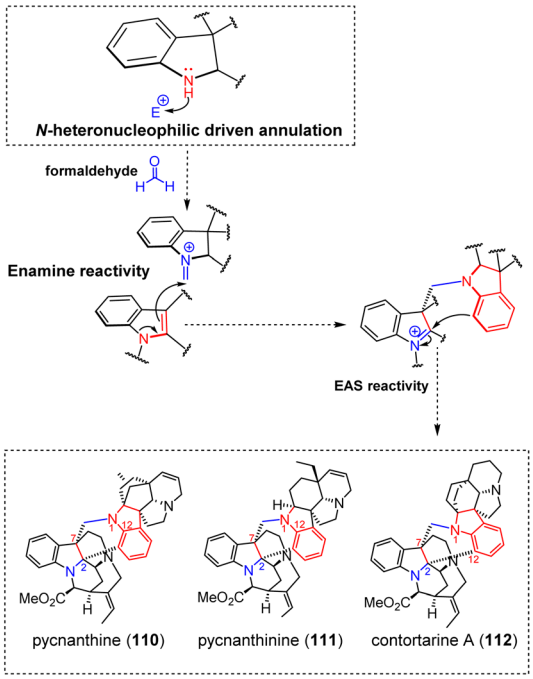

Fig. 34 Doubly-tethered oligomers resulting from a Mannich reaction combined with enamine reactivity and electrophilic aromatic substitution.

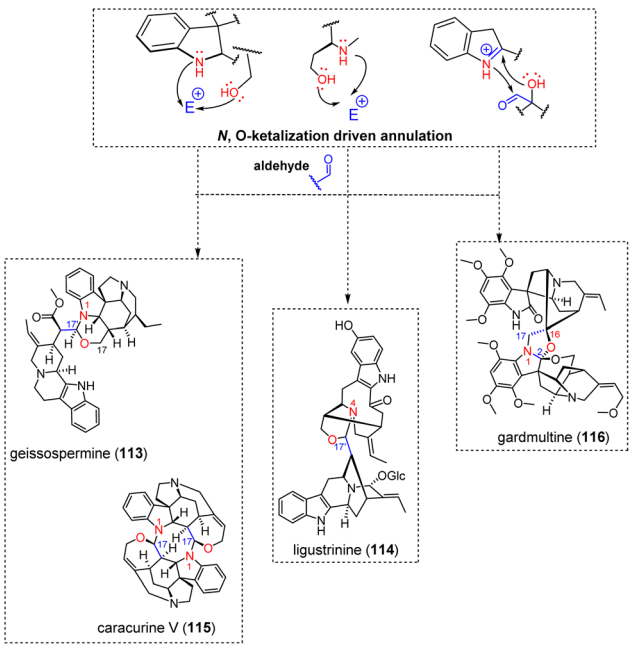

Fig. 35 Doubly-tethered oligomers resulting from *N*,*O*-ketalization.

hemiaminalization reactions may be instigated in a symmetric manner from the indoline nitrogen of an akuammicine unit to the C-17 aldehydic function of the other subunit. The seven-membered oxygenated ring of caracurine V (**115**) would then be obtained through heteronucleophilic attack of a C-18 OH group on this *N*,*O*-hemiketal. It should be noted that ketal groups sometimes occur in this specific position for some monomeric akuammicines belonging to the so-called diaboline subtype.[211] Gardmultine (**116**) (Fig. 35) and demethoxygardmultine had been simultaneously described from *Gardenia multiflora*.[212] The structure of these MIA dimers features an unusual, spiro-oxazolidine-type intermonomeric junction besides incorporating two unusual spiro-sarpagane-type components. While the southern unit strictly pertains to the spiro-sarpagane (also referred to as chitosenine) subtype[213] (16-hydroxygardneramine oxindole), the seemingly different constitution of the iminoether-containing southern component is equivalent to a masked oxindole[214] (see the example of gardneramine for related monomeric examples).[215] A first intermonomeric connection could be established by a Mannich-type heteronucleophilic attack of the N-1 atom of the gardneramine-like subunit into the oxygenated position C-17. An heteronucleophilic annulation triggered by the 16-OH on gardneramine indolenine C-2 site may then install the final spiro-oxazolidine intermonomeric junction. At last, this oxazolidine-type intermonomeric junction is reminiscent of melomorsine (**95**) that had been addressed in the former section (Fig. 27). Although a sequence initiated by an electrophilic aromatic substitution could readily account for its original constitution, an alternative path closer to that shown for geissospermine (**113**)/ligustrinine (**114**)/gardmultine (**116**) can also be proposed. In that case, the incorporation of the extraneous formaldehyde unit would result from an heteronucleophilic attack by an indolinic nitrogen. Subsequent electrophilic aromatic substitution on the corresponding N_1-exomethylene-type iminium would then avail a singly-tethered $\Delta^{1,2}$-indoleninium-containing intermediate prone to heteronucleophilic annulation, as already shown in Fig. 27.

3.2.3.5 Mannich-type reactivity. The dimerization path to the akuammicine/corynantheane-type longicaudatine F (**117**) and longicaudatine (**118**) (Fig. 36) is presumed to be initiated by a Mannich-like addition of an akuammicine type indolinic nitrogen N-1 on the C-17′ aldehydic function of a corynantheane subunit, resulting in a $\Delta^{16',17'}$ enamine function. The second connection between the two building blocks depends on the nature of the substituent undergoing the $\Delta^{16',17'}$ enamine-triggered nucleophilic attack at the C-17 position of the akuammicine unit. An aldehydic group (desacetylretulinal-type akuammicine) would result in a longicaudatine F (**117**)-type scaffold.[216] Alternatively, an hemiketal function, as observed in the akuammicine-type Wieland–Gumlich aldehyde residue, would result in a longicaudatine (**118**)-type dimer.[217] In the same spirit, the double dehydration of the bis *N*,*O*-hemiketal-containing intermediate could avail the signature diazacyclooctaediene junction of toxiferine I (**119**) (Fig. 36).[218]

Finally, doubly-tethered MIA hybrids incorporating a serine-derived component have recently been reported from *Gelsemium elegans*, namely gelsechizines A (**120**) and B (**121**) (Fig. 36).[219] Quite remarkably, these hybrid MIAs would result from an heteronucleophilic attack triggered by the non-MIA component, *viz.* the nitrogen atom of the serine derivative, targeting either the C-21 aldehydic group of a vallesiachotamane-residue (gelsechizine A (**120**)), or the C-17 aldehydic

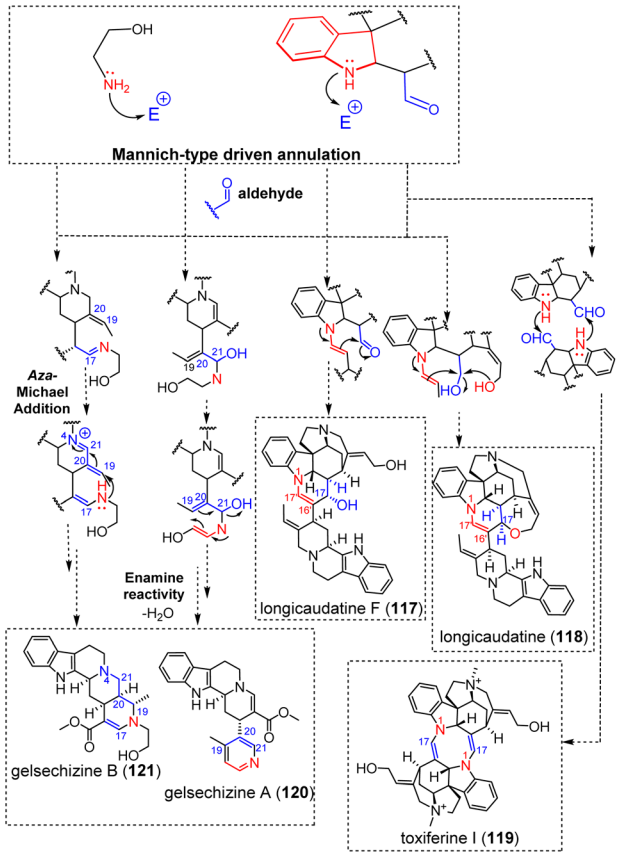

Fig. 36 Doubly-tethered oligomers resulting from Mannich-type reactivity.

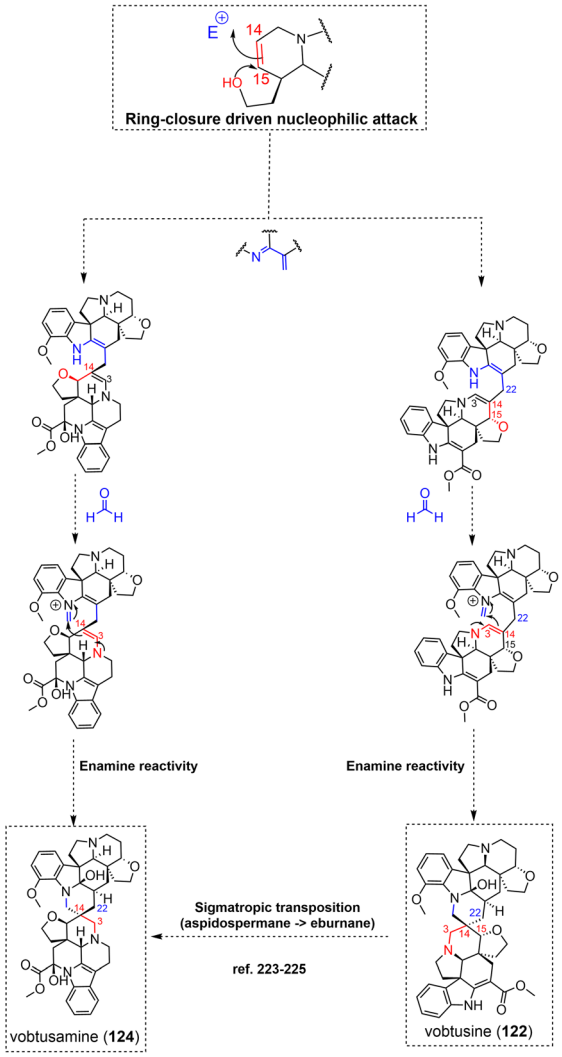

Fig. 37 Doubly-tethered oligomers resulting from ring-closure driven nucleophilic attack: putative biosynthetic pathway to vobtusine and vobtusamine (see S2‡ for a comprehensive listing).

function of a corynantheane residue (gelsechizine B (**121**)). The chemical environment of this aldehyde group determines the additional reactivity that yields the final doubly-tethered structure. As per gelsechizine A (**120**), the second intermonomeric connection seems to imply an enamine nucleophilic attack on the C-19 position of the $\Delta^{19,20}$ functionality. Regarding gelsechizine B (**121**), an aza-Michael reaction would be triggered by the addition of the nitrogen atom on the C-19 position of a conjugated $\Delta^{19,20}/\Delta^{4,21}$ iminium system analogous to that encountered in panganensine X (**29**) (Fig. 9).

3.2.4 Doubly-tethered oligomers resulting from C- and O-mediated nucleophilic attack. Four reactivities could have been outlined for this category. A detailed description of the involved mechanisms is disclosed below.

3.2.4.1 Ring closure-driven nucleophilic attack. A variety of bis-aspidospermane dimers such as vobtusine (**122**) (Fig. 37) and voacandimine A (**123**) (Fig. 38) reveal a tetrahydrofuranic ring evocative of some previously reported singly-tethered compounds like voacinol (**67**) or voacandimine C (**68**) (Fig. 20). In that case too, a ring-closure driven heteronucleophilic attack can be supposed to connect C-14 to an electrophilic partner. Vobtusine (**122**)[220] and voacandimine A (**123**)[148] derivatives may first depend on a nucleophilic attack directed on the C-22 position of a conjugated exomethylene–indolenine system to yield a singly-tethered dimeric system disclosing a C-14–C-22 bond. Further oxidation reactions would then be required to enable the formation of the second intermonomeric connection. The spiranic structure of vobtusine (**122**) seemingly requires the existence of a $\Delta^{3,14}$ enamine function on the tetrahydrofuran-containing aspidospermane unit to trigger a nucleophilic attack on an exomethylene-type N-1 iminium on the other unit. Alternatively, oxidation to a $\Delta^{3,4}$ iminium function from a similar singly-tethered intermediate could enable a direct heteronucleophilic attack by the indolinic nitrogen N-1 of the other subunit to access the scaffold of voacandimine A (**123**). A unique example of eburnane/aspidospermane dimer, namely vobtusamine (**124**) (Fig. 37),[221] could be obtained following the same sequence from a $\Delta^{3,14}$ enamine-containing eburnane. Interestingly, the authors inferred that this compound could rather be obtained following an aspidospermane to eburnane rearrangement, as proposed by Wenkert and Wickberg,[222] and subsequently validated experimentally.[223–225] In line with this hypothesis, O'Connor,

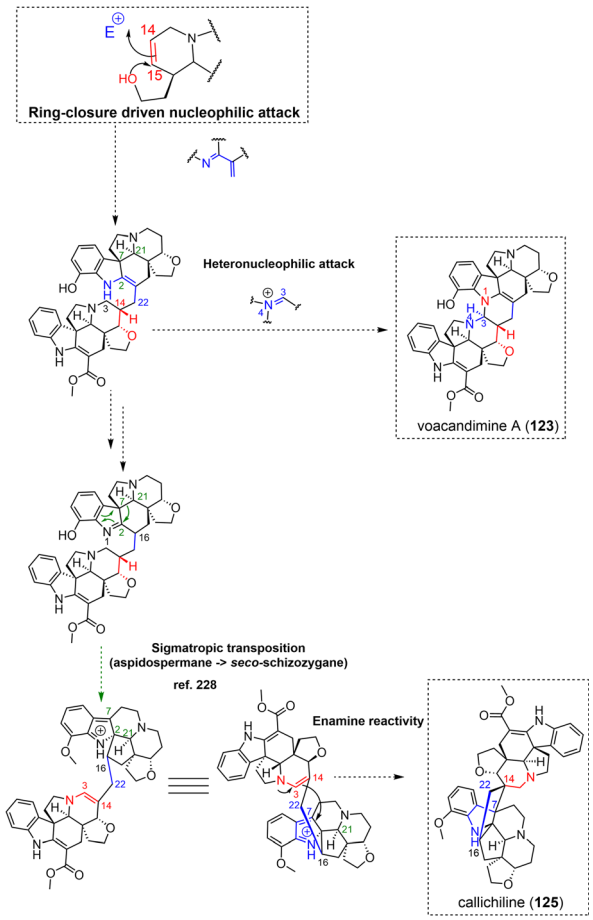

Fig. 38 Doubly-tethered oligomers resulting from ring-closure driven nucleophilic attack: putative biosynthetic pathway leading to voacandimine A and callichiline (see S2‡ for a comprehensive listing).

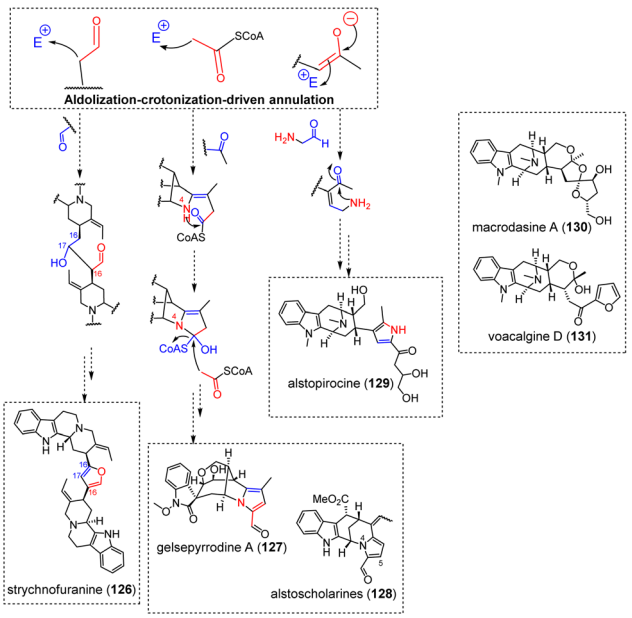

Fig. 39 Doubly-tethered oligomers resulting from aldolization–crotonization reactions (see S2‡ for a comprehensive listing).

Courdavault and co-workers had identified an enzyme capable of converting an aspidospermane-type MIA into the corresponding eburnane.[226] In their seminal report on vobtusamine (**124**), the authors could indeed transform vobtusine (**122**) into vobtusamine (**124**). The cyclopentane junction observed in callichiline (**125**) (Fig. 38) is structurally unique, and an elegant biosynthetic path to it had been suggested by Wenkert.[227] Although callichiline (**125**) discloses an heterodimeric structure comprising an aspidospermane (namely tabersonine) component and a rare *seco*-schizozygane-type subunit, its biosynthesis was proposed to proceed from two aspidospermane-type building blocks, remarkably identical to those formerly postulated to step in the biosynthesis of vobtusine (**122**), as it would only differ by the existence of a $\Delta^{1,2}$ functionality for one of them (instead of the original $\Delta^{2,16}$ unsaturation). In this indolenine configuration, a sigmatropic transposition could then convert the C-22-bonded aspidospermane-unit into the corresponding *seco*-schizozygane (namely andrangine) by dislocating the C-7–C-21 bond and installing a C-2–C-21 bond,[228] as experimentally demonstrated by Lévy *et al.* As formerly observed with vobtusine, an oxidation of the remaining aspidospermane unit to the corresponding $\Delta^{3,14}$ enamine would then be required to trigger a nucleophilic attack on the electrophilic C-7 position of the indoleninium-type andrangine, thereby availing the cyclopentanic core encountered in the structurally-unique callichiline (**125**) (Fig. 38).[132]

3.2.4.2 Aldolization. A particular case is that of strychnofuranine (**126**) (Fig. 39),[216] disclosing a unique furanic connection between two akuammicine components (*viz.* two geissoschizal components). Condensing these two aldehydic sites into the final 2,4-disubstituted furan would rely on a first sequence of aldolization/crotonization from the C-16 site of a first geissoschizal on the C-17 aldehydic site of the second unit to first provide an intermediate with a single intermonomeric bond, prone to allylic oxidation. Hemiketalization and final dehydration could afford the furanic junction appearing in strychnofuranine (**126**). Aldol-type reactions are mostly related to polyketides biosynthesis[229] and as such hybrid compounds comprising both a MIA and a polyketide component were supposed to be obtained following this kind of reactivity. Gelsepyrrodine A (**127**) (Fig. 39) represents one such example of gelsedane/polyketide-type hybrid. An aldolization reaction between acetyl-CoA and the C-19 position of the gelsedane-type 19-oxo-gelsenicine and would afford a singly-bonded gelsedane-polyketide adduct.[230] Subsequent heteronucleophilic attack of the alicyclic nitrogen N-4 on the carbonylic thioester would then give access to a transient carbinolamine function, also connected to a CoA thioester. This site could undergo a Claisen-type nucleophilic attack from an additional acetylCoA unit. Two dehydration reactions could provide the final pyrrole ring of gelsepyrrodine A (**127**). Finally, the decarboxylation of the polyketide-type side chain and its subsequent oxidation into an aldehyde leads to the final product. A related sequence can be proposed to account for the constitution of alstoscholarines (**128**) (Fig. 39). At first, an extraneous malonyl CoA unit can be

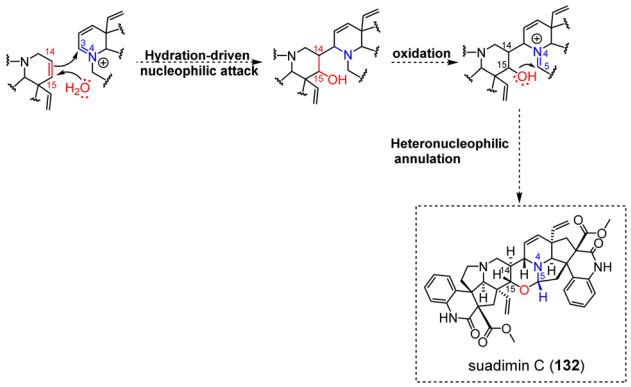

Fig. 40 Doubly-tethered oligomer resulting from an hydration-driven nucleophilic attack.

supposed to undertake an aldolization/crotonization into the C-5 aldehyde function of a rearranged akuammilane subunit (this reactivity will be further developed in the frame of alstoniasidine A (**134**) biosynthesis (Fig. 41)).[231] It can be assumed that the subsequent hydration of this singly-tethered intermediate enables a subsequent heteronucleophilic annulation initiated by the alicyclic nitrogen N-4 of the MIA, installing the final pyrrole ring after dehydration of the hemiaminal.[232] Aldolization/crotonization-based dimerization sequences are also presumed to step in the biosynthesis of some hybrid macrolane-based oligomers. Dimerization trends related to macrolane-type MIAs have already been addressed in this document, mostly relying on

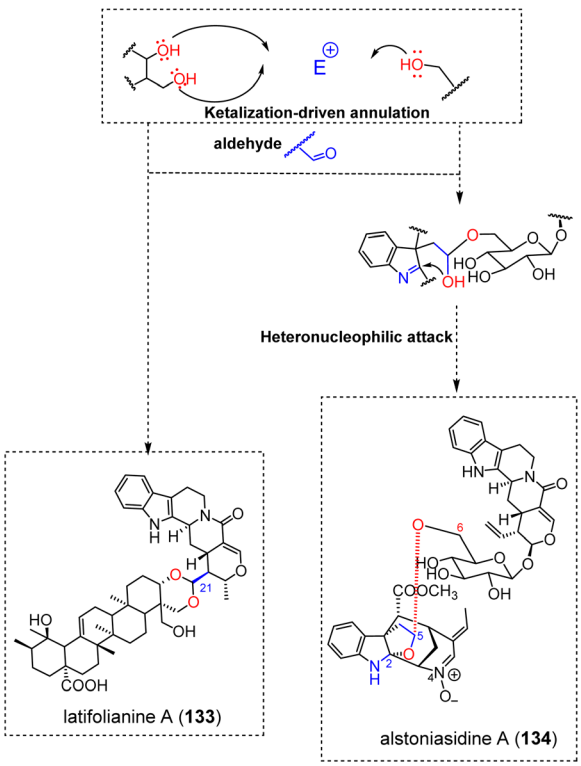

Fig. 41 Doubly-tethered oligomers resulting from acetalization reactivity.

the occurrence of Michael acceptors in their monoterpenic part (Fig. 8). Nevertheless, a few compounds incorporating a macrolane-type MIA reveal an alstomicine-type constitution,[233] *viz.* without a carbon residue at C-20, thereby revealing a nucleophilic enol function. Even though the constitution of such macrolane-type MIAs is not canonical, other such structures were reported, including alstonoxines A and B.[234] Acid hydrolysis proved capable of converting a B-type macroline into the corresponding macroline without a carbon substitute at C-20.[235] Alstopirocine (**129**) (Fig. 39) reveals an intriguing hybrid structure combining a macrolane but also a biosynthetically puzzling pyrrole substituted with a polyketide side chain. Kam *et al.* envisaged that the enolic side chain of alstomicine would initiate an aldol condensation/crotonization on an aldehyde-containing glycine analogue, presumed to evolve into a pyrrole after a Mannich-type reaction. The pyrrolic side chain would then be obtained based on a Claisen-type reaction triggered by the dienamine function of the pyrrole ring on a poly-β-ketoester.[236] Likewise, the intriguing bispiranic structures of macrodasine A (**130**) (Fig. 39) have been suggested to derive from alstomicine-type precursors.[237,238] For such compounds, the C-20 position would be alkylated by a C_6 fragment which would enable a tandem hemiketalization.[239] Singly-tethered analogues such as voacalgine D (**131**) (Fig. 39) and E are presumed to derive from a similar intermediate through different reactivity sequences. Voacalgine D (**131**) would be obtained after a hemiketalization and an aldolization/crotonization sequence to afford the furanic cycle. Alternatively, voacalgine E would derive from an oxa-Michael 1,4-addition with a similar aldolization/crotonization affording the furanic ring.[240]

3.2.4.3 Hydration-driven nucleophilic attack. The oxazinane-containing bis-Melodinus MIA dimer suadimin C (**132**) (Fig. 40) would be obtained based on a reactivity analogous to that having led to the formerly detailed suadimin A (**75**) (Fig. 21). Again, a hydration-driven nucleophilic attack triggered by the $\Delta^{14,15}$ bond on the $\Delta^{3,4}$ iminium function of the other subunit would afford a C-3–C-14 bonded intermediate. An oxidation is then presumed to occur on the C-3 bonded unit to yield the corresponding $\Delta^{4,5}$ iminium that can undergo an heteronucleophilic attack by the 15-OH group of the other subunit, installing the final 1,3-oxazinane unit.[241]

3.2.4.4 Acetalization. The unique MIA/triterpene hybrid known to date, namely latifolianine A (**133**) (Fig. 41), features a 1,3-dioxane based junction. An acetalization reaction involving the C-21 aldehydic function of naucleidinal (vallesiachotamane-type MIA) and two hydroxy groups of the ursane triterpene 3β,19α,23,24-tetrahydroxyurs-12-en-28-oic acid can easily account for the constitution of the final scaffold.[242] A few years ago, alstoniasidines A (**134**)[24] (Fig. 41) and B revealed an unprecedented sugar bridge between two MIA units. The sugar moiety instigating the intermonomeric connection belongs to the vallesiachotamane-type strictosamide. The other subunit corresponds to a thoroughly modified akuammilane-type component. Such scaffolds should be related to picrinine as a common precursor, benefitting from its characteristic ether connection between C-2 and C-5. An array of picrinine derivatives result from a disruption of N-4–C-5 connectivity. Some

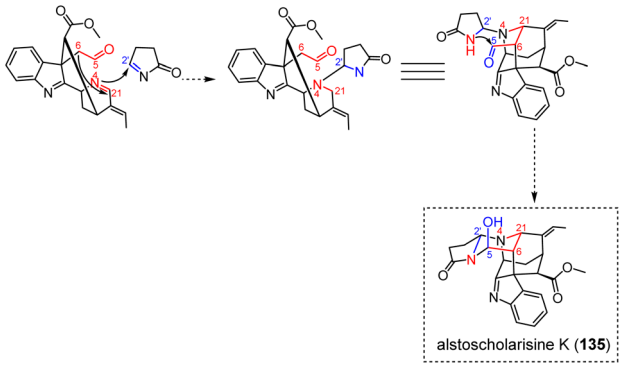

Fig. 42 Plausible enolization-driven aminalization path to alstoscholarisine K (135).

analogues, often referred to as Hofmann degradation[243]-derived compounds, disclose a more or less oxidized furanoindoline scaffold.[244,245] Alternatively, a concerted mechanism jointly disrupting both C-2-O and N-4–C-5 bonds might lead to reactive species containing both an indolenine core and an aldehydic function at C-5 has been proposed to step in the biosynthesis of various, highly-rearranged picrinine derivatives.[231,246] Back to alstoniasidines, such an aldehyde-containing analogue can initiate an acetalization reaction implying the 6-OH residue of strictosamide glucose.

3.2.4.5 Enolization-driven aminalization. Hybrid compounds were also proposed to proceed from an aldehyde-containing picrinine derivative. As such, alstoscholarisine K (**135**) (Fig. 42) is an intriguing hybrid incorporating a pyrrolic unit presumed to derive from spermine or putrescine. A nucleophilic attack would be initiated by the α-carbonylated C-6 position on a $\Delta^{4,21}$ functionality which would then trigger a second nucleophilic attack on the C-2′ position of an extraneous Δ^{1}-pyrroline. A Mannich-type nucleophilic addition by the pyrroline nitrogen into the aldehydic group would then lead to alstoscholarisine K (**135**).[247]

3.2.5 Doubly-tethered oligomers resulting from enamine reactivity. Combination of different reactions could have been identified to describe the chemical space of this section. They are described below.

3.2.5.1 Michael addition followed by heteronucleophilic annulation. The specific constitution of the monoterpenic component of gelsedane-type MIA was already shown to disclose a peculiar reactivity towards a broad range of electrophilic partners. Through the specific example of the pseudodimeric gelsedane-iridoid type gelsamydine (**62**) (Fig. 18), the possibility for the 2-ethylidenepyrroline system to undertake 1,4-Michael addition (*i.e.* from the C-19 position) has already been covered in this review. From such singly-tethered intermediates, the access to gelserancine B (**136**) (Fig. 43) is straightforward. An heteronucleophilic attack of the alicyclic nitrogen N-4 on the carbonylic lactone of the additional iridoid unit could install the final tetrahydropyridinone nucleus of gelserancine B (**136**).[248] The pyridinium-containing gelsedane/corynantheane gelsecorydine B (**137**) (Fig. 43) can also be related to the biosynthesis of the singly-tethered gelsecorydine A (**57**) (Fig. 17). An enamine-driven

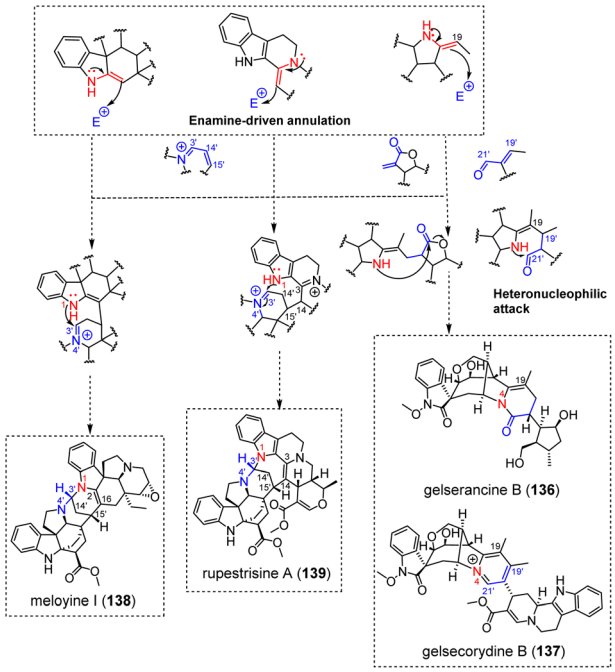

Fig. 43 Doubly-tethered oligomer resulting from enamine reactivity (Michael addition + heteronucleophilic addition).

nucleophilic attack initiated from the gelsedane C-19 position on the C-19′ position of the α,β-unsaturated aldehyde function of the vallesiachotamane unit in addition to an heteronucleophilic attack from the alicyclic nitrogen N-4 of the gelsemium subunit into the aldehydic component at the vallesiachotamane C-21′ position could yield the tetrahydropyridinium ring of gelsecorydine B (**137**)[249] after dehydration.

The aspidospermane/aspidofractane-type meloyine I (**138**)[250] and the recently reported ajmalicine/aspidofractane-based rupestrisines A (**139**) (Fig. 43) and B[251] feature an unprecedented tetrahydropyridine-based intermonomeric junction. None of the seminal phytochemical reports proposed a dimerization mechanism to account for their unusual intermonomeric connectivity. In both cases, a nucleophilic attack initiated by an enamine function (involving the alicyclic nitrogen in the case of the $\Delta^{3,14}$-containing rupestrisine A (**139**) ajmalicine unit or the indolinic nitrogen for the $\Delta^{2,16}$-containing aspidospermane unit of meloyine I (**138**)) into the C-15′ position of a conjugated iminium-containing aspidofractane can be presumed to avail a singly-tethered dimeric intermediate. Considering the $\Delta^{3',4'}$ iminium analogue of the enamine intermediate would allow final ring closure through an heteronucleophilic annulation instigated by the indolinic nitrogen N-1. Notably, the relative configurations of rupestrisines A (**139**) and B had been later revised by Kutateladze and co-workers using a machine-learning improved DU8-ML DFT-NMR workflow.[252] The structure shown for rupestrisine A (**139**) (Fig. 43) takes into account this structure revision, differing from the initial one by the configuration of C-3′.

3.2.5.2 Unconjugated iminium addition in combination with heteronucleophilic annulation. Husson, Lounasmaa *et al.*

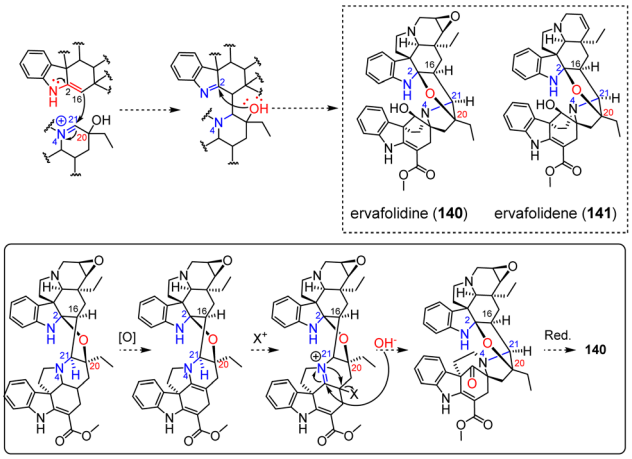

Fig. 44 Top: doubly-tethered oligomer resulting from enamine reactivity (iminium addition + heteronucleophilic addition). Bottom: putative rearrangement from pandolinane to isopandolinane.

reported on the intriguing structures of ervafolidine (**140**) and ervafolidene (**141**) (Fig. 44) in the early 1980s.[253] Beyond the dimerization mechanism, the MIA subtype of the southern counterpart raised some biosynthetic questions since these atypical dimers were first described. The dimerization would rely on the condensation of a $\Delta^{2,16}$ enamine derived from the aspidospermane unit on a $\Delta^{4,21}$ iminium-containing 20-*epi*-pandoline. This reactivity would be followed by the heteronucleophilic annulation triggered by the 20-OH group of the 20-*epi*-pandoline component on the C-2 position of the indolenine-type aspidospermane setting up the intermonomeric ether connection. To complete the biosynthesis of ervafolidine (**140**) and ervafolidene (**141**), its southern component must now rearrange itself into the final isopandolinane-type constitution, *i.e.* rearrange the piperidine ring into the corresponding ketone-containing spiropyrrolidine (Fig. 44). For this purpose, Henriques *et al.* suggested to consider an oxidized pandoline component revealing a $\Delta^{3,4}$ iminium. Nucleophilic attack by an OH- on this functionality could then lead to a carbinol amine and then to an aziridinium intermediate that can open to yield the corresponding ketone.[253] Various organic synthesis studies support this presumed biosynthesis sequence.[254,255]

3.2.5.3 Conjugate 1,6-addition in combination with aza 1,6-addition. Monogagaine (**142**)[256] and flabellipparicine (**143**)[257] (Fig. 45) are rare MIA dimers featuring a vallesamane building block, along with a more or less transformed vobasane constituent. The C-3 site of the vobasanoid component has already been described as an electrophilic site of considerable generality, as it can undergo a conjugate 1,6-addition from a wealth of nucleophilic partners. As per monogagaine (**142**) and flabellipparicine (**143**), this usual 1,6-addition would be triggered by the exomethylene function of the conjugated $\Delta^{16,22}$ exomethylenic functionality of the vallesamane unit to afford a singly-bonded intermediate. In both cases, the driving force for this nucleophilic attack would be an heteronucleophilic attack by the indolic nitrogen of the vobasanoid component on the C-16 position of the vallesamane (*viz.* apparicine) counterpart.[258]

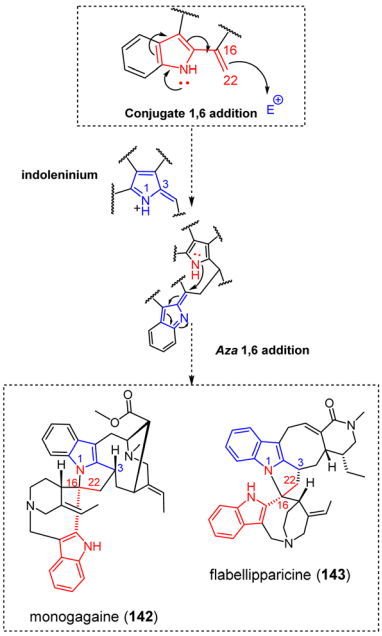

Fig. 45 Doubly-tethered oligomer resulting from conjugated 1,6-addition and aza 1,6-addition.

3.2.5.4 Nucleophilicity and electrophilicity of the pleiocarpamane skeleton. Some salient reactivity trends of the pleiocarpamane-type MIAs had been outlined earlier in this review through the examples of pycnanthine (**110**), pycnanthinine (**111**) and contortarine A (**112**) that shed light on both the nucleophilicity of pleiocarpamane scaffold C-7 position and the electrophilicity of C-2 (Fig. 34). The pleiocarpamane/vobasane-type hunterizeyline F (**144**)[259] (Fig. 46) results from a nucleophilic attack triggered by the enamine function comprised in the strained indolic system of the pleiocarpamane-type MIA on the C-3 electrophilic site of a vobasinyl residue. Heteronucleophilic annulation by the vobasane indolic nitrogen on the C-2 position of the indoleninium-containing pleiocarpamane would then avail the five-membered nitrogenated heterocycle connecting the pleiocarpamane and vobasane components of hunterizeyline F (**144**) (Fig. 46). Although structurally different, the biosynthesis of villalstonine (**145**)[201] (Fig. 46) proceeds *via* a similar mechanism. The nucleophilic attack of the pleiocarpamane enamine function at C-7 should be directed on the exomethylenic C-21 site of the α,β-unsaturated ketone system of macroline (formally a type A macroline Fig. 8) to perform a 1,4-Michael addition (see alstomacrophylline (**25**) (Fig. 9) for an analogous reactivity). An hemiketalization reaction should then take place in the macrolane unit from the C-17 OH group on the no longer-conjugated ketone carbonyl at C-19. Finally, heteronucleophilic annulation by the hemiketalic OH group on pleiocarpamane C-2 indoleninium provides the final structure of villalstonine (**145**). The early biomimetic synthesis of villalstonine (**145**) substantiates this putative biosynthetic pathway.[201]

Pleiocarpamane derivatives were shown to react with diverse phenolic substances. Voacalgine A (**146**) (Fig. 47) represents a pleiocarpamane-type MIA fused with a pyrocatechuic-type benzoic acid moiety. First erroneously elucidated after its first

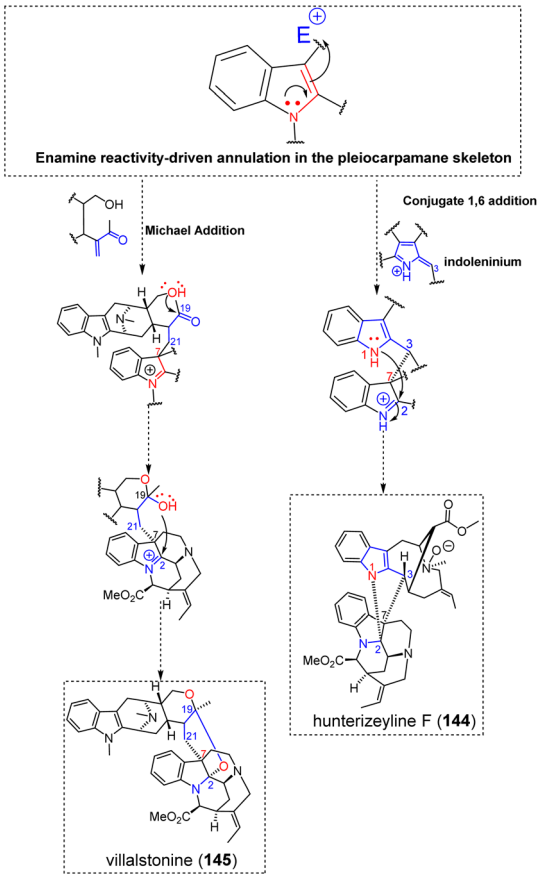

Fig. 46 Doubly-tethered MIA dimers resulting from the characteristic reactivity of the pleiocarpamane skeleton.

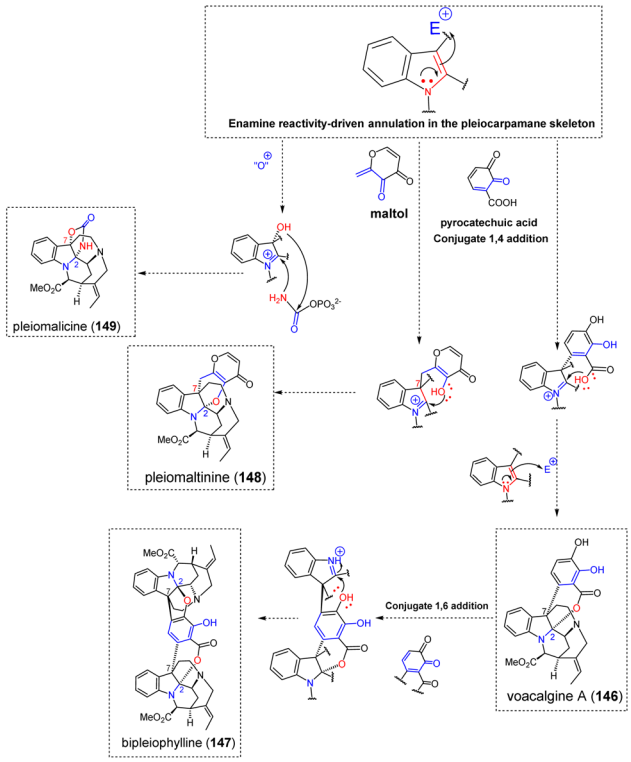

Fig. 47 Doubly-tethered heterodimers resulting from the characteristic reactivity of the pleiocarpamane skeleton.

isolation in 2015,[240] its structure was revised to the disclosed regioisomer a few years later, in the frame of its hemisynthesis.[260] The postulated biosynthesis of voacalgine A (**146**) involves the oxidation of the catechol moiety of pyrocatechuic acid into the corresponding *ortho*-quinone. A 1,4-Michael addition initiated by the pleiocarpamane enamine function on the electrophilic site contiguous to the carboxylic acid function of this oxidized unit could yield a singly-tethered indoleninium, prone to further heteronucleophilic annulation through attack of the carboxylic acid OH group on the C-2 electrophilic position of the indoleninium.[260] Oxidation of the catechol unit of voacalgine A (**146**) would enable a subsequent 1,6-addition by a second pleiocarpamane component through a similar enamine-driven nucleophilic attack. A heteronucleophilic attack from the contiguous phenolic group on the C-2 indoleninium site of this second pleiocarpamane unit would lead to bipleiophylline (**147**) (Fig. 47),[261] the sole MIA dimer known to date comprising two MIA components anchored on an aromatic spacer platform. Again, this speculative biosynthetic scenario received support from synthetic reports.[260,262] A slightly different, yet related MIA-phenolic hybrid is represented by the pleiocarpamane-γ-pyrone-type pleiomaltinine (**148**) (Fig. 47). Along with its original report, Kam *et al.* suggested that the biosynthesis of pleiomaltinine should proceed from an oxidized form of the co-isolated maltol to reveal a conjugated exomethylenic system prone to undergo a nucleophilic attack by the pleiocarpamine $\Delta^{2,7}$ enamine moiety. An heteronucleophilic annulation by the contiguous phenolic site on pleiocarpamine indoleninium C-2 could then yield pleiomaltinine (**148**).[236] Again, this putative scenario was further supported by synthesis, using 3-siloxy-4-pyrone derivatives that disclose a reactivity analogous to that of the putative oxidized pyrone.[263] In a similar spirit of reactivity, pleiomalicine (**149**) (Fig. 47) oligomerization assembly may start with the oxidation of the enamine part of pleiocarpamine into a 7-hydroxy-indoleninium precursor. It is worth noting that this oxygen addition at C-7, enabling dearomatization of indole, can be encountered in other MIAs such as terengganensine A[264] and rhazidine.[265] At last, an heteronucleophilic attack by the 7-OH group on a carbamoyl phosphate unit could install a singly-tethered intermediate prone to yield the final scaffold by heteronucleophilic annulation on the indoleninium C-2 position.[236]

3.2.5.5 Aldehyde addition combined to a Mannich-type reaction. As a unique trimeric instance in this section, trirosaline (**150**) (Fig. 48) represents an intriguing tris-ajmalicine-type MIA and the first trimer ever reported from the emblematic plant, *Catharanthus roseus*.[266] Its oligomerization process would rely on the condensation of a $\Delta^{5,6}$ enamine, which is derived from a first ajmalicine unit on the retro-Mannich-derived C-5′ aldehydic function of a *seco*-ajmalicine unit. The second inter-monomeric N–C connection could be obtained through a Mannich-type reaction from the *seco*-ajmalicine N-4′ on the C-6″ oxidized ajmalicine of a third ajmalicine residue. This latter

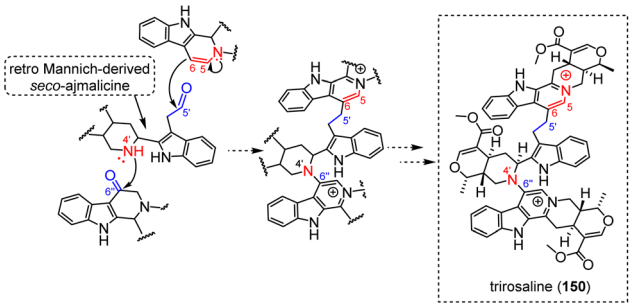

Fig. 48 Plausible biosynthetic path to trirosaline (aldehyde addition and Mannich-type reaction).

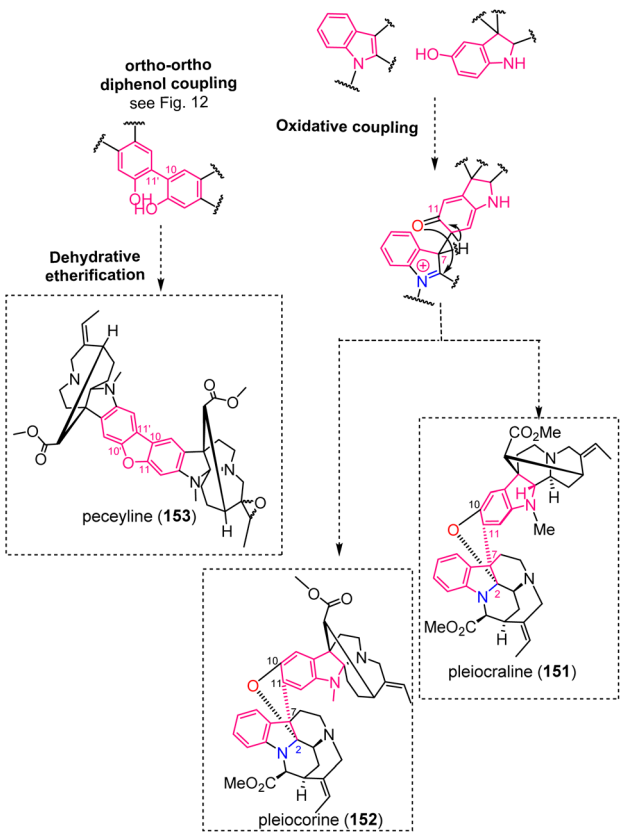

Fig. 49 Doubly-tethered oligomers resulting from phenolic couplings (see S2‡ for a comprehensive listing, pink color indicates groups involved in the radical coupling reactivities).

reactivity is, in some ways, reminiscent of undulatine (**32**) (Fig. 9) bridging mode.

3.2.6 Doubly-tethered oligomers resulting from cycloadditions and radical couplings. Two main coupling modes seem to be involved in this section. Selected compounds are summarized below.

3.2.6.1 Phenolic coupling. Pleiocraline (**151**)[267] and pleiocorine (**152**)[268] are two pleiocarpamane–akuammilane MIA dimers that share a common benzofuroindoline junction (Fig. 49). This connection mode is presumed to derive from an oxidative coupling between the C-7 site of the pleiocarpamane unit with the C-11 *ortho*-phenolic site of the akuammilane counterpart. Such a reactivity had already been considered for the singly-tethered haplophytine (**48**) and cimiciphytine (**49**) (Fig. 14), where the canthinone component reveals some degree of structural analogy with the pleiocarpamane scaffold. The singly-tethered C-7–C-11 intermediate can undergo a final heteronucleophilic annulation on the C-2 pleiocarpamane indoleninium to install the sought-after benzofuroindoline motif. Notably, in the context of their synthesis of haplophytine (**48**),[119] Nicolaou and Chen accessed doubly-tethered intermediates analogous to pleiocraline (**151**) and pleiocorine (**152**), further strengthening the analogy between these two kinds of MIA dimers. The isopleiocarpamane/vincorinane—type peceyline (**153**) (Fig. 49) features a dibenzofuran junction involving the benzene ring of both indoline systems.[269] The biaryl C–C linkage between C-10 and C-11′ is first presumed to arise through a radicalar process (see ceylanine (**44**), Fig. 14), probably benefitting from the occurrence of *ortho*-phenolic functionalities increasing the spin density at the connected sites. Subsequently, a dehydrative etherification would cause a ring closure and install the final furanic junction by forming an ether bond between C-11 and C-10′. This process is of considerable generality in the biosynthesis of dibenzofuran-type natural products.[270]

3.2.6.2 (Hetero)-Diels–Alder. Dimeric MIAs obtained through a Diels–Alder reaction are quite scarce. A first interesting case is represented by secamines, rare MIA dimers mainly described in the 1970s with partial stereochemical assignments. Secodine-type alkaloids are prone to dimerization owing to their acrylic ester system. Therefore, presecamine

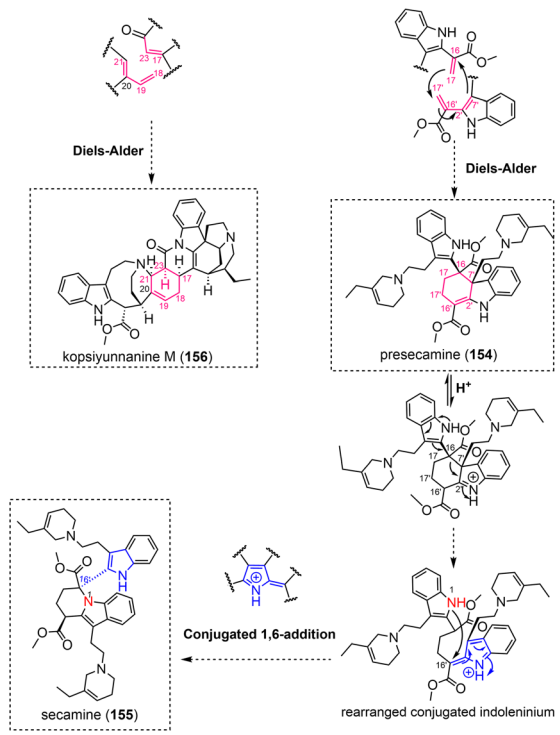

Fig. 50 Doubly-tethered oligomers resulting from Diels–Alder cycloadditions (see S2‡ for a comprehensive listing, pink color refers to structural elements related to Diels–Alder reaction).

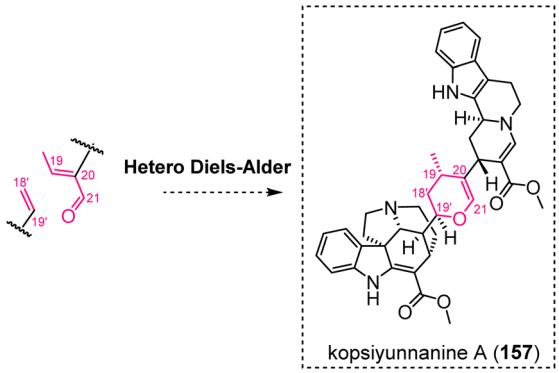

Fig. 51 Doubly-tethered oligomer resulting from an hetero-Diels–Alder cycloaddition. (see S2‡ for a comprehensive listing, pink color indicates structural features involved in hetero-Diels–Alder reaction).

(**154**)[271] (Fig. 50) is a dimeric secodine obtained through a Diels–Alder reaction involving the $\Delta^{16,17}$ functionality of a first secodine as the dienophile and the $\Delta^{2',7'}$ and $\Delta^{16',17'}$ of a second secodine building block as the dienic system. Presecamine (**154**) was shown to rearrange quantitatively to secamine (**155**) (Fig. 50) in dilute HCl at room temperature.[271] Cordell *et al.* proposed a rearrangement mechanism giving rise to a conjugated indoleninium as shown in Fig. 50, that could undergo 1,6-addition from the indolic nitrogen on the C-16′ position of the other secodine subunit.[271] A further case of Diels-Alder derived MIA dimer is the stemmadeninane/strychnane-based kopsiyunnanine M (**156**) (Fig. 50).[272]

The dienic system is represented by the $\Delta^{20,21}$ and the vinylic $\Delta^{18,19}$ functionalities of the stemmadeninane unit, reacting on the characteristic $\Delta^{17,23}$ functionality of the strychnane counterpart. Another last example of cycloaddition-related dimerization process is that of kopsiyunnanine A (**157**) (Fig. 51).[273] This condylocarpane/vallesiachotamane-based MIA dimer could be obtained through a hetero-Diels–Alder reaction involving the α,β-unsaturated aldehyde of vallesiachotamane as the diene (*i.e.* $\Delta^{19,20}$ and the aldehydic group at C-21) and the vinylic $\Delta^{18',19'}$ functionality of an oxidized derivative of 18,19-dehydrotubotaiwine as the dienophile.[273] Although unique in the broad group of MIA oligomers, hetero-Diels–Alder reaction appears to be more common in the bis-diterpenoids group[274] and is also invoked to access dimeric triterpenes and sterols,[275,276] affording the signature dihydropyran-type intermonomeric junction. Diels–Alder-based dimerization reactions are also involved in the biosynthesis of borreverine/isoborreverine-type dimeric structures that proceed from borrerine.[277] Enamine reactivity followed by heteronucleophilic annulation (borreverine) or heteronucleophilic attack (isoborreverine) further step in the biosynthesis of these compounds that lie outside of the scope of the current review.[278,279]

3.3 Oligomers featuring a mixed tethering mode

A limited number of oligomers result from a combination of the two above mentioned tethering modes. They are disclosed in Fig. 52.

3.3.1 Iminium trapping.

The strychnane/akuammicine/akuammicine-type strychnohexamine (**158**)[280] (Fig. 52) discloses a characteristic, toxiferine I (**119**)-like (Fig. 36), diazacyclooctadiene inter-akuammicine junction that had previously been related to a double hemiaminalization (heteronucleophilic attack from an indolinic N-1 on the aldehydic C-17 group of the other akuammicine component, in a symmetric manner) and subsequent dehydration of these *N*,*O*-hemiketalic groups (Fig. 36). Likewise, the connection between the strychnane and northern akuammicine component is strictly analogous to that previously reported to occur in the biosynthesis of bis-strychnane-type MIA dimers strychnogucine A (**73**) and sungucine (**76**) (*viz.* hydration-driven $\Delta^{17',23'}$ enamine nucleophilic attack on a $\Delta^{4,5}$ iminium) (Fig. 21).

A remarkable example of oligomeric MIA with mixed tethering modes is alasmontamine A (**159**) (Fig. 52),[132] the sole example of tetrameric MIA known to date, comprising four aspidospermane units. More precisely, this structure should be considered as a dimeric vobtusine (**122**). The biosynthetic path to vobtusine (**122**) supposedly steps through a ring closure-driven nucleophilic attack from the $\Delta^{14,15}$ functionality on a conjugated exomethylene indolenine system (as reported to occur in the biosynthesis of both voacandimine A (**123**) and voatriafricanine A (**160**)). The spiranic junction of vobtusine would then derive from the enamine nucleophilic attack of a newly installed $\Delta^{3,14}$ moiety into an exomethylene-type N-1 iminium of the other aspidospermane unit (Fig. 37). The connection between the two vobtusine building blocks can easily be related to an enamine ($\Delta^{5,6}$)-driven nucleophilic attack into a $\Delta^{4',5'}$ iminium function of the other vobtusine counterpart. As of 2024, a MIA dimer disclosing this precise connectivity does not seem to have been reported, but this reactivity can be related to that having led to the bis-aspidofractane arbolodinine A (**51**) that involved a similar $\Delta^{4,5}$ iminium electrophilic partner but involved a different $\Delta^{3,14}$ enamine (Fig. 16).

3.3.2 Electrophilic aromatic substitution on indoleninium.

The constitution of the first ever-reported vobasane/aspidospermane/aspidospermane-type voatriafricanines A (**160**)[281] (Fig. 52) and B can be easily delineated by referring to formerly developed reactivity trends. The aspidospermane/aspidospermane connection is reminiscent of that seen in voacandimine A (**123**) (Fig. 38), although it relates to a different diastereoisomeric series. Briefly, this junction was proposed to arise from the ring closure-driven nucleophilic attack of a $\Delta^{14,15}$ functionality into the conjugated C-22 site of the exomethylene indolenine unit of the other aspidospermane unit, followed by heteronucleophilic annulation of the indolinic nitrogen into the C-3 site of the $\Delta^{3,4}$ iminium obtained after the first reaction related to enamine reactivity. The incorporation of the vobasane unit relies on an electrophilic aromatic substitution triggered by the northern aspidospermane unit monomer C-10 site on the electrophilic C-3′ position of the vobasane residue.

3.4 Triply-tethered oligomers

A few dimeric MIAs feature three intermonomeric connections. Most often, these junctions can be related to a doubly-bonded dimeric structure but involve an additional reaction.

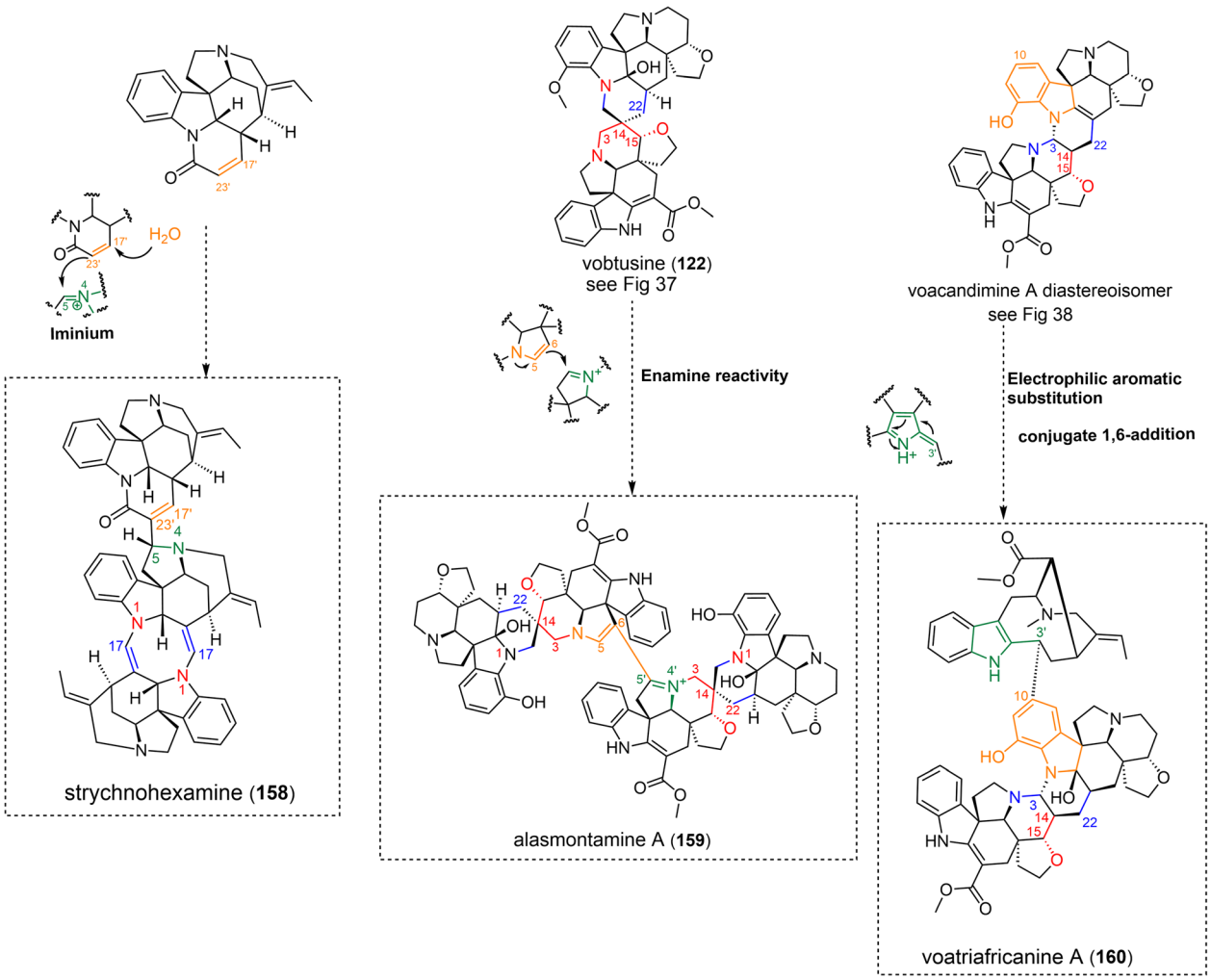

Fig. 52 Oligomers featuring mixed tethering modes (see S2‡ for a comprehensive listing, red and blue-colored moieties refer to a first set of nucleophilic and electrophilic sites, respectively; orange and green colored moieties refer to a second set of nucleophilic and electrophilic sites, respectively).

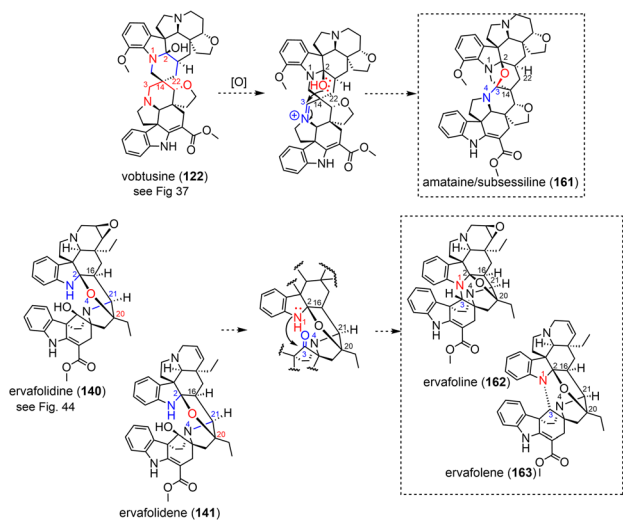

Fig. 53 Triply-tethered oligomers resulting from heteronucleophilic annulation-driven oligomerization.

3.4.1 (Hetero)nucleophilic annulation-driven oligomerization. As a first example to introduce this category, the triply-tethered scaffold of amataine/subsessiline (**161**)[220] (Fig. 53) can be easily related to the spiranic junction seen in vobtusine (**122**).[282] Converting vobtusine (**122**) into amataine/subsessiline (**161**) would merely imply an heteronucleophilic annulation of the 2-OH group into the $\Delta^{3,4}$ iminium of the other aspidospermane counterpart. Likewise, the triply-connected aspidospermane and isopandolinane subunits appearing in ervafoline (**162**) (Fig. 53) and ervafolene (**163**) (Fig. 53) should be related to their doubly-bonded analogues ervafolidine (**140**) and ervafolidene (**141**) (Fig. 44).[283] The complex biosynthetic path to the doubly-tethered ervafolidine (**140**) and ervafolidene (**141**) revealed these dimeric structures to derive from the $\Delta^{2,16}$ enamine reactivity guided condensation of an aspidospermane unit into a $\Delta^{4,21}$-iminium-containing pandolinane unit, followed by the heteronucleophilic attack of the pandolinane 20-OH group on the C-2 site of the aspidospermane indoleninium. The pandolinane would then rearrange to an isopandolinane (Fig. 44). Notably, the rearrangement into the isopandolinane

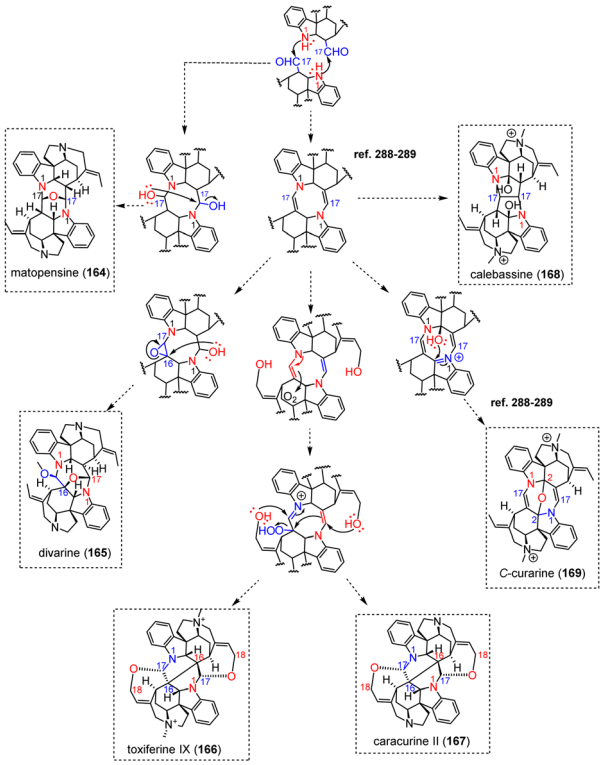

Fig. 54 Plausible biosynthetic path to diazacyclooctadiene-containing MIA dimers and related compounds.

scaffold also resulted in installing an oxygenated moiety at C-3 that can undergo further heteronucleophilic annulation from the indolinic N-1 nitrogen of the aspidospermane counterpart, resulting in triply-tethered structures such as ervafoline (**162**) and ervafolene (**163**) (Fig. 53).[253]

Finally, the diazacyclooctadiene junction of bis-akuammicine type MIA as it appears in toxiferine I (**119**) (Fig. 54) was experimentally shown to represent an entry point into many triply-tethered MIA dimers.[284] These dimeric compounds can readily undergo further chemical change, shown to depend on the conditions of pH, heat and the presence of oxygen.[80] In these conditions, the central ring of these dimeric structures can undergo changes in oxygenation level (Fig. 54). The triple connection appearing in matopensine (**164**)[285] can be related to the non-dehydrated precursor of the diazacyclooctadiene scaffold, from which it could derive by dehydrative etherification. Divarine (**165**)[286] features a similar junction but distinct tethering sites compared with matopensine (**164**). An intermediate revealing both a *N*,*O*-hemiketalic group and an epoxide function can be supposed to step in the biosynthesis of this MIA dimer as shown in Fig. 54. The epoxide ring opening at C-16 initiated by the *N*,*O*-hemiketalic OH group at the C-17 position of the other component can be presumed to yield the intermonomeric connectivity appearing in divarine (**165**), only requiring subsequent *O* methylation to obtain the final product. Toxiferine IX (**166**)/caracurine II (**167**)-type triply-tethered akuammicine dimers (*viz.* featuring an additional C-16 to C-16′ bond) has been investigated by Battersby and co-workers in the late 1960s.[287] It was noted that the dimerization of toxiferin I into caracurine II (**167**) depended on acid and oxygen. A tentative mechanism has been proposed that would be initiated by an enamine nucleophilic attack of O_2 at C-16, hinting a plausible artefactual origin for such compounds. A second nucleophilic attack triggered by the second enamine function of this eight-membered junction into the peroxyhemiketal, could then yield the complex triple intermonomeric connection appearing in toxiferine IX (**166**)/caracurine II (**167**).

Photooxidation reactions were shown to lead to another subtype of triply-tethered akuammicine dimers. Since the late 1950s,[288,289] Bernauer and co-workers reported on unusual, photosensitized oxygen transfer reactions to several calabash curares. The diazacyclooctadiene-containing *C*-dihydrotoxiferine I and toxiferine I (**119**) were respectively shown to transform into calebassine (**168**) and *C*-alkaloid A when irradiated in aerated solutions in the presence of eosin as sensitizer. Exposed to light and air in the absence of sensitizer, alternative scaffolds containing an additional ether bond (*viz.* respectively *C*-curarine (**169**) and *C*-alkaloid E) would be obtained instead.[288,289] A radical hydroxylation at C-2 can be envisaged for *C*-curarine (**169**), which could evolve into the sought-after ether connectivity by heteronucleophilic attack to the C-2 oxidized indoleninium akuammicine counterpart. In neither case could a definite reaction mechanism be established although transannular reactions analogous to that converting toxiferine I to *C*-alkaloid A did not seem to have been reported prior to these photooxidation studies.[290,291]

The diazacyclooctane junction and the ether connection between the two aspidospermane components appearing in hazuntiphylline (**170**)[292] (Fig. 55) can be presumed to be analogous with the biosynthetic scheme leading to leucofoline (**103**)-like (*viz.* stepwise aza-Michael, Fig. 31). Two distinct aza-Michael reactions from the indolinic N-1 of both components on the C-22 exomethylene of the indolenine-exomethylene system of the other counterpart can be supposed to install the eight-membered intermonomeric junction. A possible hydroxylation at the C-2 position of both units could set the stage for the final dehydrative etherification yielding the three connections between both aspidospermane units. It is also plausible that this ether connection results from an heteronucleophilic attack from this OH-2 group on an indoleninium.

Our literature survey resulted in locating a single example of triply-tethered MIA-containing entity not involving two MIAs or

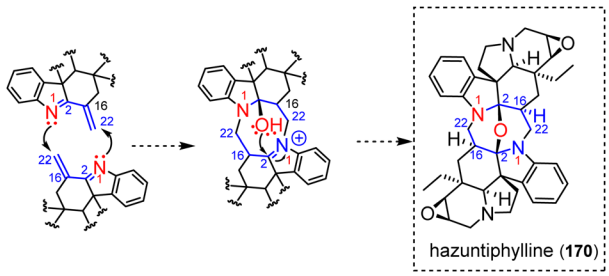

Fig. 55 Plausible biosynthetic chemical logic for the assembly of hazuntiphylline.

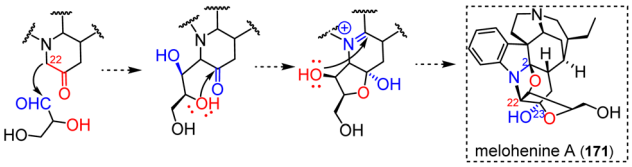

Fig. 56 Plausible biosynthetic path to melohenine A.

a MIA and a pseudodimer: melohenine A (**171**) (Fig. 56).[129] This example is remarkable given the modest size of the extraneous unit instigating these three connections, *viz.* glyceraldehyde. The biosynthesis is presumed to proceed from an oxidized form of the strychnane-like dihydrodeoxyisostrychnidine, which is capable of initiating aldolization into glyceraldehyde phosphate from C-22, followed by an hemiketalization reaction at C-23 to afford a doubly-tethered intermediate. An heteronucleophilic annulation on a $\Delta^{1,2}$- indoleninium could then lead to the final scaffold.

3.4.2 Mannich-type reactivity-driven oligomerization. Triply-tethered MIA oligomers involving Mannich-type reactivity throughout dimerization are, to our knowledge, limited to a few pseudodimers comprising an additional tryptamine unit. The importance of the Pictet–Spengler reaction in accessing this specific class of pseudodimers has already been highlighted previously through the specific example of usambarine (**109**) (Fig. 33) and this reaction alone accounts for 61 of the 74 tryptamine-containing pseudodimers described to date. A few pseudodimers incorporating an additional tryptamine unit derive from Pictet–Spengler condensation but require an additional intermonomeric connection, such as janussines A/B (**172**) (Fig. 57). Janussines can be regarded as pseudodimers incorporating either an ajmalicine-derived corynantheane or an akagerane-type MIA.[113] Accordingly, biosynthetic schemes from either of these scaffolds could lead to the core structure of janussines. In any case, a Pictet–Spengler reaction would first occur to give rise to a doubly-tethered structure, as formerly described for the usambarine-type pseudodimers (Fig. 33).[202] Such a reaction could for example imply the aldehyde group at C-17 of the corynantheane component. Subsequently, a nucleophilic attack from the tryptamine nitrogen N-1 on the carbonylated C-19 site of the corynantheane building block would instigate a third connection between the two monomeric blocks. An alternative, yet chemically analogous, biosynthetic path to janussines using both decussine and 7-hydroxytryptamine can be found elsewhere.[293] The doubly bridged oxojanussine can be assumed to correspond to an enamine dioxygenation product of these latter. The pseudodimeric roxburghine derivatives, illustrated here by roxburghine A (**173**) (Fig. 57), were inferred to derive from a *seco*-tetrahydroalstonine as a MIA precursor since Merlini's initial phytochemical report.[294] A Mannich-type heteronucleophilic attack of tryptamine aliphatic nitrogen into the C-17 aldehydic function of *seco*-tetrahydroalstonine is presumed to avail a singly-tethered, enamine-containing pseudodimer amenable to a doubly-tethered analogue through a second heteronucleophilic attack by the newly formed secondary amine on the C-19 ketone group of the *seco*-tetrahydroalstonine unit. Winterfeldt demonstrated that such analogues could readily afford the corresponding *trans*-quinolizidine through ring closure.[295] Accordingly, the condensation of tryptamine with an indoloquinolizidine precursor could yield a roxburghine A (**173**)-like octacyclic ring structure.[296] This reactivity is somehow evocative of a Bischler–Napieralski-type sequence that had been repeatedly applied to the synthesis of different ipecac monoterpenoid isoquinoline alkaloids revealing similar building blocks, including pseudodimeric derivatives thereof.[297,298]

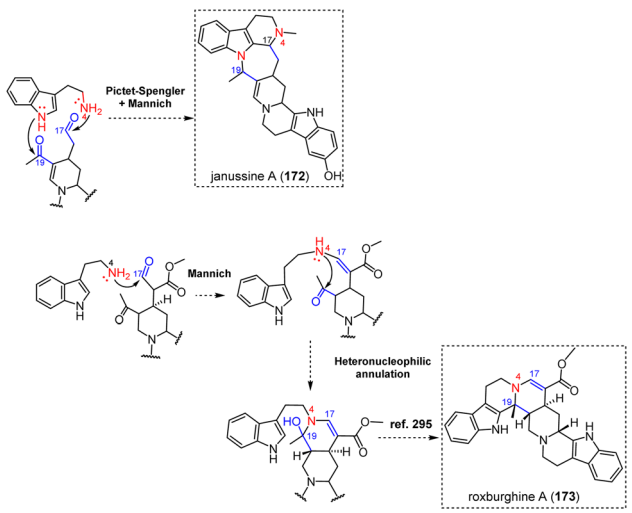

Fig. 57 Plausible biosynthetic path to triply-tethered MIA pseudodimers.

4 Outlook and concluding remarks

The body of work highlighted here demonstrates that numerous oligomerization steps follow a limited number of assembly reactions.[299] For instance, in the case of electrophilic aromatic substitutions, eight electrophilic motifs have been enumerated and identified throughout this endeavour. In addition, MIA skeletons reactivity mappings have been generated during this work and are depicted in ESI (S1).‡ Moreover, an exhaustive list of non-MIA adducts could have been compiled and a MIA oligomer network (Fig. 3) has been built. We foresee that this global overview will be used by the community as a unique assistance for structure elucidation and anticipation of MIA oligomers. Ultimately, the comprehensive repository of MIA oligomers machine-readable metadata (ESI‡) associated to this review has been uploaded on LOTUS[16] and could be leveraged for chemoinformatics purposes. Altogether, we hope that our literature survey will provide a versatile platform to assist natural product chemists in assessing the structural novelty of future oligomeric MIAs.

Although some efforts have been made to determine the biosynthesis of these complex natural products,[300] it is important to point out that most of the biosynthetic pathways covered here are highly speculative. In this context, several biosynthetic routes are possible to reach certain dimers discussed in this

manuscript and it is hardly possible to favour one over the others. As an illustration, different mechanistic scenarios leading to a few dimers have been developed in this manuscript, among many other available examples (see melomorsine (**95**) and bisleucocurine A (**105**) for some such examples).

Prior to concluding our review, we were willing to compare the wealth of processes involved in MIA oligomerization with other groups of alkaloids. Few alkaloid families can rival MIA in terms of numbers of representatives, hampering a fair comparison with most phytochemical classes. The main such example that came to our mind was the group of bisbenzylisoquinoline alkaloids, that comprises a bit more than 500 entries.[301,302] Nevertheless, this diversity relies on a much more limited set of assembly modes that is relatable to a combination of diphenyl ether linkages and/or benzylphenyl ether (=methyleneoxy) linkage. Plausible mechanisms of formation for this latter bridging mode, not known to the best of our knowledge in the realm of MIA, have been thoroughly addressed elsewhere.[303] Number (up to 3) and sites of connections lead to further refine the classification of these dimeric compounds. As *N*-methylcoclaurine is the gateway to benzylisoquinolines, most bisbenzylisoquinolines share its oxygenation pattern, probably limiting available dimerization mechanisms. Although very limited in relation to the current topic, these bridging modes can lead to a few junctions that have not yet been observed within MIAs, due to certain specific combinations of coupling modes and assembly sites, especially when the methyleneoxy bridge specific to bisbenzylisoquinolines is involved. Two such examples are benzodioxin-comprising bisbenzylisoquinolines (obtained as a consequence of two contiguous diphenyl ether couplings) that have repeatedly been reported.[304] The seven-membered 1,4-dioxepine junction in racemosidine A results from the combination of an ether coupling and a contiguous methyleneoxy bond.[305] Notably, cissampereine-type dimers, revealing a simple methyleneoxy connection, are presumed to derive from such intermediates.[303] Triply-tethered repanduline-type bisbenzylisoquinolines,[306] revealing a spiro-1,4-dioxane junction would imply an ether-bonded precursor that would enable the subsequent installation of a methyleneoxy functionality through an original dearomatizing sequence.[307] These assembly logics can be extended to most homo- and heterodimeric bisbenzylisoquinoline-derived scaffolds (*e.g.* aporphine, protoberberines, pavines, *seco*-phenanthrenes *etc.*). However, some dimers revealing more unusual connectivities are obtained by mechanisms that are strictly analogous to those encountered in this review. As such, several bis-aporphines (ovigeridimerine,[308] ovihernangerine, oviisocorydine[309]) are being bridged through a urea junction that is exactly similar to that being reported in geleganidine C (**71**) (Fig. 20), presumably involving an heteronucleophilic attack of an extraneous formaldehyde unit. Likewise, the methylene-bridged lagesianine B[310] is strongly reminiscent of the putative dimerization reaction having led to melofusine I (**70**) (Fig. 20). The co-isolated bisbenzylisoquinoline-type isopyruthaldine and isopythaldine[311] are the unique such dimers linked through a methylene group, which guided some authors to assume that these compounds should arise through an electrophilic aromatic substitution with formaldehyde[312] (see the example of pleiokomenine A (**33**) (Fig. 10). As the last example of extraneous methylene unit-containing dimer, the unique case of the bisbenzylisoquinoline medelline, isolated by Cavé in 1986,[313] deserved to be mentioned here. This compound features a methylenedioxy bridge between its two components, that can be traced back to an heteronucleophilic attack initiated from two O atoms instead of a melofusine I-type sequence initiated by two N atoms. The presence of a nearby ether connectivity results in a 1,3,6-oxacine intermonomeric junction. Such a reactivity has yet to be described in the realm of MIA. Another disturbing link between the world of isoquinolines and that of MIAs lies in the tendency of dopamine to undergo Pictet–Spengler reactions with secologanine to produce the so-called monoterpenoid ipecac alkaloids.[314] These reactions produce a hybrid structure that is very reminiscent of strictosidine, namely deacetyllipecoside giving a straight access to a series of alkaloids analogous to type I MIAs albeit lacking their pyrrole nucleus due to the amine-containing partner being dopamine instead of tryptamine. Among many others, one can quote the examples of the "corynantheane-like" protoemetine,[315] and of the "vallesiachotamane-like" alangiside[316] and various azaberberines often referred to as alamarine derivatives[317,318] (these latter being reminiscent of angustine). Due to their structural similarity, these protoemetine-type ipecac alkaloids show strikingly similar reactivity to corynantheane-type alkaloids, as shown by the constitution of cephaeline/emetine which denotes Pictet–Spengler-type condensation with an additional dopamine unit.[203] Closer still to the MIA, various tubulosine[319,320] derivatives condense with a tryptamine unit, which is extremely similar to usambarine (**109**)-type corynantheane-tryptamine pseudodimers (Fig. 33). Ipecac alkaloids had also been shown to instigate phenylpropene adducts through an amide connection,[321] as observed for some MIAs like cylindrocarpine[322] (see the example of alstiphyllanine I (**86**) for a related compound including a gallate derivative instead (Fig. 24)). Similarly, aporphine-gallate adducts linked by an amide bond have been described very recently.[323] It is interesting to note that benzylisoquinoline alkaloids, mostly aporphines, tend to react with carbamic acid too.[324,325] Nevertheless, these adducts constantly arise through a *N*-triggered nucleophilic attack that does not seem to be reported for any MIA so far. The tertiary nature of the alicyclic nitrogen of most MIA probably accounts for this, even though some alkaloids isolated from *Gelsemium* sources disclose secondary amines that could afford such hybrid structures in the future. To draw a final parallel with the world of MIAs, benzylisoquinolines are also about to enter the era of trimeric compounds, with the first example of such a compound published in 2018: neoliensinine.[326]

It is interesting to note that some specific alkaloid series are associated with typical substituents that may step in some specific bridging modes. One such example is that of tropanic alkaloids that tend to be substituted with diverse organic acids (*e.g.* mesaconic acid, itaconic acid, angelic acid or senecic acid).[327] Both carboxylic acid ends of mesaconic acid can be esterified by tropanic alkaloids units to yield a wealth of different dimers.[328] Ditropane diesters of itaconic acid have also been described.[329] Likewise, tropane alkaloids substituted with a tropic acid residue are prone to spontaneous dimerization

through a Diels-Alder-type cyclization to obtain belladonnine/scopadonnine derivatives.[330] Photoinduced [2 + 2] cycloadditions, unknown to date for MIA and benzylisoquinolines families, produce cyclobutane-centered tropane dimers. These dimers rely on the unsaturations occurring on an organic acid-type substituent and/or of a phenylpropene residue.[331] Truxillin-type[332] MIA dimers could be envisaged from the numerous MIA dimers disclosing a phenylpropene residue, but such compounds had not been described so far. Remarkable trimers have made use of several of these reactivities, such as grahamine, which requires both a mesaconic acid bridging group and a [2 + 2] cycloaddition.[333] Other trimers are biosynthesized by mechanisms close to MIA chemistry, such as the recently reported trissaccardine, based on two aza-Michael additions.[334] Tropane dimers being bridged through an urea function had also been reported, as formerly known from MIA and benzylisoquinolines.[335]

It appeared clearly throughout this review that numerous oligomerization chemical logics extend beyond MIA skeleton boundaries (see hazuntiphylline (**170**) (aspidospermane) and *C*-curarine (**169**) (akuammicine) Fig. 54) and often serve as the starting points to several scaffolds either through highly evolved enzymatic pathways or diversification opportunities through spontaneous reaction or both.[336] Among those diversification opportunities, Potier-Polonovski fragmentation and retro Mannich often lead to structural rearrangements of certain MIA skeletons resulting in unexpected oligomerizations (see, trirosaline (**150**), angustiphylline (**84**)). Moreover, a glance at the reactivity table (S2, ESI‡) shows, for example, that dimerizations based on the Pictet–Spengler reaction have so far been strictly linked to the biosynthesis of pseudodimeric MIAs incorporating an additional tryptamine unit. Similarly, esterification and amidification reactions appear to have been exclusively involved in the incorporation of phenylpropanoids/gallates/anthranilates.

Advances in the characterization, isolation techniques, and synthesis of this fascinating class of phytochemicals have significantly enriched the understanding of their chemistry. The landmark advances in the fields of mass spectrometry, NMR, and chemoinformatics provide natural chemists with ever-expanding capacities to pinpoint minor, structurally new metabolites since the very first steps of phytochemical processing and to target their isolation through a hypothesis-driven pipeline. MIA in particular strongly benefitted from the molecular networking strategies thanks to the upload of MS/MS data related to 172 structurally diverse MIAs[337] to the GNPS[338] repositories. We foresee that the number of newly described MIA oligomers, trimers in particular, will increase in the coming years enabling, hopefully, the discovery of new assembly patterns.

We hope that this global overview of the unified chemical logic underlying the assembly of MIA oligomers will provide new insights on the biosynthesis and inspiring prospects for biomimetic total syntheses.

5 Data availability

The data supporting this article have been included as part of the ESI.‡ The comprehensive repository of MIA oligomers machine-readable metadata (InChI and SMILES) associated to this review has been uploaded on LOTUS and is accessible at **https://www.wikidata.org/**.

6 Author contributions

Pierre Le Pogam: conceptualization, writing – original draft, review & editing, supervision, validation, Mehdi A. Beniddir: conceptualization, writing – original draft, review & editing, supervision, validation.

7 Conflicts of interest

There are no conflicts to declare.

8 Acknowledgement

M. A. B. and P. L. P. were supported by the National French Agency (ANR grant 20-CE43-0010). M.A.B. warmly thanks all his students (past and present) who have been involved in MIA discovery program for their enthusiasm and their efforts, rendering these discoveries a true pleasure to pursue. The authors warmly thank Adriano Rutz for the upload of the MIA oligomer biosource to LOTUS.

9 Notes and references

1 S. A. Snyder, A. M. ElSohly and F. Kontes, *Nat. Prod. Rep.*, 2011, **28**, 897–924.
2 Q. T. Khong, D. Li, B. A. P. Wilson, K. Ranguelova, M. Dalilian, E. A. Smith, A. Wamiru, E. I. Goncharova, T. Grkovic, D. Voeller, S. Lipkowitz, M. J. Schnermann, B. R. O'Keefe and L. Du, *Org. Lett.*, 2022, **24**, 9468–9472.
3 C. Cuello, E. Stander, H. Jansen, T. Dugé De Bernonville, A. Oudin, C. Birer Williams, A. Lanoue, N. Giglioli Guivarc'h, N. Papon, R. Dirks, M. Jensen, S. O'Connor, S. Besseau and V. Courdavault, *F1000Research*, 2022, **11**, 1541.
4 J. Zhang, L. G. Hansen, O. Gudich, K. Viehrig, L. M. M. Lassen, L. Schrübbers, K. B. Adhikari, P. Rubaszka, E. Carrasquer-Alvarez, L. Chen, V. D'Ambrosio, B. Lehka, A. K. Haidar, S. Nallapareddy, K. Giannakou, M. Laloux, D. Arsovska, M. A. K. Jørgensen, L. J. G. Chan, M. Kristensen, H. B. Christensen, S. Sudarsan, E. A. Stander, E. Baidoo, C. J. Petzold, T. Wulff, S. E. O'Connor, V. Courdavault, M. K. Jensen and J. D. Keasling, *Nature*, 2022, **609**, 341–347.
5 M. J. Dror, J. Misa, D. A. Yee, A. M. Chu, R. K. Yu, B. B. Chan, L. S. Aoyama, A. P. Chaparala, S. E. O'Connor and Y. Tang, *J. Ind. Microbiol. Biotechnol.*, 2023, kuad047.
6 S. A. Bradley, B. J. Lehka, F. G. Hansson, K. B. Adhikari, D. Rago, P. Rubaszka, A. K. Haidar, L. Chen, L. G. Hansen, O. Gudich, K. Giannakou, B. Lengger, R. T. Gill, Y. Nakamura, T. D. de Bernonville, K. Koudounas, D. Romero-Suarez, L. Ding, Y. Qiao, T. M. Frimurer, A. A. Petersen, S. Besseau, S. Kumar, N. Gautron, C. Melin, J. Marc, R. Jeanneau,

S. E. O'Connor, V. Courdavault, J. D. Keasling, J. Zhang and M. K. Jensen, *Nat. Chem. Biol.*, 2023, **19**, 1551–1560.
7 M. Sottomayor and A. Ros Barceló, *Protoplasma*, 2003, **222**, 97–105.
8 J. Garnier, M. Koch and N. Kunesch, *Phytochemistry*, 1969, **8**, 1241–1254.
9 G. A. Cordell and J. E. Saxton, *The Alkaloids: Chemistry and Physiology*, 1981, 20, pp. 1–295.
10 T.-S. Kam and Y.-M. Choo, in *The Alkaloids: Chemistry and Biology*, ed. G. A. Cordell, Academic Press, 2006, vol. 63, pp. 181–337.
11 M. Kitajima and H. Takayama, *The Alkaloids: Chemistry and Biology*, 2016, 76, pp. 259–310.
12 L. Szabó, *Molecules*, 2008, **13**, 1875–1896.
13 X.-H. Cai, M.-F. Bao, Y. Zhang, C.-X. Zeng, Y.-P. Liu and X.-D. Luo, *Org. Lett.*, 2011, **13**, 3568–3571, In 2011, the description of alstrostines A and B revealed a potential new precursor towards monoterpene indole alkaloids that would include a tryptophane unit and two seco-iridoid components, which may thus fall into the category of pseudodimers.
14 C. Kornpointner, A. Berger, F. Traxler, A. Hadžiabdić, M. Massar, J. Matek, L. Brecker and J. Schinnerl, *Phytochemistry*, 2020, **173**, 112296.
15 A. Berger, K. Valant-Vetschera, J. Schinnerl and L. Brecker, *Phytochem. Rev.*, 2022, **21**, 915–939.
16 A. Rutz, M. Sorokina, J. Galgonek, D. Mietchen, E. Willighagen, A. Gaudry, J. G. Graham, R. Stephan, R. Page, J. Vondrášek, C. Steinbeck, G. F. Pauli, J.-L. Wolfender, J. Bisson and P.-M. Allard, *Elife*, 2022, **11**, e70780.
17 P. Shannon, A. Markiel, O. Ozier, N. S. Baliga, J. T. Wang, D. Ramage, N. Amin, B. Schwikowski and T. Ideker, *Genome Res.*, 2003, **13**, 2498–2504.
18 E. Otogo N'Nang Obiang, G. Genta-Jouve, J.-F. Gallard, B. Kumulungui, E. Mouray, P. Grellier, L. Evanno, E. Poupon, P. Champy and M. A. Beniddir, *Org. Lett.*, 2017, **19**, 6180–6183.
19 W. Zhang, X.-J. Huang, S.-Y. Zhang, D.-M. Zhang, R.-W. Jiang, J.-Y. Hu, X.-Q. Zhang, L. Wang and W.-C. Ye, *J. Nat. Prod.*, 2015, **78**, 2036–2044.
20 E. Okuyama, L.-H. Gao and M. Yamazaki, *Chem. Pharm. Bull.*, 1992, **40**, 2075–2079.
21 T.-S. Kam, S.-J. Tan, S.-W. Ng and K. Komiyama, *Org. Lett.*, 2008, **10**, 3749–3752.
22 E. Otogo N'Nang, G. Bernadat, E. Mouray, B. Kumulungui, P. Grellier, E. Poupon, P. Champy and M. A. Beniddir, *Org. Lett.*, 2018, **20**, 6596–6600.
23 E. Otogo N'Nang, J. F. Gallard, P. Champy, P. Le Pogam and M. A. Beniddir, *Magn. Reson. Chem.*, 2022, **60**, 1178–1184.
24 X. Wei, Z. Dai, J. Yang, A. Khan, H.-F. Yu, Y.-L. Zhao, Y.-F. Wang, Y.-P. Liu, Z.-F. Yang, W.-Y. Huang, X.-H. Wang, X.-D. Zhao and X.-D. Luo, *Bioorg. Med. Chem.*, 2018, **26**, 1776–1783.
25 G. Cauchie, E. O. N'Nang, J. J. J. van der Hooft, P. Le Pogam, G. Bernadat, J.-F. Gallard, B. Kumulungui, P. Champy, E. Poupon and M. A. Beniddir, *Org. Lett.*, 2020, **22**, 6077–6081.
26 J.-J. Wei, W.-Q. Wang, W.-B. Song, J. Li and L.-j. Xuan, *Phytochem. Lett.*, 2018, **23**, 1–4.
27 J. M. Müller, *Experientia*, 1957, **13**, 479–481.
28 H. Arai, K. Zaima, E. Mitsuta, H. Tamamoto, A. Saito, Y. Hirasawa, A. Rahman, I. Kusumawati, N. C. Zaini and H. Morita, *Bioorg. Med. Chem.*, 2012, **20**, 3454–3459.
29 E. Davioud, C. Kan, J.-C. Quirion, B. C. Das and H.-P. Husson, *Phytochemistry*, 1989, **28**, 1383–1387.
30 B. Hong, D. Grzech, L. Caputi, P. Sonawane, C. E. R. López, M. O. Kamileen, N. J. Hernández Lozada, V. Grabe and S. E. O'Connor, *Nature*, 2022, **607**, 617–622.
31 C. Schlatter, E. E. Waldner, H. Schmid, W. Maier and D. Gröger, *Helv. Chim. Acta*, 1969, **52**, 776–789.
32 C. Schlatter, E. E. Waldner, H. Schmid, D. Gröger, K. Stolle and K. Mothes, *Helv. Chim. Acta*, 1966, **49**, 1714–1715.
33 We inform the readers that this review effort outlined only one unclassified MIA, named tenuiphylline. This puzzling case is addressed in S3, ESI‡
34 J. Le Men and W. I. Taylor, *Experientia*, 1965, **21**, 508–510.
35 M. E. Tanner, *Nat. Prod. Rep.*, 2015, **32**, 88–101.
36 C. T. Walsh, *ACS Chem. Biol.*, 2014, **9**, 2718–2728.
37 T. A. van Beek, R. Verpoorte and P. Q. Kinh, *Planta Med.*, 1985, **51**, 277–279.
38 H. Fouotsa, P. Mkounga, A. M. Lannang, J. Vanheuverzwijn, Z. Zhou, K. Leblanc, S. Rharrabti, A. E. Nkengfack, J.-F. Gallard, V. Fontaine, F. Meyer, E. Poupon, P. Le Pogam and M. A. Beniddir, *Org. Biomol. Chem.*, 2022, **20**, 98–105.
39 B. González, N. Veiga, G. Hernández, G. Seoane and I. Carrera, *J. Nat. Prod.*, 2023, **86**, 1500–1511.
40 J. P. Kutney, *Nat. Prod. Rep.*, 1990, **7**, 85–103.
41 M. Hiroki, A. Abulikemu, C. Totsuka, Y. Hirasawa, T. Kaneda and H. Morita, *J. Nat. Med.*, 2024, **78**, 216–225.
42 A. Brossi and M. Suffness, *The Alkaloids: Antitumor Bisindole Alkaloids from Catharanthus roseus (L.)*, Academic Press, 1990.
43 N. Neuss and S. S. Tafur, *United States Pat.*, US3968113A, 1977.
44 A. El-Sayed, G. A. Handy and G. A. Cordell, *J. Nat. Prod.*, 1983, **46**, 517–527.
45 Y. Hirasawa, A. Kase, A. Okamoto, K. Suzuki, M. Hiroki, T. Kaneda, N. Uchiyama and H. Morita, *J. Nat. Med.*, 2024, **78**, 382–392.
46 C.-H. Wang, G.-C. Wang, Y. Wang, X.-Q. Zhang, X.-J. Huang, D.-M. Zhang, M.-F. Chen and W.-C. Ye, *Fitoterapia*, 2012, **83**, 765–769.
47 C. Szántay, *Pure Appl. Chem.*, 1990, **62**, 1299–1302.
48 I. Chardon-Loriaux and H.-P. Husson, *Tetrahedron Lett.*, 1975, **16**, 1845–1848.
49 I. Chardon-Loriaux, M.-M. Debray and H.-P. Husson, *Phytochemistry*, 1978, **17**, 1605–1608.
50 F. Reuß and P. Heretsch, *Nat. Prod. Rep.*, 2021, **38**, 693–701.
51 J. Bruneton, A. Cavé, E. W. Hagaman, N. Kunesch and E. Wenkert, *Tetrahedron Lett.*, 1976, **17**, 3567–3570.

52 K.-H. Lim and T.-S. Kam, *Helv. Chim. Acta*, 2009, **92**, 1895–1902.
53 K.-H. Lim and T.-S. Kam, *Tetrahedron Lett.*, 2009, **50**, 3756–3759.
54 D. W. Thomas, H. Achenbach and K. Biemann, *J. Am. Chem. Soc.*, 1966, **88**, 1537–1544.
55 Y.-H. Fu, Y.-T. Di, H.-P. He, S.-l. Li, Y. Zhang and X.-J. Hao, *J. Nat. Prod.*, 2014, **77**, 57–62.
56 The specific case of vobtusamine is, however, very particular. It was indeed suggested that the eburnane half of this compound would occur as a consequence of an aspidospermane to eburnane rearrangement as experimentally validated by Wenkert from vobtusine.
57 C.-Y. Gan, W. T. Robinson, T. Etoh, M. Hayashi, K. Komiyama and T.-S. Kam, *Org. Lett.*, 2009, **11**, 3962–3965.
58 G. Pandey, A. Mishra and J. Khamrai, *Org. Lett.*, 2017, **19**, 3267–3270.
59 M. Damak, A. Ahond and P. Potier, *Bull. Soc. Chim. Fr.*, 1980, **9**, 490–495.
60 C.-E. Nge, K.-S. Sim, S.-H. Lim, N. F. Thomas, Y.-Y. Low and T.-S. Kam, *J. Nat. Prod.*, 2016, **79**, 2709–2717.
61 E. Otogo N'Nang, G. Cauchie, P. Retailleau, S. T. Agnandji, J.-F. Gallard, E. Mouray, P. Grellier, P. Champy, P. Le Pogam and M. A. Beniddir, *J. Nat. Prod.*, 2023, **86**, 1202–1210.
62 J. Bruneton, A. Bouquet and A. Cavé, *Phytochemistry*, 1974, **13**, 1963–1967.
63 A. Cavé, J. Bruneton, A. Ahond, A. M. Bui, H. P. Husson, C. Kan, G. Lukacs and P. Potier, *Tetrahedron Lett.*, 1973, **14**, 5081–5084.
64 Y.-P. Liu, Y.-L. Zhao, T. Feng, G.-G. Cheng, B.-H. Zhang, Y. Li, X.-H. Cai and X.-D. Luo, *J. Nat. Prod.*, 2013, **76**, 2322–2329.
65 A. Arnone, G. Nasini and L. Merlini, *J. Chem. Soc., Perkin Trans. 1*, 1987, 571–575.
66 T.-S. Kam, K.-H. Lee and S.-H. Goh, *Phytochemistry*, 1991, **30**, 3441–3444.
67 T. Kouamé, A. T. Okpekon, N. F. Bony, A. D. N'Tamon, J.-F. Gallard, S. Rharrabti, K. Leblanc, E. Mouray, P. Grellier, P. Champy, M. A. Beniddir and P. Le Pogam, *Molecules*, 2020, **25**, 2654.
68 N. Yoshikado, S. Taniguchi, N. Kasajima, F. Ohashi, K. I. Doi, T. Shibata, T. Yoshida and T. Hatano, *Heterocycles*, 2009, **77**, 793–800.
69 M. Oshima, H. Aoyama, Y. Shimozu, S. Taniguchi, T. Miura and T. Hatano, *Heterocycles*, 2019, **98**, 804–812.
70 Z.-W. Liu, M. Song, J.-Y. Wang, D.-Z. Wang, B. Sun, L. Shi, R.-W. Jiang, M. Ma and X.-Q. Zhang, *Phytochemistry*, 2023, **211**, 113678.
71 T. P. Lien, C. Kamperdick, T. Van Sung, G. Adam and H. Ripperger, *Phytochemistry*, 1998, **49**, 1797–1799.
72 J. W. Medley and M. Movassaghi, *Angew. Chem., Int. Ed.*, 2012, **51**, 4572–4576.
73 P. Obitz, S. Endreß and J. Stöckigt, *Phytochemistry*, 1995, **40**, 1407–1417.
74 M. T. Rahman and J. M. Cook, in *Studies in Natural Products Chemistry*, ed. Atta-Ur-Rahman, Elsevier, 2020, vol. 64, pp. 1–57.
75 M. T. Rahman, V. V. N. P. B. Tiruveedhula and J. M. Cook, *Molecules*, 2016, **21**, 1525.
76 J. S.-Y. Yeap, H. M. Saad, C.-H. Tan, K.-S. Sim, S.-H. Lim, Y.-Y. Low and T.-S. Kam, *J. Nat. Prod.*, 2019, **82**, 3121–3132.
77 S.-K. Wong, J. S.-Y. Yeap, C.-H. Tan, K.-S. Sim, S.-H. Lim, Y.-Y. Low and T.-S. Kam, *Tetrahedron*, 2021, **78**, 131802.
78 A. Jossang, P. Fodor and B. Bodo, *J. Org. Chem.*, 1998, **63**, 7162–7167.
79 S. Subhadhirasakul, H. Takayama, N. Aimi, D. Ponglux and S.-I. Sakai, *Chem. Pharm. Bull.*, 1994, **42**, 1427–1431.
80 J.-M. Nuzillard, P. Thépenier, M.-J. Jacquier, G. Massiot, L. Le Men-Olivier and C. Delaude, *Phytochemistry*, 1996, **43**, 897–902.
81 K.-H. Lim and T.-S. Kam, *Org. Lett.*, 2006, **8**, 1733–1735.
82 X.-H. Gao, P.-Q. Wu, Y.-Y. Fan, B. Zhou and J.-M. Yue, *Chin. J. Chem.*, 2023, **41**, 2296–2304.
83 J. Chen, S. Kongkiatpaiboon and X.-H. Cai, *Phytochemistry*, 2024, **222**, 114075.
84 J. M. Nuzillard, T. M. Pinchon, C. Caron, G. Massiot and L. Le Men-Olivier, *C. R. Acad. Sci.*, 1989, **309**, 195–198.
85 V. M. Malikov, M. R. Sharipov and S. Y. Yunusov, *Chem. Nat. Compd.*, 1972, **8**, 741–742.
86 G. Massiot, J. M. Nuzillard, B. Richard and L. Le Men-Olivier, *Tetrahedron Lett.*, 1990, **31**, 2883–2884.
87 C. Chen, J.-W. Liu, L.-L. Guo, F. Xiong, X.-Q. Ran, Y.-R. Guo, Y.-G. Yao, X.-J. Hao, R.-C. Luo and Y. Zhang, *Phytochemistry*, 2022, **203**, 113392.
88 Y. Fan, J. Shen, Z. Liu, K. Xia, W. Zhu and P. Fu, *Nat. Prod. Rep.*, 2022, **39**, 1305–1324.
89 Y. Yu, S.-M. Zhao, M.-F. Bao and X.-H. Cai, *Org. Chem. Front.*, 2020, **7**, 1365–1373.
90 R. Torrenegra, J. A. P. Pedrozo, H. Achenbach and P. Bauereiß, *Phytochemistry*, 1988, **27**, 1843–1848.
91 L. Zhang, Z. Hua, Y. Song and C. Feng, *Fitoterapia*, 2014, **97**, 142–147.
92 F.-R. Li, L. Liu, Y.-P. Liu, J.-T. Wang, M.-L. Yang, A. Khan, X.-J. Qin, Y.-D. Wang and G.-G. Cheng, *Phytochemistry*, 2021, **184**, 112673.
93 B.-J. Zhang, C. Liu, M.-F. Bao, X.-H. Zhong, L. Ni, J. Wu and X.-H. Cai, *Tetrahedron*, 2017, **73**, 5821–5826.
94 A. B. Nama, T. Paululat, G. R. Ebede, P. H. D. Betote, D. E. Pegnyemb, J. N. Mbing, J. T. Ndongo, H. Ihmels and H. Laatsch, *Phytochem. Lett.*, 2023, **54**, 63–69.
95 M. Damak, A. Ahond and P. Potier, *Bull. Soc. Chim. Fr.*, 1981, **2**, 213–216.
96 E. C. Miranda and B. Gilbert, *Experientia*, 1969, **25**, 575–576.
97 J. Abaul, P. Bourgeois, E. Philogene, M. Damak, A. Ahond, C. Poupat and P. Potier, *C. R. Acad. Sci. Ser. 2*, 1984, **298**, 627–629.
98 M. Lin, B. Yang and D. Q. Yu, *Acta Pharm. Sin.*, 1986, **21**, 114–118.
99 C. R. Edwankar, R. V. Edwankar, J. R. Deschamps and J. M. Cook, *Angew. Chem., Int. Ed.*, 2012, **51**, 11762–11765.
100 P. A. Keller, N. R. Yepuri, M. J. Kelso, M. Mariani, B. W. Skelton and A. H. White, *Tetrahedron*, 2008, **64**, 7787–7795.

101 E. Valencia, A. Madinaveitia, J. Bermejo and A. G. Gonzalez, *J. Nat. Prod.*, 1995, **58**, 134–137.
102 W. Hüttel and M. Müller, *ChemBioChem*, 2007, **8**, 521–529.
103 A. Pervin and A. Muzaffar, *Heterocycles*, 1988, **27**, 2051–2057.
104 J. Qu, L. Fang, X.-D. Ren, Y. Liu, S.-S. Yu, L. Li, X.-Q. Bao, D. Zhang, Y. Li and S.-G. Ma, *J. Nat. Prod.*, 2013, **76**, 2203–2209.
105 L.-Z. Lin, G. A. Cordell, C.-Z. Ni and J. Clardy, *Tetrahedron Lett.*, 1989, **30**, 1177–1180.
106 M.-X. Sun, Y. Cui, Y. Li, W.-Q. Meng, Q.-Q. Xu, J. Zhao, J.-C. Lu and K. Xiao, *Phytochemistry*, 2019, **162**, 232–240.
107 J. C. Quirion, H. P. Husson, C. Kan and I. R. C. Bick, *Nat. Prod. Lett.*, 1993, **2**, 41–48.
108 S. Laha and R. G. Luthy, *Environ. Sci. Technol.*, 1990, **24**, 363–373.
109 M. Gill and R. J. Strauch, *Z. Naturforsch. C*, 1984, **39**, 1027–1029.
110 M. Baunach, L. Ding, T. Bruhn, G. Bringmann and C. Hertweck, *Angew. Chem., Int. Ed.*, 2013, **52**, 9040–9043.
111 P. Yates, F. N. MacLachlan, I. D. Rae, M. Rosenberger, A. G. Szabo, C. R. Willis, M. P. Cava, M. Behforouz, M. V. Lakshmikantham and W. Zeiger, *J. Am. Chem. Soc.*, 1973, **95**, 7842–7850.
112 E. F. Rogers, H. R. Snyder and R. F. Fischer, *J. Am. Chem. Soc.*, 1952, **74**, 1987–1989.
113 A. Adesomoju, M. Lakshmikantham and M. Cava, *Heterocycles*, 1983, **20**, 1511–1517.
114 Z.-L. Song, C.-A. Fan and Y.-Q. Tu, *Chem. Rev.*, 2011, **111**, 7523–7556.
115 A. A. Adesomoju, V. H. Rawal, M. V. Lakshmikantham and M. P. Cava, *J. Org. Chem.*, 1983, **48**, 3015–3017.
116 P. D. Rege, Y. Tian and E. J. Corey, *Org. Lett.*, 2006, **8**, 3117–3120.
117 K. C. Nicolaou, S. M. Dalby, S. Li, T. Suzuki and D. Y. K. Chen, *Angew. Chem., Int. Ed.*, 2009, **48**, 7616–7620.
118 H. Satoh, K.-I. Ojima, H. Ueda and H. Tokuyama, *Angew. Chem., Int. Ed.*, 2016, **55**, 15157–15161.
119 K. C. Nicolaou, S. M. Dalby, S. Li, T. Suzuki and D. Y.-K. Chen, *Angew. Chem., Int. Ed.*, 2009, **48**, 7616–7620.
120 Y.-L. Du and K. S. Ryan, *Curr. Opin. Chem. Biol.*, 2016, **31**, 74–81.
121 Y. Masui, C. Kawabe, K. Mastumoto, K. Abe and T. Miwa, *Phytochemistry*, 1986, **25**, 1470–1471.
122 J.-G. Shi, H.-Q. Wang, M. Wang, Y.-C. Yang, W.-Y. Hu and G.-X. Zhou, *J. Nat. Prod.*, 2000, **63**, 782–786.
123 H. H. Wasserman, R. W. DeSimone, D. L. Boger and C. M. Baldino, *J. Am. Chem. Soc.*, 1993, **115**, 8457–8458.
124 B.-B. Shi, J.-S. Lu, J. Wu, M.-F. Bao and X.-H. Cai, *Org. Chem. Front.*, 2021, **8**, 2601–2607.
125 D. Grierson, in *Organic Reactions*, 2004, pp. 85–295.
126 D. F. Dickel, C. L. Holden, R. C. Maxfield, L. E. Paszek and W. I. Taylor, *J. Am. Chem. Soc.*, 1958, **80**, 123–125.
127 M. Mentel and R. Breinbauer, *Curr. Org. Chem.*, 2007, **11**, 159–176.
128 J.-W. Liu, Z.-Q. Huo, Q. Zhao, X.-J. Hao, H.-P. He and Y. Zhang, *Fitoterapia*, 2019, **138**, 104347.
129 T. Feng, X.-H. Cai, Y. Li, Y.-Y. Wang, Y.-P. Liu, M.-J. Xie and X.-D. Luo, *Org. Lett.*, 2009, **11**, 4834–4837.
130 M. Wu, P. Wu, H. Xie, G. Wu and X. Wei, *Planta Med.*, 2011, **77**, 284–286.
131 S. Shao, H. Zhang, C.-M. Yuan, Y. Zhang, M.-M. Cao, H.-Y. Zhang, Y. Feng, X. Ding, Q. Zhou, Q. Zhao, H.-P. He and X.-J. Hao, *Phytochemistry*, 2015, **116**, 367–373.
132 Y. Hirasawa, S. Miyama, T. Hosoya, K. Koyama, A. Rahman, I. Kusumawati, N. C. Zaini and H. Morita, *Org. Lett.*, 2009, **11**, 5718–5721.
133 C. F. Alcover, G. Bernadat, F. A. Kabran, P. Le Pogam, K. Leblanc, A. E. Fox Ramos, J.-F. Gallard, E. Mouray, P. Grellier, E. Poupon and M. A. Beniddir, *J. Nat. Prod.*, 2020, **83**, 1207–1216.
134 R. Verpoorte, M. Frédérich, C. Delaude, L. Angenot, G. Dive, P. Thépenier, M.-J. Jacquier, M. Zèches-Hanrot, C. Lavaud and J.-M. Nuzillard, *Phytochem. Lett.*, 2010, **3**, 100–103.
135 H. Irie, K. Ishizuka, S. Kawashima, N. Masaki, K. Osaki, T. Shingu, S. Uyeo, H. Kaneko and S. Naruto, *J. Chem. Soc., Chem. Commun.*, 1972, 871.
136 A. Itoh, T. Tanahashi, N. Nagakura and T. Nishi, *Phytochemistry*, 2003, **62**, 359–369.
137 N.-P. Li, M. Liu, X.-J. Huang, X.-Y. Gong, W. Zhang, M.-J. Cheng, W.-C. Ye and L. Wang, *J. Org. Chem.*, 2018, **83**, 5707–5714.
138 W. Zhang, W. Xu, G.-Y. Wang, X.-Y. Gong, N.-P. Li, L. Wang and W.-C. Ye, *Org. Lett.*, 2017, **19**, 5194–5197.
139 J. Lin, J. Wu, M.-F. Bao, S. Kongkiatpaiboon and X.-H. Cai, *Phytochemistry*, 2024, **222**, 114077.
140 H. Takayama, Y. Tominaga, M. Kitajima, N. Aimi and S. Sakai, *J. Org. Chem.*, 1994, **59**, 4381–4385.
141 L. Lin, G. A. Cordell, C. Ni and J. Clardy, *J. Org. Chem.*, 1989, **54**, 3199–3202.
142 T. A. van Beek, R. Verpoorte and A. B. Svendsen, *Tetrahedron Lett.*, 1984, **25**, 2057–2060.
143 P. Pachaly, A. Kroll-Horstmann and K. Sin, *Die Pharmazie*, 2000, **55**, 777.
144 T. T. Nguyen, D. H. Nguyen, B. T. Zhao, D. D. Le, D. H. Choi, Y. H. Kim, T. H. Nguyen and M. H. Woo, *Bioorg. Chem.*, 2017, **74**, 221–227.
145 Y.-C. Li, J. Yang, X.-R. Zhou, X.-H. Liang and Q.-Y. Fu, *Z. Naturforsch. B*, 2016, **71**, 193–195.
146 A.-M. Bui, B. C. Das and P. Potier, *Phytochemistry*, 1980, **19**, 1473–1475.
147 T. R. Govindachari, G. Sandhya, S. Chandrasekharan and K. Rajagopalan, *J. Chem. Soc., Chem. Commun.*, 1987, 1137–1138.
148 M. Kitajima, M. Iwai, N. Kogure, R. Kikura-Hanajiri, Y. Goda and H. Takayama, *Tetrahedron*, 2013, **69**, 796–801.
149 K. M. Flynn, I.-S. Myeong, T. Pinto and M. Movassaghi, *J. Am. Chem. Soc.*, 2022, **144**, 9126–9131.
150 X.-H. Cai, H. Jiang, Y. Li, G.-G. Cheng, Y.-P. Liu, T. Feng and X.-D. Luo, *Chin. J. Nat. Med.*, 2011, **9**, 259–263.
151 C. Kan-Fan, G. Massiot, B. C. Das and P. Potier, *J. Org. Chem.*, 1981, **46**, 1481–1483.
152 T. Gan and J. M. Cook, *Tetrahedron Lett.*, 1996, **37**, 5037–5038.

153 F. Mayerl and M. Hesse, *Helv. Chim. Acta*, 1978, **61**, 337–351.
154 T. Gan and J. M. Cook, *J. Org. Chem.*, 1998, **63**, 1478–1483.
155 M. Frédérich, M.-C. De Pauw, C. Prosperi, M. Tits, V. Brandt, J. Penelle, M.-P. Hayette, P. DeMol and L. Angenot, *J. Nat. Prod.*, 2001, **64**, 12–16.
156 J. Lamotte, L. Dupont, O. Dideberg, K. Kambu and L. Angenot, *Tetrahedron Lett.*, 1979, **20**, 4227–4228.
157 W. I. Taylor, *J. Org. Chem.*, 1965, **30**, 309–310.
158 H. Mehri, S. Baassou and M. Plat, *J. Nat. Prod.*, 1991, **54**, 372–379.
159 T. Kouamé, G. Bernadat, V. Turpin, M. Litaudon, A. T. Okpekon, J.-F. Gallard, K. Leblanc, S. Rharrabti, P. Champy, E. Poupon, M. A. Beniddir and P. Le Pogam, *Org. Lett.*, 2021, **23**, 5964–5968.
160 Y. Zhang, Y.-X. Yuan, M. Goto, L.-L. Guo, X.-N. Li, S. L. Morris-Natschke, K.-H. Lee and X.-J. Hao, *J. Nat. Prod.*, 2018, **81**, 562–571.
161 Y. Zhang, L. Guo, G. Yang, F. Guo, Y. Di, S. Li, D. Chen and X. Hao, *Fitoterapia*, 2015, **100**, 150–155.
162 A. E. Nugroho, Y. Hirasawa, N. Kawahara, Y. Goda, K. Awang, A. H. A. Hadi and H. Morita, *J. Nat. Prod.*, 2009, **72**, 1502–1506.
163 M. Bert, G. Baudouin, F. Tillequin and M. Koch, *Heterocycles*, 1986, **24**, 1567–1570.
164 E. Otogo N'Nang, P. Le Pogam, T. Ndong Mba, C. Sima Obiang, E. Mouray, P. Grellier, B. Kumulungui, P. Champy and M. A. Beniddir, *J. Nat. Prod.*, 2021, **84**, 1409–1413.
165 W.-F. Ku, S.-J. Tan, Y.-Y. Low, K. Komiyama and T.-S. Kam, *Phytochemistry*, 2011, **72**, 2212–2218.
166 K. Koyama, Y. Hirasawa, K. Zaima, T. C. Hoe, K.-L. Chan and H. Morita, *Bioorg. Med. Chem.*, 2008, **16**, 6483–6488.
167 P. Potier and M. Janot, *C. R. Acad. Sci. Paris Ser. C*, 1973, **276**, 1727–1729.
168 X.-H. Zhong, M.-F. Bao, C.-X. Zeng, B.-J. Zhang, J. Wu, Y. Zhang and X.-H. Cai, *Phytochem. Lett.*, 2017, **20**, 77–83.
169 P. Krishnan, F.-K. Lee, K.-W. Chong, C.-W. Mai, A. Muhamad, S.-H. Lim, Y.-Y. Low, K.-N. Ting and K.-H. Lim, *Org. Lett.*, 2018, **20**, 8014–8018.
170 K.-H. Lim, C.-W. Mai, S.-K. Wong, Y.-Y. Low, S.-H. Lim and P. Krishnan, *Phytochem. Lett.*, 2024, **61**, 97–103.
171 A. P. G. Macabeo, K. Krohn, D. Gehle, R. W. Read, J. J. Brophy, G. A. Cordell, S. G. Franzblau and A. M. Aguinaldo, *Phytochemistry*, 2005, **66**, 1158–1162.
172 N. Kogure, N. Ishii, M. Kitajima, S. Wongseripipatana and H. Takayama, *Org. Lett.*, 2006, **8**, 3085–3088.
173 B. V. Milborrow and C. Djerassi, *J. Chem. Soc. C*, 1969, 417–424.
174 J. Sakamoto, Y. Umeda, K. Rakumitsu, M. Sumimoto and H. Ishikawa, *Angew. Chem., Int. Ed.*, 2020, **59**, 13414–13422.
175 J. Chen, Y. Yu, J. Wu, M.-F. Bao, S. Kongkiatpaiboon, J. Schinnerl and X.-H. Cai, *Bioorg. Chem.*, 2021, **116**, 105314.
176 B.-J. Zhang, X.-F. Teng, M.-F. Bao, X.-H. Zhong, L. Ni and X.-H. Cai, *Phytochemistry*, 2015, **120**, 46–52.
177 A. E. Nugroho, W. Zhang, Y. Hirasawa, Y. Tang, C. P. Wong, T. Kaneda, A. H. A. Hadi and H. Morita, *J. Nat. Prod.*, 2018, **81**, 2600–2604.
178 T. Kanchanapoom, P. Sahakitpichan, N. Chimnoi, C. Petchthong, W. Thamniyom, P. Nangkoed and S. Ruchirawat, *Phytochem. Lett.*, 2021, **41**, 83–87.
179 A. Mauger, M. Jarret, C. Kouklovsky, E. Poupon, L. Evanno and G. Vincent, *Nat. Prod. Rep.*, 2021, **38**, 1852–1886.
180 M. A. Beniddir, M.-T. Martin, M.-E. Tran Huu Dau, P. Grellier, P. Rasoanaivo, F. Guéritte and M. Litaudon, *Org. Lett.*, 2012, **14**, 4162–4165.
181 M. A. Beniddir, M.-T. Martin, M.-E. Tran Huu Dau, P. Rasoanaivo, F. Guéritte and M. Litaudon, *Tetrahedron Lett.*, 2013, **54**, 2115–2119.
182 Y.-L. He, W.-M. Chen and X.-Z. Feng, *J. Nat. Prod.*, 1994, **57**, 411–414.
183 E. E. Waldner, M. Hesse, W. I. Taylor and H. Schmid, *Helv. Chim. Acta*, 1967, **50**, 1926–1939.
184 S.-H. Lim, S.-J. Tan, Y.-Y. Low and T.-S. Kam, *J. Nat. Prod.*, 2011, **74**, 2556–2562.
185 S. Zhao, X. Liao and J. M. Cook, *Org. Lett.*, 2002, **4**, 687–690.
186 K. P. Pandey, M. T. Rahman and J. M. Cook, *Molecules*, 2021, **26**, 3459.
187 Y. Hirasawa, R. Yasuda, W. Minami, M. Hirata, A. E. Nugroho, T. Tougan, N. Uchiyama, T. Hakamatsuka, T. Horii and H. Morita, *Tetrahedron Lett.*, 2021, **83**, 153423.
188 Y.-L. Wang, C.-R. Guo, Y. Mu, Y.-L. Lin, H.-J. Yan, Z.-W. Wang and X.-J. Wang, *Tetrahedron Lett.*, 2019, **60**, 151042.
189 Y. Hirasawa, Y. Kakizoe, T. Tougan, N. Uchiyama, T. Horii and H. Morita, *J. Nat. Med.*, 2024, **78**, 768–773.
190 S. Michel, F. Tillequin and M. Koch, *J. Chem. Soc. Chem. Commun.*, 1987, 229–230.
191 F. Zhang, K. Yang, H. Liu, T. Yang, R. Zhou, X. Zhang, G. Zhan and Z. Guo, *Phytochemistry*, 2023, **209**, 113610.
192 C.-Y. Gan, T. Etoh, M. Hayashi, K. Komiyama and T.-S. Kam, *J. Nat. Prod.*, 2010, **73**, 1107–1111.
193 P. Kokkonda, K. R. Brown, T. J. Seguin, S. E. Wheeler, S. Vaddypally, M. J. Zdilla and R. B. Andrade, *Angew. Chem., Int. Ed.*, 2015, **54**, 12632–12635.
194 C.-Y. Gan, Y.-Y. Low, W. T. Robinson, K. Komiyama and T.-S. Kam, *Phytochemistry*, 2010, **71**, 1365–1370.
195 A.-M. Bui, B. C. Das, E. Guittet and P. Potier, *J. Nat. Prod.*, 1991, **54**, 514–518.
196 A. E. Nugroho, Y. Hirasawa, T. Hosoya, K. Awang, A. H. A. Hadi and H. Morita, *Tetrahedron Lett.*, 2010, **51**, 2589–2592.
197 A. T. Tchinda, O. Jansen, J.-N. Nyemb, M. Tits, G. Dive, L. Angenot and M. Frédérich, *J. Nat. Prod.*, 2014, **77**, 1078–1082.
198 Z.-W. Li, C.-L. Fan, B. Sun, L. Huang, Z.-Q. Wang, X.-J. Huang, S.-Q. Zhang, W.-C. Ye, Z.-L. Wu and X.-Q. Zhang, *Chem.–Eur. J.*, 2024, **30**, e202303519.
199 J. M. Cook and P. W. Le Quesne, *J. Org. Chem.*, 1971, **36**, 582–586.
200 D. E. Burke, J. M. Cook and P. W. Le Quesne, *J. Chem. Soc. Chem. Commun.*, 1972, 697.

201 D. E. Burke, J. M. Cook and P. W. Le Quesne, *J. Am. Chem. Soc.*, 1973, **95**, 546–552.
202 E. Seguin and M. Koch, *Planta Med.*, 1979, **37**, 175–177.
203 N. Nagakura, G. Höfle, D. Coggiola and M. H. Zenk, *Planta Med.*, 1978, **34**, 381–389.
204 J. T. Ndongo, J. N. Mbing, M. F. Tala, A. Monteillier, D. E. Pegnyemb, M. Cuendet and H. Laatsch, *Phytochemistry*, 2017, **144**, 189–196.
205 A. A. Gorman and H. Schmid, *Monatshefte für Chemie und verwandte Teile anderer Wissenschaften*, 1967, 98, pp. 1554–1566.
206 M.-M. Janot, *Tetrahedron*, 1961, **14**, 113–125.
207 H. Rapoport and R. E. Moore, *J. Org. Chem.*, 1962, **27**, 2981–2985.
208 H. M. de Sousa, A. B. da Silva, M. K. A. Ferreira, A. W. da Silva, J. E. S. A. de Menezes, E. S. Marinho, M. M. Marinho, H. S. dos Santos and O. D. L. Pessoa, *Planta Med.*, 2023, **89**, 979–989.
209 M. J. G. Tits and L. Angenot, *Planta Med.*, 1978, **34**, 57–61.
210 R. Verpoorte and A. B. Svendsen, *J. Pharm. Sci.*, 1978, **67**, 171–174.
211 F. C. Ohiri, R. Verpoorte and A. B. Svendsen, *J. Ethnopharmacol.*, 1983, **9**, 167–223.
212 S.-I. Sakai, N. Aimi, K. Yamaguchi, E. Yamanaka and J. Haginiwa, *J. Chem. Soc., Perkin Trans. 1*, 1982, 1257–1262.
213 S.-I. Sakai, N. Aimi, K. Yamaguchi, H. Ohhira, K. Hori and J. Haginiwa, *Tetrahedron Lett.*, 1975, **16**, 715–718.
214 N. Aimi, S.-I. Sakai and Y. Ban, in *The Alkaloids: Chemistry and Pharmacology*, ed. A. Brossi, Academic Press, 1990, vol. 36, pp. 1–68.
215 N. Aimi, S. Sakai, Y. Iitaka and A. Itai, *Tetrahedron Lett.*, 1971, **12**, 2061–2064.
216 G. Massiot, B. Massoussa, M.-J. Jacquier, P. Thépénier, L. Le Men-Olivier, C. Delaude and R. Verpoorte, *Phytochemistry*, 1988, **27**, 3293–3304.
217 G. Massiot, M. Zeches, C. Mirand, L. Le Men-Olivier, C. Delaude, K. H. C. Baser, R. Bavovada, N. G. Bisset and P. J. Hylands, *J. Org. Chem.*, 1983, **48**, 1869–1872.
218 A. R. Battersby, *Pure Appl. Chem.*, 1963, **6**, 471–482.
219 N.-P. Li, J.-S. Liu, J.-W. Liu, H.-Y. Tian, H.-L. Zhou, Y.-R. Zheng, X.-J. Huang, J.-Q. Cao, W.-C. Ye and L. Wang, *Bioorg. Chem.*, 2021, **107**, 104624.
220 N. Kunesch, Y. Rolland, J. Poisson, P. L. Majumder, R. Majumder, A. Chatterjee, V. C. Agwada, J. Naranjo, M. Hesse and H. Schmid, *Helv. Chim. Acta*, 1977, **60**, 2854–2859.
221 B. Danieli, G. Lesma, G. Palmisano, S. Tollari and B. Gabetta, *J. Org. Chem.*, 1983, **48**, 381–383.
222 E. Wenkert and B. Wickberg, *J. Am. Chem. Soc.*, 1965, **87**, 1580–1589.
223 G. Hugel, G. Massiot, J. Lévy and J. Le Men, *Tetrahedron*, 1981, **37**, 1369–1375.
224 B. Danieli, G. Lesma, G. Palmisano and B. Gabetta, *J. Chem. Soc. Chem. Commun.*, 1981, 908–909.
225 L. Calabi, B. Danieli, G. Lesma and G. Palmisano, *J. Chem. Soc., Perkin Trans. 1*, 1982, 1371–1379.
226 F. Kellner, F. Geu-Flores, N. H. Sherden, S. Brown, E. Foureau, V. Courdavault and S. E. O'Connor, *Chem. Commun.*, 2015, **51**, 7626–7628.
227 A. T. McPhail, E. W. Hagaman, N. Kunesch, E. Wenkert and J. Poisson, *Tetrahedron*, 1983, **39**, 3629–3637.
228 J. Lévy, P. Maupérin, M. D. de Maindreville and J. Le Men, *Tetrahedron Lett.*, 1971, **12**, 1003–1006.
229 B. J. Rawlings, *Nat. Prod. Rep.*, 1997, **14**, 523–556.
230 M.-X. Sun, H.-H. Gao, J. Zhao, L. Zhang and K. Xiao, *Tetrahedron Lett.*, 2015, **56**, 6194–6197.
231 X.-H. Cai, Z.-Z. Du and X.-D. Luo, *Org. Lett.*, 2007, **9**, 1817–1820.
232 J. M. Wood, D. P. Furkert and M. A. Brimble, *Nat. Prod. Rep.*, 2019, **36**, 289–306.
233 T.-S. Kam and Y.-M. Choo, *J. Nat. Prod.*, 2004, **67**, 547–552.
234 T.-S. Kam and Y.-M. Choo, *Tetrahedron*, 2000, **56**, 6143–6150.
235 T. Kishi, M. Hesse, C. W. Gemenden, W. I. Taylor and H. Schmid, *Helv. Chim. Acta*, 1965, **48**, 1349–1362.
236 S.-J. Tan, Y.-M. Choo, N. F. Thomas, W. T. Robinson, K. Komiyama and T.-S. Kam, *Tetrahedron*, 2010, **66**, 7799–7806.
237 S.-J. Tan, W. T. Robinson, K. Komiyama and T.-S. Kam, *Tetrahedron*, 2011, **67**, 3830–3838.
238 T.-S. Kam and Y.-M. Choo, *Tetrahedron Lett.*, 2003, **44**, 8787–8789.
239 T.-S. Kam, Y.-M. Choo and K. Komiyama, *Tetrahedron*, 2004, **60**, 3957–3966.
240 Y. Hirasawa, H. Arai, A. Rahman, I. Kusumawati, N. C. Zaini, O. Shirota and H. Morita, *Tetrahedron*, 2013, **69**, 10869–10875.
241 X.-H. Gao, Y.-Y. Fan, Q.-F. Liu, S.-H. Cho, G. F. Pauli, S.-N. Chen and J.-M. Yue, *Org. Lett.*, 2019, **21**, 7065–7068.
242 J. J. Kezetas Bankeu, D. U. Kenou Kagho, Y. S. Fotsing Fongang, R. M. Kouipou Toghueo, B. M. Mba'ning, G. R. Tchouya Feuya, F. Boyom Fekam, J. C. Tchouankeu, S. A. Ngouela, N. Sewald, B. N. Lenta and M. S. Ali, *J. Nat. Prod.*, 2019, **82**, 2580–2585.
243 K. Jewers and J. McKenna, *J. Chem. Soc.*, 1958, 2209–2217.
244 X.-W. Yang, X.-J. Qin, Y.-L. Zhao, P. K. Lunga, X.-N. Li, S.-Z. Jiang, G.-G. Cheng, Y.-P. Liu and X.-D. Luo, *Tetrahedron Lett.*, 2014, **55**, 4593–4596.
245 B.-Y. Hu, Y.-L. Zhao, Y.-J. He, Y. Qin and X.-D. Luo, *Phytochemistry*, 2024, **217**, 113926.
246 G.-Y. Zhu, X.-J. Yao, L. Liu, L.-P. Bai and Z.-H. Jiang, *Org. Lett.*, 2014, **16**, 1080–1083.
247 H.-F. Yu, C.-F. Ding, L.-C. Zhang, X. Wei, G.-G. Cheng, Y.-P. Liu, R.-P. Zhang and X.-D. Luo, *Org. Lett.*, 2021, **23**, 5782–5786.
248 J.-H. Gu, W. Zhang, W.-Y. Cai, X.-X. Fu, H.-L. Zhou, N.-P. Li, H.-Y. Tian, J.-S. Liu, W.-C. Ye and L. Wang, *Org. Chem. Front.*, 2021, **8**, 1918–1925.
249 N.-P. Li, M. Liu, X.-J. Huang, X.-Y. Gong, W. Zhang, M.-J. Cheng, W.-C. Ye and L. Wang, *J. Org. Chem.*, 2018, **83**, 5707–5714.
250 X.-H. Cai, Y. Li, Y.-P. Liu, X.-N. Li, M.-F. Bao and X.-D. Luo, *Phytochemistry*, 2012, **83**, 116–124.

251 Z.-W. Wang, J.-P. Zhang, Q.-H. Wei, L. Chen, Y.-L. Lin, Y.-L. Wang, T. An and X.-J. Wang, *Tetrahedron Lett.*, 2021, **87**, 153525.
252 I. M. Novitskiy and A. G. Kutateladze, *J. Org. Chem.*, 2022, **87**, 4818–4828.
253 A. Henriques, C. Kan, A. Chiaroni, C. Riche, H. P. Husson, S. K. Kan and M. Lounasmaa, *J. Org. Chem.*, 1982, **47**, 803–811.
254 G. Costa, C. Riche and H. P. Husson, *Tetrahedron*, 1977, **33**, 315–320.
255 L. Duhamel, J. M. Poirier and P. Granger, *J. Org. Chem.*, 1979, **44**, 3576–3578.
256 T. A. v. Beek, P. P. Lankhorst, R. Verpoorte, G. Massiot, R. Fokkens, C. Erkelens, P. Perera and C. Tibell, *Z. Naturforsch. B*, 1985, **40**, 693–701.
257 Y.-S. Cai, A. M. Sarotti, T.-L. Zhou, R. Huang, G. Qiu, C. Tian, Z.-H. Miao, A. Mándi, T. Kurtán, S. Cao and S.-P. Yang, *J. Nat. Prod.*, 2018, **81**, 1976–1983.
258 It can also be envisaged that an heteronucleophilic attack initiated by the vobasane N-1 position onto the C-16 position of the $\Delta^{16,22}$ function of the vallesamane component could be the driving force for its 1,6-conjugate addition onto the C-3 site of the vobasane component.
259 M.-F. Bao, C.-X. Zeng, Y.-P. Liu, B.-J. Zhang, L. Ni, X.-D. Luo and X.-H. Cai, *J. Nat. Prod.*, 2017, **80**, 790–797.
260 D. Lachkar, N. Denizot, G. Bernadat, K. Ahamada, M. A. Beniddir, V. Dumontet, J.-F. Gallard, R. Guillot, K. Leblanc, E. O. N'Nang, V. Turpin, C. Kouklovsky, E. Poupon, L. Evanno and G. Vincent, *Nat. Chem.*, 2017, **9**, 793–798.
261 T.-S. Kam, S.-J. Tan, S.-W. Ng and K. Komiyama, *Org. Lett.*, 2008, **10**, 3749–3752.
262 K. Okada, K.-i. Ojima, H. Ueda and H. Tokuyama, *J. Am. Chem. Soc.*, 2023, **145**, 16337–16343.
263 R. E. Ziegler, S.-J. Tan, T.-S. Kam and J. A. Porco Jr, *Angew. Chem., Int. Ed.*, 2012, **51**, 9348–9351.
264 S. Uzir, A. M. Mustapha, A. H. A. Hadi, K. Awang, C. Wiart, J.-F. Gallard and M. Païs, *Tetrahedron Lett.*, 1997, **38**, 1571–1574.
265 S. Markey, K. Biemann and B. Witkop, *Tetrahedron Lett.*, 1967, **8**, 157–160.
266 S. Szwarc, A. Jagora, S. Derbré, K. Leblanc, S. Rharrabti, C. Said-Hassane, C. El Kalamouni, J.-F. Gallard, P. Le Pogam and M. A. Beniddir, *Org. Lett.*, 2024, **26**, 274–279.
267 B. C. Das, J. P. Cosson and G. Lukacs, *J. Org. Chem.*, 1977, **42**, 2785–2786.
268 B. C. Das, J. P. Cosson, G. Lukacs and P. Potier, *Tetrahedron Lett.*, 1974, **15**, 4299–4302.
269 N. Kunesch, A. Cavé, E. W. Hagaman and E. Wenkert, *Tetrahedron Lett.*, 1980, **21**, 1727–1730.
270 M. Millot, A. Dieu and S. Tomasi, *Nat. Prod. Rep.*, 2016, **33**, 801–811.
271 G. A. Cordell, G. F. Smith and G. N. Smith, *J. Chem. Soc. D*, 1970, 191–192.
272 M. Kitajima, M. Nakazawa, Y. Wu, N. Kogure, R.-P. Zhang and H. Takayama, *Tetrahedron*, 2016, **72**, 6692–6696.
273 Y. Wu, M. Kitajima, N. Kogure, R. Zhang and H. Takayama, *Tetrahedron Lett.*, 2008, **49**, 5935–5938.
274 Y. Chang, C. Sun, C. Wang, X. Huo, W. Zhao and X. Ma, *Nat. Prod. Rep.*, 2022, **39**, 2030–2056.
275 M. Kobayashi, K. Kawazoe, T. Katori and I. Kitagawa, *Chem. Pharm. Bull.*, 1992, **40**, 1773–1778.
276 Y. Inouye, Y. Sugo, T. Kusumi and N. Fusetani, *Chem. Lett.*, 1994, **23**, 419–420.
277 F. Tillequin, M. Koch, M. Bert and T. Sevenet, *J. Nat. Prod.*, 1979, **42**, 92–95.
278 F. Tillequin, M. Koch, J.-L. Pousset and A. Cave, *J. Chem. Soc. Chem. Commun.*, 1978, 826–828.
279 L. S. Fernandez, M. S. Buchanan, A. R. Carroll, Y. J. Feng, R. J. Quinn and V. M. Avery, *Org. Lett.*, 2009, **11**, 329–332.
280 G. Philippe, E. Prost, J.-M. Nuzillard, M. Zèches-Hanrot, M. Tits, L. Angenot and M. Frédérich, *Tetrahedron Lett.*, 2002, **43**, 3387–3390.
281 H. Fouotsa, P. Le Pogam, P. Mkounga, A. M. Lannang, G. Bernadat, J. Vanheuverzwijn, Z. Zhou, K. Leblanc, S. Rharrabti, A. E. Nkengfack, J. F. Gallard, V. Fontaine, F. Meyer, E. Poupon and M. A. Beniddir, *J. Nat. Prod.*, 2021, **84**, 2755–2761.
282 V. C. Agwada, J. Naranjo, M. Hesse, H. Schmid, Y. Rolland, N. Kunesch, J. Poisson and A. Chatterjee, *Helv. Chim. Acta*, 1977, **60**, 2830–2853.
283 M. Zeches, G. Lukacs, G. M. L. Le Men-Olivier and M.-M. Debray, *J. Nat. Prod.*, 1982, **45**, 707–713.
284 N. G. Bisset, *Acta Amazonica*, 1988, **18**, 255–290.
285 G. Massiot, B. Massoussa, P. Thepenier, M.-J. Jacquier and L. Le Men-Olivier, *Heterocycles*, 1983, **20**, 2339–2342.
286 R. Mukherjee, B. C. Das, P. A. Keifer and J. N. Shoolery, *Heterocycles*, 1994, **38**, 1965–1970.
287 A. R. Battersby, H. F. Hodson, G. V. Rao and D. A. Yeowell, *J. Chem. Soc. C*, 1967, 2335–2339.
288 K. Bernauer, H. Schmid and P. Karrer, *Helv. Chim. Acta*, 1957, **40**, 1999–2003.
289 K. Bernauer, F. Berlage, H. Schmid and P. Karrer, *Helv. Chim. Acta*, 1958, **41**, 1202–1206.
290 A. Schönberg, in *Preparative Organic Photochemistry*, ed. A. Schönberg, Springer Berlin Heidelberg, Berlin, Heidelberg, 1968, pp. 373–406.
291 S. P. Singh, V. I. Stenberg and S. S. Parmar, *Chem. Rev.*, 1980, **80**, 269–282.
292 A.-M. Bui, B. C. Das, E. Guittet, J.-Y. Lallemand and P. Potier, *J. Nat. Prod.*, 1986, **49**, 321–325.
293 G. Massiot, P. Thépenier, M.-J. Jacquier, L. Le Men-Olivier, R. Verpoorte and C. Delaude, *Phytochemistry*, 1987, **26**, 2839–2846.
294 L. Merlini, R. Mondelli, G. Nasini and M. Hesse, *Tetrahedron*, 1970, **26**, 2259–2279.
295 E. Winterfeldt, *Chem. Ber.*, 1964, **97**, 2463–2468.
296 H. Riesner and E. Winterfeldt, *J. Chem. Soc. Chem. Commun.*, 1972, 786–787.
297 A. R. Battersby and J. C. Turner, *J. Chem. Soc.*, 1960, 717–725.
298 E. E. Van Tamelen, P. E. Aldrich and J. B. Hester, Jr., *J. Am. Chem. Soc.*, 1959, **81**, 6214–6221.

299 B. R. Lichman, *Nat. Prod. Rep.*, 2021, **38**, 103–129.
300 L. Caputi, J. Franke, S. C. Farrow, K. Chung, R. M. E. Payne, T.-D. Nguyen, T.-T. T. Dang, I. Soares Teto Carqueijeiro, K. Koudounas, T. Dugé de Bernonville, B. Ameyaw, D. M. Jones, I. J. C. Vieira, V. Courdavault and S. E. O'Connor, *Science*, 2018, **360**, 1235–1239.
301 P. L. Schiff, in *Alkaloids: Chemical and Biological Perspectives*, ed. S. W. Pelletier, Pergamon, 1999, vol. 14, pp. 1–284.
302 C. Weber and T. Opatz, in *The Alkaloids: Chemistry and Biology*, ed. H.-J. Knölker, Academic Press, 2019, vol. 81, pp. 1–114.
303 M. Shamma and J. Moniot, *Heterocycles*, 1975, **3**, 297–300.
304 I. R. C. Bick and S. Sotheeswaran, *Aust. J. Chem.*, 1978, **31**, 2077–2083.
305 J.-Z. Wang, Q.-H. Chen and F.-P. Wang, *J. Nat. Prod.*, 2010, **73**, 1288–1293.
306 C. D. Critchett, H. R. W. Dharmaratne, S. Sotheeswaran, A. M. Galal, P. L. Schiff and I. R. C. Bick, *Aust. J. Chem.*, 1989, **42**, 2043–2046.
307 J. Harley-Mason, A. S. Howard, W. I. Taylor, M. J. Vernengo, I. R. C. Bick and P. S. Clezy, *J. Chem. Soc. C*, 1967, 1948–1951.
308 C. Jih-Jung, T. Ian-Lih, T. Ishikawa, W. Chyl-Jia and C. Ih-Sheng, *Phytochemistry*, 1996, **42**, 1479–1484.
309 J.-J. Chen, T. Ishikawa, C.-Y. Duh, I.-L. Tsai and I.-S. Chen, *Planta Med.*, 1996, **62**, 528–533.
310 M. L. R. Ferreira, I. C. de Pascoli, I. R. Nascimento, J. Zukerman-Schpector and L. M. X. Lopes, *Phytochemistry*, 2010, **71**, 469–478.
311 R. S. Istatkova and S. A. Philipov, *Phytochemistry*, 2000, **54**, 959–964.
312 K. W. Bentley, *Nat. Prod. Rep.*, 2002, **19**, 332–356.
313 D. Cortes, J. Saez, R. Hocquemiller, A. Cavé and A. Cavé, *Heterocycles*, 1986, **24**, 607–610.
314 N. Nagakura, G. Höfle and M. H. Zenk, *J. Chem. Soc. Chem. Commun.*, 1978, 896–898.
315 Y.-S. Cai, C. Wang, C. Tian, W.-T. Sun, L. Chen, D. Xiao, S.-Y. Zhou, G. Qiu, J. Yu, K. Zhu and S.-P. Yang, *J. Nat. Prod.*, 2019, **82**, 2645–2652.
316 A. Itoh, T. Tanahashi and N. Nagakura, *Phytochemistry*, 1991, **30**, 3117–3123.
317 S. C. Pakrashi, B. Achari, E. Ali, P. P. Ghosh Dastidar and R. R. Sinha, *Tetrahedron Lett.*, 1980, **21**, 2667–2670.
318 A. Bhattacharjya, R. Mukhopadhyay and S. C. Pakrashi, *Tetrahedron Lett.*, 1986, **27**, 1215–1216.
319 P. Brauchli, V. Deulofeu, H. Budzikiewicz and C. Djerassi, *J. Am. Chem. Soc.*, 1964, **86**, 1895–1896.
320 A. Itoh, T. Tanahashi and N. Nagakura, *J. Nat. Prod.*, 1995, **58**, 1228–1239.
321 N. Nagakura, A. Itoh and T. Tanahashi, *Phytochemistry*, 1993, **32**, 761–765.
322 C. Djerassi, A. A. P. G. Archer, T. George, B. Gilbert, J. N. Shoolery and L. F. Johnson, *Experientia*, 1960, **16**, 532–534.
323 P. Teerapongpisan, V. Suthiphasilp, P. Kumboonma, T. Maneerat, T. Duangyod, R. Charoensup, P. Promnart and S. Laphookhieo, *Phytochemistry*, 2024, **220**, 114020.
324 Y.-W. Ge, S. Zhu, M.-Y. Shang, X.-Y. Zang, X. Wang, Y.-J. Bai, L. Li, K. Komatsu and S.-Q. Cai, *Phytochemistry*, 2013, **86**, 201–207.
325 Y.-G. Guo, Y.-H. Ding, G.-J. Wu, S.-L. Zhu, Y.-F. Sun, S.-K. Yan, F. Qian, H.-Z. Jin and W.-D. Zhang, *Fitoterapia*, 2018, **127**, 96–100.
326 G.-M. Yang, J. Sun, Y. Pan, J.-L. Zhang, M. Xiao and M.-S. Zhu, *Fitoterapia*, 2018, **124**, 58–65.
327 W. J. Griffin and G. D. Lin, *Phytochemistry*, 2000, **53**, 623–637.
328 O. Muñoz, R. Hartmann and E. Breitmaier, *J. Nat. Prod.*, 1991, **54**, 1094–1096.
329 A. San-Martín, C. Labbé, O. Muñoz, M. Castillo, M. Reina, G. De La Fuente and A. González, *Phytochemistry*, 1987, **26**, 819–822.
330 H. W. Voigtländer and W. Rosenberg, *Arch. Pharmazie*, 1959, **292**, 632–642.
331 S. Cretton, T. A. Bartholomeusz, M. Humam, L. Marcourt, Y. Allenbach, D. Jeannerat, O. Muñoz and P. Christen, *J. Nat. Prod.*, 2011, **74**, 2388–2394.
332 M. Lounasmaa and T. Tamminen, in *The Alkaloids: Chemistry and Pharmacology*, ed. G. A. Cordell, Academic Press, 1993, vol. 44, pp. 1–114.
333 R. Hartmann, A. San-Martin, O. Muñoz and E. Breitmaier, *Angew. Chem., Int. Ed.*, 1990, **29**, 385–386.
334 Z.-Y. Chan, P. Krishnan, S. M. Modaresi, L.-W. Hii, C.-W. Mai, W.-M. Lim, C.-O. Leong, Y.-Y. Low, S.-K. Wong, K.-T. Yong, A. Z.-X. Leong, M.-K. Lee, K.-N. Ting and K.-H. Lim, *J. Nat. Prod.*, 2021, **84**, 2272–2281.
335 S. F. Aripova, E. G. Sharova and S. Y. Yunusov, *Chem. Nat. Compd.*, 1982, **18**, 606–607.
336 S. A. Snyder, A. Gollner and M. I. Chiriac, *Nature*, 2011, **474**, 461–466.
337 A. E. Fox Ramos, P. Le Pogam, C. Fox Alcover, E. Otogo N'Nang, G. Cauchie, H. Hazni, K. Awang, D. Bréard, A. M. Echavarren, M. Frédérich, T. Gaslonde, M. Girardot, R. Grougnet, M. S. Kirillova, M. Kritsanida, C. Lémus, A.-M. Le Ray, G. Lewin, M. Litaudon, L. Mambu, S. Michel, F. M. Miloserdov, M. E. Muratore, P. Richomme-Peniguel, F. Roussi, L. Evanno, E. Poupon, P. Champy and M. A. Beniddir, *Sci. Data*, 2019, **6**, 15.
338 M. Wang, J. J. Carver, V. V. Phelan, L. M. Sanchez, N. Garg, Y. Peng, D. D. Nguyen, J. Watrous, C. A. Kapono, T. Luzzatto-Knaan, C. Porto, A. Bouslimani, A. V. Melnik, M. J. Meehan, W.-T. Liu, M. Crusemann, P. D. Boudreau, E. Esquenazi, M. Sandoval-Calderon, R. D. Kersten, L. A. Pace, R. A. Quinn, K. R. Duncan, C.-C. Hsu, D. J. Floros, R. G. Gavilan, K. Kleigrewe, T. Northen, R. J. Dutton, D. Parrot, E. E. Carlson, B. Aigle, C. F. Michelsen, L. Jelsbak, C. Sohlenkamp, P. Pevzner, A. Edlund, J. McLean, J. Piel, B. T. Murphy, L. Gerwick, C.-C. Liaw, Y.-L. Yang, H.-U. Humpf, M. Maansson, R. A. Keyzers, A. C. Sims, A. R. Johnson, A. M. Sidebottom, B. E. Sedio, A. Klitgaard, C. B. Larson,

C. A. Boya P, D. Torres-Mendoza, D. J. Gonzalez, D. B. Silva, L. M. Marques, D. P. Demarque, E. Pociute, E. C. O'Neill, E. Briand, E. J. N. Helfrich, E. A. Granatosky, E. Glukhov, F. Ryffel, H. Houson, H. Mohimani, J. J. Kharbush, Y. Zeng, J. A. Vorholt, K. L. Kurita, P. Charusanti, K. L. McPhail, K. F. Nielsen, L. Vuong, M. Elfeki, M. F. Traxler, N. Engene, N. Koyama, O. B. Vining, R. Baric, R. R. Silva, S. J. Mascuch, S. Tomasi, S. Jenkins, V. Macherla, T. Hoffman, V. Agarwal, P. G. Williams, J. Dai, R. Neupane, J. Gurr, A. M. C. Rodriguez, A. Lamsa, C. Zhang, K. Dorrestein, B. M. Duggan, J. Almaliti, P.-M. Allard, P. Phapale, L.-F. Nothias, T. Alexandrov, M. Litaudon, J.-L. Wolfender, J. E. Kyle, T. O. Metz, T. Peryea, D.-T. Nguyen, D. VanLeer, P. Shinn, A. Jadhav, R. Muller, K. M. Waters, W. Shi, X. Liu, L. Zhang, R. Knight, P. R. Jensen, B. O. Palsson, K. Pogliano, R. G. Linington, M. Gutierrez, N. P. Lopes, W. H. Gerwick, B. S. Moore, P. C. Dorrestein and N. Bandeira, *Nat. Biotechnol.*, 2016, **34**, 828–837.